CHAPTER **3**

High-Throughput Organic Synthesis in Microreactors

Charlotte Wiles[1,2,*] and **Paul Watts**[1,*]

Contents

Abstract

With an average lead time of 10–12 years for a compound to pro-
gress from initial identification through clinical trials and finally into a
medicine, the pharmaceutical industry are interested in the devel-
opment of techniques which have the potential to reduce the time
taken to generate prospective lead compounds and translate the
protocols into production. As such, one of the areas of synthetic
chemistry that has benefited greatly from microreaction technology
(MRT), over the past 15 years, has been that of pharmaceutical

1   Department of Chemistry, The University of Hull, Cottingham Road, Hull HU6 7RX, UK
2   Chemtrix BV, Burgemeester Lemmensstraat 358, 6163JT Geleen, The Netherlands

* Corresponding author.
E-mail address: c.wiles@chemtrix.com
E-mail address: p.watts@hull.ac.uk

research and development (Glasnov and Kappe, 2007; Mason et al., 2007); with interest in the technology stemming from the perceived ease with which reaction conditions can be optimized and subsequently employed across a range of substrates in order to generate compound libraries (Kirschning et al., 2006; Wiles and Watts, 2007a; Wiles and Watts 2008a). The rapid translation of reaction methodology from the microreactors employed within an R&D facility to production, achieved by a process referred to as scale-out, numbering-up, or upscaling, also has the potential to reduce the time taken to take a compound to market (Yoshida, 2008).

Based on this notion, research into the use of microreactors as tools for high-throughput organic synthesis has grown in popularity, with the last 5 years seeing an emerging trend in the types of compounds prepared changing from proof of concept reactions, to the synthesis of molecules of direct relevance to the pharmaceutical industry. With this in mind, the chapter begins with an overview of the seminal examples that helped to foster interest in microreactors as high-throughput tools, illustrating liquid phase (Sections 2.1–2.3), catalytic (Section 2.4) and photochemical (Section 2.6) reactions, and concludes with a selection of current examples into the synthesis of industrially relevant molecules using MRT (Section 3).

1. INTRODUCTION

When considering the use of microreaction technology, from the perspective of high-throughput organic synthesis, the main benefit that this technique offers is increased reaction control, which in itself affords many practical advantages to the user. As a result of the small reactor dimensions, rapid mixing of reactants, and an even temperature distribution are observed, which not only increase the uniformity of reaction conditions, but also afford increased reaction safety, selectivity, reproducibility, and efficiency when compared to conventional batch reactors; where hot spot formation can lead to the formation of by-products and the risk of thermal runaway.

From a screening perspective, the rapid mixing and equilibration of reaction conditions is advantageous as parameters such as time, temperature, pressure, and stoichiometry can be varied with ease and have an immediate effect on the microreaction, compared to batch vessels where changes take time to have an effect on the whole of the reaction mixture. As such, reaction screening can be performed in a shorter time frame, using less raw materials than a conventional reaction evaluation; whilst enabling the reaction conditions identified to be employed in the production of larger quantities of the material for clinical trials and subsequent production campaigns if required. With these factors in mind, the following sections provide practical examples of the advantages associated with microreaction technology (MRT), starting with liquid-phase

reactions (Sections 2.1–2.3) and moving on to those reactions that have employed solid-supported reagents, catalysts, and scavengers (Section 2.4–2.5) into the continuous flow process.

2. THE USE OF MICROREACTORS FOR HIGH-THROUGHPUT ORGANIC SYNTHESIS

2.1 Enhanced reaction control

An early example that illustrated the ability to reduce reaction times as a consequence of conducting reactions in miniaturized, continuous flow reactors was reported by Fernandez-Suarez et al. (2002) who investigated a series of Domino reactions within a soda-lime glass microreactor. As Scheme 1 illustrates, the reactions involved a base-catalyzed Knoevenagel condensation followed by an intramolecular hetero-Diels–Alder reaction. To synthesize cycloadduct **1** under continuous flow, a solution of *rac*-citronellal **2** (0.10 M) and a premixed solution containing barbituric acid **3** (0.12 M) and ethylenediamine diacetate (EDDA) **4** (0.17 M), in MeOH:H$_2$O (80:20), were introduced into the reaction channels from inlets A and B, respectively. Reagents were mobilized within the reactor using a series of computer-controlled pumps, with reactions performed over a period of 30 min prior to analysis of the reaction products off-line by liquid chromatography–mass spectrometry (LC–MS). Employing an initial residence time of 2 min, the authors reported 60% conversion to cycloadduct **1**, which was further increased to 68% conversion by extending the residence time to 6 min. With this information in hand, the authors synthesized a series of cycloadducts under the aforementioned conditions, affording the respective compounds in yields ranging from 59 to 75%.

In another glass (borosilicate) microreactor [channel dimensions = 350 μm (wide) × 52 μm (deep) × 2.5 cm (long)], Wiles et al. (2004b) prepared a series of 1,2-azoles, illustrating the synthesis of a pharmaceutically relevant core motif. Reactions were performed using electroosmotic flow (EOF) as the pumping mechanism and employed separate
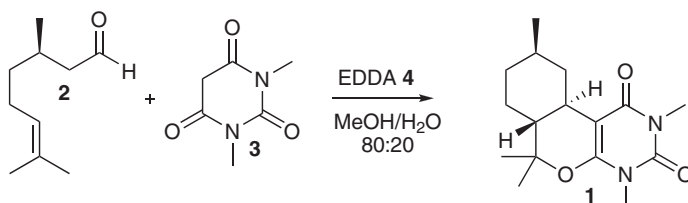
Scheme 1 An example of the Domino reactions performed by Fernandez-Suarez et al. (2002) in a soda-lime microreactor.
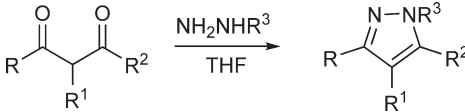
reactant solutions of 1,3-diketones (1.0 M) and the hydrazine derivative (1.0 M) in anhydrous THF.

Application of a positive voltage resulted in pumping of the reactants through the microchannel network, into a central channel where the reaction occurred and toward the reactor outlet (0 V cm^{-1}). Employing a range of applied fields enabled the reactant residence time to be optimized, resulting in the synthesis of numerous 1,2-azoles in excellent purity, compared to analogous batch reactions. As Table 1 illustrates, reactions involving hydrazine monohydrate (R^3 = H) afforded excellent conversions; however, when a substituted hydrazine derivative, benzyl hydrazine hydrochloride (R^3 = CH$_2$Ph), was employed only 42% conversion to the target 1,2-azole was obtained. This was later optimized to 100% by the use of a stopped flow technique, which served to increase the reactant residence time within the microreactor. Should the technique be required for the production of larger quantities of material, the same effect could be obtained by increasing the length of the microchannel in order to obtain an increased residence time under continuous flow.

Employing a staked plate microreactor (channel dimensions = 100 μm, total volume = 2 ml), Acke and Stevens (2007) reported the continuous flow synthesis of a series of chromenones via a multicomponent route consisting of a sequential Strecker reaction-intramolecular nucleophilic addition and tautomerization, as depicted in Scheme 2.

To synthesize these pharmaceutically interesting compounds, methanolic solutions of acetic acid 6 (2.0 eq.)/2-formylbenzoic acid 7 (1.0 eq.) and aniline 8 (2.0 eq.)/potassium cyanide 9 (1.2 eq.) were introduced into the reactor from separate inlets, thus ensuring the formation of HCN and the

Table 1 A summary of the results obtained for the synthesis of 1,2-azoles using EOF as the pumping mechanism

R	R^1	R^2	R^3	Applied field (V cm^{-1})[a]	Conversion (%)
CH$_3$	H	CH$_3$	H	292, 318	100
Ph	H	CH$_3$	H	364, 341	100
–(CH$_2$)$_4$–		Ph	H	260, 303	100
Ph	H	Ph	H	386, 364	100
Ph	CH$_3$	CH$_3$	H	292, 318	100
Ph	H	CH$_3$	CH$_2$Ph	318, 318	42 (100)[b]

[a]All reaction products were collected at 0 V cm^{-1}.
[b]Stopped flow was used.
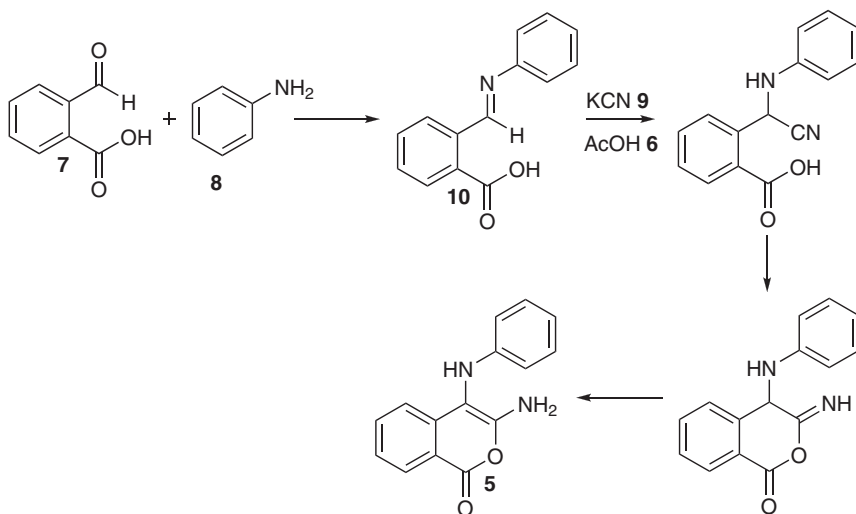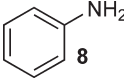
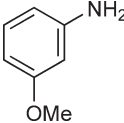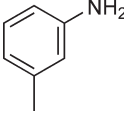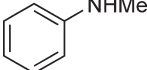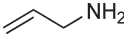**Scheme 2** Reaction protocol employed for the synthesis of 3-diamino-1*H*-isochromen-1-one **5** under continuous flow conditions.

imine **10** occurred within the confines of the microchannel. In order to prevent precipitation of the reaction products within the residence time unit, and the reactor outlet, a maximum concentration of 0.15 M was selected for the 2-formyl benzoic acid **7**. Employing a residence time of 40 min, the authors reported an isocoumarin **5** yield of 66%, which equates to a throughput of 1.80 g h^{-1}; as the target materials were found to be unstable in solution, the chromenones were stored in a solid form. To demonstrate the flexibility of the reaction setup, a series of amines were employed in place of aniline **8** to afford the target products in yields ranging from 6 to 75% (Table 2). Although these yields may be viewed as moderate to good, several of the examples reported demonstrated an increase in yield compared to analogous batch reactions.

Building on this research, Acke et al. (2008) extended their investigation to include the ring closing of vicinal amino groups in order to introduce an imidazole core into the compounds skeleton. Employing the synthesis of 1*H*-isochromeno[3,4-*d*]imidazol-5-one **11** as a model reaction (Scheme 3), the authors investigated the effect of solvent, temperature, acid/orthoester stoichiometry and reactant concentration within a stacked plate microreactor.

Using this approach, the authors found the optimal reaction conditions to be a reactant concentration of 0.2 M, dimethylformamide (DMF) as the reaction solvent, a reaction temperature of 22 °C, 10 mol% *p*-TsOH **12**, and 5.0 eq. of the orthoester **13**. Under the aforementioned conditions, the target material **11** was obtained in 43% yield, with a residence time of

Table 2   A selection of chromenones synthesized under flow by Acke et al. (2007)
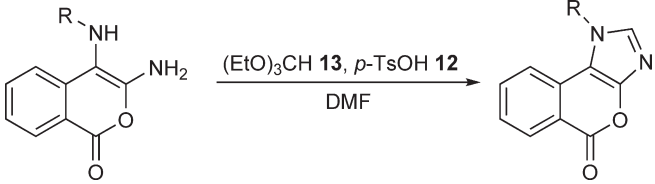
Amine	Yield (%)	Throughput (g h^{-1})
NH$_2$ **8**	66	1.80
NH$_2$ OMe	75	2.28
NH$_2$	9	1.98
NHMe	49	1.41
NH$_2$	6	0.14
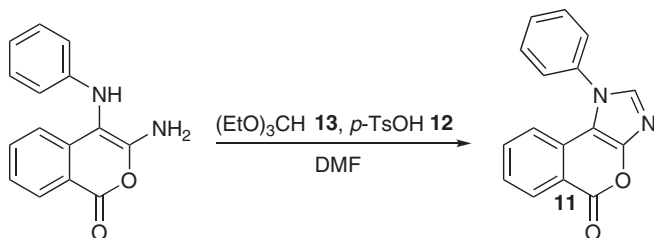
Scheme 3   Illustration of the model reaction employed to evaluate the ring closure of 3-amino-4-(arylamino)-1H-isochromen-1-ones under continuous flow.

19.6 min, which was successfully increased to 80% as a result of increasing the residence time to 59 min. Although quantitative conversion to **11** was obtained, the use of DMF as the reaction solvent led to a relatively large loss of product **11** upon isolation. However, having demonstrated the ability to perform the desired ring closure, the authors subsequently evaluated the generality of the protocol for a series of substituted isochromen-1-ones, as illustrated in Table 3, affording the target compounds in a continuous output of 0.18–2.21 g h^{-1}.

The conversion of carboxylic acids to esters is a fundamental transformation in the synthetic chemists' toolbox, as such Wiles et al. (2003) investigated the ability to efficiently synthesize a series of methyl, ethyl,

Table 3 Summary of the 1*H*-isochromeno[3,4-*d*]imidazol-5-ones synthesized in a stacked plate microreactor using *p*-TsOH **12** as the promoter

R	Yield (%)[a]	Throughput (g h^{-1})
3-Methoxyphenyl	55	0.39
3-Tolyl	27	0.18
4-Tolyl	78	0.52
4-Methoxyphenyl	75	0.53
4-Fluorophenyl	92	0.62

[a]Residence time = 118 min.

and benzyl ester under continuous flow, using EOF as the pumping mechanism. Employing a borosilicate glass microreactor [channel dimensions = 350 µm (wide) × 52 µm (deep) × 2.5 cm (long)] with three inlets and one outlet, the authors investigated the use of a mixed anhydride, to synthesize esters from carboxylic acids, as depicted in Scheme 4.

Solutions of triethylamine (Et$_3$N) **14** (1.0 M), premixed carboxylic acid/alkyl chloroformate (1.0 M respectively), and 4-dimethylaminopyridine **15** (0.5 M) in MeCN were introduced into the reactor from separate inlets and the reaction products collected at the outlet in MeCN, prior to analysis by gas chromatography–mass spectrometry (GC–MS). Under optimized reaction conditions, the authors were able to synthesize the methyl **16**, ethyl **17**, and benzyl **18** esters in quantitative conversion, with no anhydride or deprotection by-products detected (as observed in conventional batch reactions). In addition to the Boc-glycine derivatives illustrated in Scheme 4, the authors also esterified a series of aromatic carboxylic acids with yields ranging from 91 to 100%, depending on the additional functional groups present.
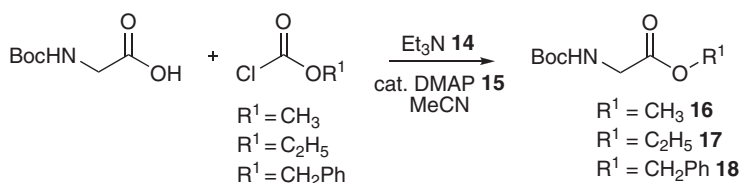
Scheme 4 A selection of the esters synthesized in an EOF-based microreactor.

Of the homogeneous reactions investigated within microstructured reactors, the acylation of amines represents one of the most frequently reported classes of reaction observed to benefit from continuous processing (Kikutani et al. 2002a, 2002b; Schwalbe et al., 2002, 2004). In a recent example by Hooper and Watts (2007), the atom efficiency of reactions conducted within microfluidic systems was demonstrated via the incorporation of deuterium labels into an array of small organic compounds. Employing the base-mediated acylation of primary amines as a model reaction, see Scheme 5, the authors demonstrated the ease by which reactions could firstly be conducted using unlabeled precursors and once the optimal reaction conditions were identified, substitution with the labeled reagent enabled the rapid and efficient synthesis of the deuterated analog.

To conduct the model reaction illustrated, two borosilicate glass reactors were employed in series [Reactor $1 = 201 \, \mu m$ (wide) $\times 75 \, \mu m$ (deep) $\times 2 \, cm$ (long), Reactor $2 = 158 \, \mu m$ (wide) $\times 60 \, \mu m$ (deep) $\times 1.5 \, cm$ (long)] and reagents delivered to the reaction channels using a syringe pump. To ensure long-term operation of the reactor setup, the authors found it necessary to employ a mixed solvent in order to obtain a balance between by-product solubility ($Et_3N \cdot HCl$) and stability of the acylating agent 19. With this in mind, solutions of benzylamine 20 and triethylamine 14 in MeCN (0.1 M, respectively) were introduced into the reactor from separate inlets and mixed using a T-mixer, prior to the addition of the acyl halide (0.05 M) as a solution in anhydrous THF. Employing a total flow rate of $40 \, \mu l \, min^{-1}$, equating to a residence time of 2.6 s, the authors obtained N-benzamide 21 in 95% conversion [determined by off-line high-performance liquid chromatography (HPLC) analysis].

The ease of method transfer was subsequently demonstrated via substitution of acetyl chloride 19 with acetyl [D_3]chloride 22, whereby operating the reactor under the aforementioned conditions, the authors obtained comparable results (98% conversion). This investigation provided important results for those in the area of isotope labeling as it demonstrated the ability to perform and optimize reactions using cheap, readily available precursors and then substitute labeled precursors to obtain the respective

$R^1 = CH_3$ 19
$R^1 = CD_3$ 22

$R^1 = CH_3$ 21
$R^1 = CD_3$
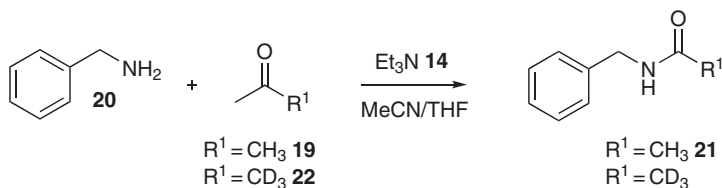
Scheme 5   Schematic illustrating the methodology employed for the incorporation of deuterium labels into small organic compounds.

labeled analog. For applications such as this, microreaction technology affords a means of reducing the development costs associated with the production of small molecule libraries, whilst also affording a rapid and efficient means of producing the labeled compounds.

2.2 Thermal control

Through the examples discussed thus far it can be seen that reaction times can be dramatically reduced as a result of moving from a batch vessel to a microreactor, typically seconds or minutes, a feature that can be attributed to the increased mixing efficiency and excellent thermal control obtained through the efficient dissipation of heat generated during a reaction. This makes microreactors ideal vessels to perform reactions that are temperature sensitive, along with those that are highly exothermic and would prove too hazardous to be performed batchwise. In addition, in the case of those reactions that require activation, thermal control is required in order to heat the microreactors and as the following section illustrates, this has been achieved by the use of thermal jackets, baths, and microwave irradiation.

2.2.1 Increased reaction temperature and pressure

van Meene et al. (2006) demonstrated the ability to conduct reactions above room temperature within a microreactor, reporting the synthesis of α-aminophosphonates via the Kabachnick–Fields reaction (Scheme 6). Using a stainless-steel flow reactor, maintained at 50 °C, the authors found that employing a residence time of 78 min (600 µl min^{-1}) afforded quantitative conversion of the aldimine **23** to the respective α-aminophosphonate **24** and after subjecting the reaction products to an off-line acid–base extraction, an isolated yield of 94% **24** was obtained. Under the aforementioned reaction conditions, a further four derivatives were synthesized, with isolated yields ranging from 68 to 91%.

Compared to conventional batch protocols, where catalysts such as LiClO$_4$ and InCl$_3$ are frequently employed, the continuous flow approach proved advantageous as the reaction was conducted in the absence of a catalyst and without the need for lengthy reaction times, maintained at reflux.
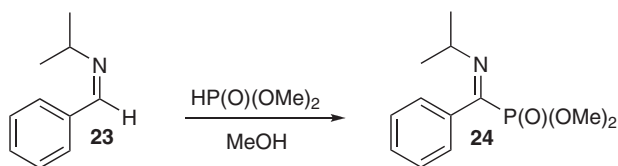

Scheme 6   Example of the α-aminophosphonates synthesized under continuous flow.
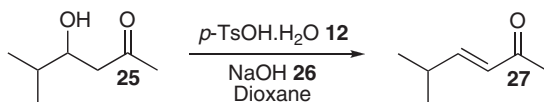
Scheme 7 Acid-catalyzed elimination used to dehydrate β-hydroxyketones.

Tanaka et al. (2007) recently demonstrated the use of an IMM micro-mixer for an investigation into the development of a continuous flow method for the dehydration of β-hydroxyketones to the target unsaturated products, as depicted in Scheme 7. A typical protocol involved the intro-duction of 4-hydroxy-5-methylhexan-2-one **25** (1×10^{-2} M) and p-TsOH. H_2O **12** (1×10^{-2} M) in dioxane into the micromixer, the reaction mixture was then heated in a microchannel prior to quenching the resulting reac-tion mixture with aq. NaOH **26** (1.0 M). Using this approach, the authors found the optimal reaction conditions to be a residence time of 47 s (200 μl min^{-1}) and a reaction temperature of 110 °C, which afforded the target alkene **27** in quantitative yield. In comparison, batch reactions typically afforded a respectable 71% yield; however, the product **27** was accompa-nied by a large proportion of by-products. Compared to previous batch methodology, the continuous flow approach provides a facile approach for the dehydration of β-hydroxyketones and as discussed in Section 3. (Scheme 71), enables production quantities of synthetically useful material to be generated with ease.

One approach that is becoming more common within research laboratories, and proves impractical when considering the need to scale a process, is the activation of reactions by employing high tem-peratures and pressure. However through the use of microreaction technology, such reaction conditions can be employed safely and with ease, as the high-temperature/pressure regime recently employed by Hessel et al. (2005) for the Kolbe–Schmitt reaction of resorcinol **28**, to afford 2,4-hydroxybenzoic acid **29** (Scheme 8) demonstrates. As the reaction is industrially relevant, potassium hydrogen carbonate **30** was selected as it is a cheap, readily available raw material making it feasible to use in the large-scale synthesis of **29** (100–1,000 l h^{-1}); furthermore, water was selected as the reaction medium as it is a safe and inexpensive solvent.
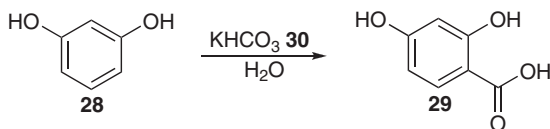

Scheme 8 Kolbe–Schmitt synthesis of 2,4-dihydrobenzoic acid **29** from resorcinol **28**.

Utilizing a stainless-steel capillary-based reactor, the authors initially evaluated the effect of pressure on a reaction conducted at 120 °C and found that with a fixed residence time of 6.5 min an increase in yield from 23 to 47% was observed upon increasing reactor pressure from 1 to 32 bar. In an analogous batch reaction, conducted at reflux, the authors obtained 2,4-dihydroxybenzoic acid **29** in ∼40% yield, after 2 h, with only 90% selectivity. By overpressuring the reaction vessel to 40 bar, the authors were able to increase the boiling point of water to 250 °C, enabling the evaluation of reaction temperature to be conducted over a wide range with relative ease, without encountering a complex biphasic reaction mixture. Maintaining a moderate overpressure, the effect of reaction temperature was subsequently investigated, with results comparable to batch obtained at 140 °C and a residence time of 12 min. The use of higher reaction temperatures was however found to be disadvantageous as it led to decomposition of the target benzoic acid **29** via decarboxylation, the technique did, however, afford a 440-fold increase in the space time yield (cf. a 1 l flask) representing a throughput of 110 g **29** h^{-1}.

Kawanami et al. (2007) demonstrated the ability to perform a series of copper-free Sonogashira C–C coupling reactions in water through the use of a superheated Hastelloy micromixer [0.5 mm (i.d.)] and tubular flow reactor [1.7 mm (i.d.) × 10 m (length)]. Employing a flow process consisting of rapid collision mixing between a substrate and water (to afford particle dispersion) followed by rapid heating (to induce reaction) and cooling to afford a binary phase (consisting of reaction products and water), the authors were able to obtain the target compounds in excellent yield and selectivity when compared to the use of organic solvents. Conducting the reaction illustrated in Scheme 9 at 250 °C and 16 MPa, near quantitative coupling of 4-iodobenzene **31** to phenylacetylene **32** was obtained employing 2 mol% of catalyst **33** in 0.1–4.0 s. Upon collection, the reaction products floated on the surface of the water and the catalyst precipitated as Pd^0, as such the diphenylacetylene **34** was isolated by a facile process of filtration and phase separation.

In addition to the rate acceleration observed, the technique of rapid mixing and heating afforded an unprecedented catalytic turnover frequency of $4.3 \times 10^6 \, h^{-1}$. Using this approach, the authors subsequently investigated the C–C coupling reactions between phenyl acetylene **32** and a further nine aryl halides to afford yields ranging from 62 to 100%.
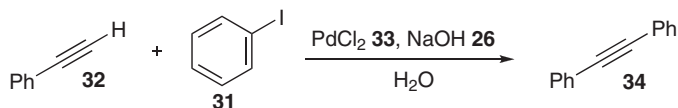
Scheme 9 Model reaction used to demonstrate the rate acceleration attained using superheated water as a reaction solvent.
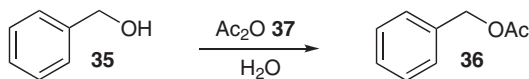
Scheme 10   An example of the hydrolysis free O-acylation conducted in subcritical water.

In a second example, Sato et al. (2007) demonstrated the highly selective, hydrolysis free O-acylation of alcohols using subcritical water (Scheme 10). Employing a reaction temperature of 200 °C, a pressure of 5 MPa, the acylation of benzyl alcohol **35** was achieved in <10 s, using acetic anhydride **37** as the acylating agent, and afforded the target benzyl acetate **36** in 99% yield, compared to 17% in a batch process. The use of subcritical water coupled with the microflow reactor has great synthetic potential as it removes the need for organic solvents enabling reactions to be performed in an environmentally benign solvent system, whilst affording a facile means of isolating the reaction products, facilitating reuse of the solvent.

In addition to providing heat to a reaction vessel through the use of a thermal jacket, oil bath, or convective heater, the past 5 years have seen numerous authors successfully combine the emerging technologies of microwave chemistry and microreaction technology, noting an array of advantages including reduced reaction times and increased product selectivity. Comer and Organ (2005a) recently demonstrated the use of microwave irradiation as an alternative heating source for a series of Suzuki–Miyaura reactions conducted in glass capillary reactors [200 μm (i.d)]. To perform a reaction, the authors introduced reactants into the flow reactor through a stainless-steel mixing chamber, under pressure-driven flow, and investigated the coupling of 4-iodooct-4-ene **38** (0.20 M) and 4-methoxyboronic acid **39** (0.24 M) using THF as the reaction solvent and palladium tetrakis(triphenylphosphine) **40** as the catalyst (Scheme 11). Under 100 W, the authors obtained 100% conversion to 1-methoxy-4-(1-propylpent-1-enyl) benzene **41** with a residence time of 28 min.

The reaction was subsequently repeated using an array of aryl halides and boronic acids, affording the target compounds in 37% to quantitative yield. Compared to conventional batch reactions, these results illustrate dramatic improvements in yield largely due to the suppression of competing side reactions.
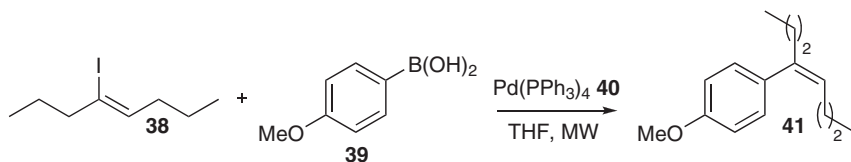

Scheme 11   Schematic illustrating the Suzuki–Miyaura reaction, using microwave heating.

Other reactions evaluated by the authors include the Wittig–Horner olefination and a series of ring-closing metathesis reactions, employing Grubb's II catalyst; in all the cases, a reduction in power consumption, increase in yield and reduction in reaction time was obtained as a result of employing microwave-assisted continuous flow reactions (Comer and Organ, 2005b).

Using a coiled perfluoroalkoxy alkane tube, with an internal diameter of 750 µm (total volume = 3 ml), Benali et al. (2008) investigated the effect of microwaves on a bromination reaction (Scheme 12), the product of which was required in a large amount for a drug discovery program. Employing microwave power of 300 W, affording a reaction temperature of 120 °C, coupled with a flow rate of 0.65 ml min^{-1}, the authors were able to obtain the target compound in 89% yield and 91% purity. Unfortunately, the time taken for the system to reach a steady state, due to the reactor volume, resulted in a large amount of waste generation and the authors sought an alternative method for microwave reaction optimization.

To increase the rate of optimization and reduce the volume of material used, the authors subsequently investigated the formation of discreet sample plugs separated by a fluorous solvent, perfluoromethyldecalin, enabling a large number of reactions to be performed in series, each with a relatively small reactant volume. Initial investigations therefore focused on the halide displacement reaction illustrated in Scheme 13 and importantly identified that analogous conversions were obtained across plug volumes ranging from 200 to 4000 µl (∼85% conversion to 42);
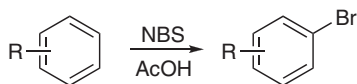
Scheme 12 Bromination reactions used to evaluate continuous flow microwave-assisted reaction optimization.
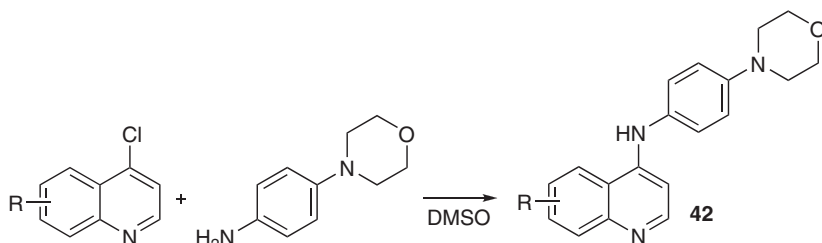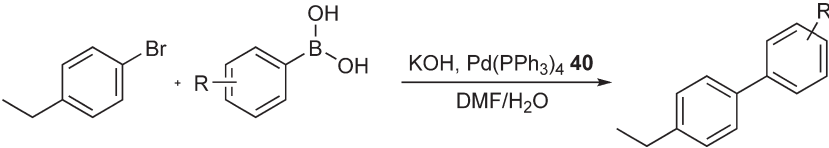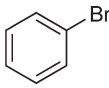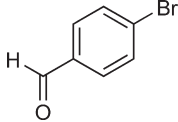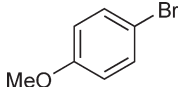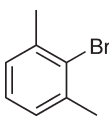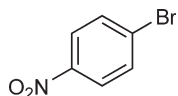

Scheme 13 Microwave-assisted displacement of an aromatic chloride by a 2° amine used to evaluate the effect of plug size in the continuous flow reactor.

meaning that reactions could readily be scaled once optimized using 200 µl volumes of reactants.

The facile approach to reaction optimization, followed by scale-out was subsequently demonstrated using the Suzuki–Miyaura cross-coupling reaction. As Table 4 illustrates, excellent results were obtained using a range of aryl bromides, with comparable or better yields obtained than the analogous batch reactions. Employing a constant reaction stream for a period of 35 min, equivalent to a reaction volume of 30 ml, the authors were able to synthesize a target biphenyl in an overall yield of 58%, corresponding to a throughput of $0.5\,g\,h^{-1}$.

Table 4   Suzuki–Miyaura reaction used as a model to demonstrate the optimization of microwave induced continuous flow reactions

| Aryl bromide	Yield (%)	
	Batch	Flow
	100	100
	100	91
	100	96
	49	100
	100	86

2.2.2 Reduced reaction temperatures

In addition to introducing energy into reactors via heating, or removal of heat generated during a reaction, some synthetic processes need to be conducted at reduced temperatures in order to prevent decomposition of unstable intermediates or to preserve reaction stereoselectivity.

An early example of a microreaction conducted at a reduced reaction temperature was demonstrated by Wiles et al. (2004c) and was used to illustrate the stereoselective alkylation of an Evans auxiliary **43** under continuous flow, as depicted in Scheme 14. Employing a borosilicate glass microreactor [microchannel = 152 μm (wide) × 51 μm (deep) × 2.3 cm (long)] and microtee (Upchurch Scientific, USA), submerged in a solid CO_2/ether ice bath ($-100\,°C$), the authors investigated the deprotonation of 4-methyl-5-phenyl-3-propionyloxazolidin-2-one **43**, using NaHMDS **44** (in anhydrous THF) within a T-reactor. The *in situ* generated enolate **45** was subsequently reacted with benzyl bromide **46** and the reaction products collected at room temperature where immediate quenching was employed. Analysis of the resulting reaction mixture, by GC–MS, enabled the conversion of **43** to diastereomers **47** and **48** to be assessed and the ratio of diastereomers quantified.

Using a total flow rate of $30\,\mu l\,min^{-1}$, the authors obtained 41% conversion to **47** and **48** and a diastereoselectivity of 91:9 (**47**:**48**), with 59% residual *N*-acyl oxazolidinone **43**. In an analogous batch reaction, conducted at $-100\,°C$, the diastereomers **47** and **48** were obtained in an overall yield of 68% and a ratio of 85:15 (**47**:**48**); however, 10% decomposition to afford **49** was observed (Scheme 15).

Consequently, by increasing control over the reaction temperature the authors were able to enhance the diastereoselectivity of the reaction and remove the decomposition pathway observed in batch. The authors acknowledge that further work is required to optimize the deprotonation
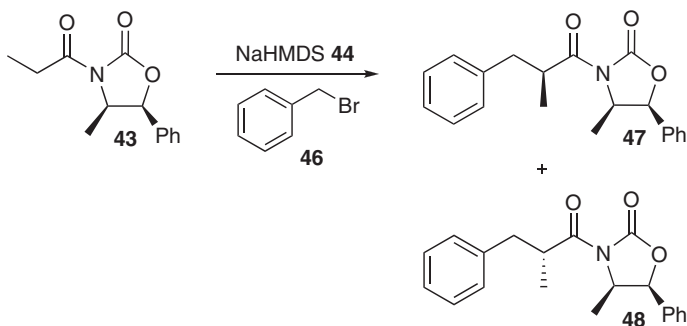
Scheme 14 The alkylation of *N*-acyl oxazolidinone **43** to afford diastereomers **47** and **48** investigated under continuous flow at $-100\,°C$.
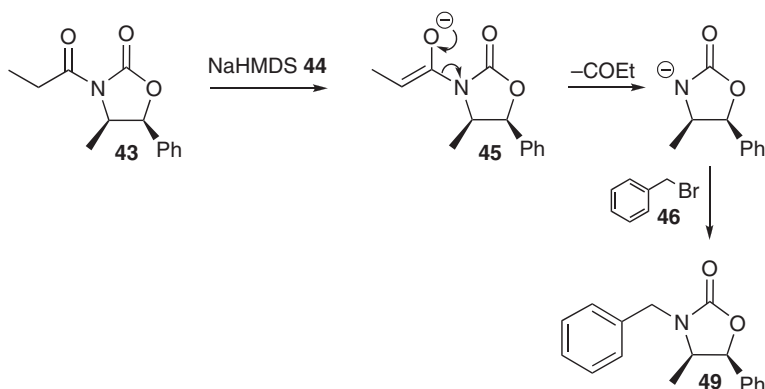
Scheme 15 The decomposition of enolate **45** observed when the reaction is conducted under batch conditions.

step in order to increase the conversion of **43** to **47**/**48**; however, the technique effectively demonstrated the ability to perform temperature-sensitive reactions in microfabricated reactors.

More recently, Matsuoka et al. (2006) reported the ability to supercool fluid streams within octadecylsilane-treated Pyrex microchannels, demonstrating a link between channel dimensions and the freezing point of water which range from −20 to −28 °C as the channel was reduced in width from 300 to 100 μm. Interestingly, a dimension-independent freezing temperature of −15 °C was obtained when bare Pyrex microchannels were employed. Having identified this phenomenon and found it to be independent of flow rate, the authors subsequently investigated the ability to perform asymmetric syntheses within such as system and employed the reaction depicted in Scheme 16 as a model.

Employing a biphasic reaction mixture comprising of the phase transfer catalyst (S,S)-3,4,5-trifluorophenyl-NAS bromide in aq. KOH and an organic phase containing the imine **50** and benzyl bromide **46**, the authors investigated the effect of reaction temperature on the product **51** ratio obtained. Using an untreated microchannel with dimensions of 100 μm (wide) × 40 μm (deep) × 0.6 cm (long), segmented two-phase flow was
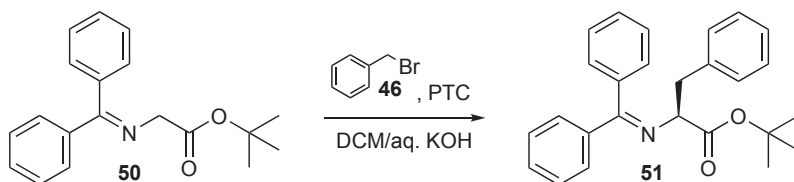
Scheme 16 Model reaction used to illustrate the application of supercooled microflows in asymmetric synthesis.

observed and the authors found that as the reaction temperature decreased from 20 to $-20\,°C$, the enantiomeric excess (*ee*) increased from 43 to >50%. Using supercooled microflow, the authors were able to evaluate the effect of reaction temperatures inaccessible within a batch reactor, whereby freezing of the aq. KOH phase was observed at $4\,°C$. Whilst the authors note that further increases in *ee* are required if the methodology is to be of widespread synthetic utility, the technique represents a means of accessing reaction conditions that are unattainable through the use of conventional bulk processes.

Another example where reactions needed to be conducted at moderately low temperatures $(0–20\,°C)$ was the continuous flow synthesis of oligosaccharides reported by Carrel et al. (2007) which built on previous experience gained through the synthesis of disaccharides (Flogel et al., 2006; Geyer and Seeberger, 2007; Ratner et al., 2005). In an extension to this project, the researchers demonstrated the synthesis of a homotetramer **52** using iterative glycosylations under continuous flow (Scheme 17). In order to optimize the reaction conditions required for the glycosylation steps, the authors introduced a solution of the nucleophile into the reactor from inlet 1, glycosyl phosphate **53** (2.0 eq.) from inlet 2 and the activator, trimethylsilyl trifluoromethanesulfonate (TMSOTf) **54** (2.0 eq.), from inlet 3. Employing a deprotective quench, consisting of piperidine **55** (25% in DMF) and tetra-*n*-butylammonium fluoride (TBAF) **56**, the effect of conducting the reaction over a range of residence times (10 s to 10 min) and temperatures (0 and $20\,°C$) was investigated.
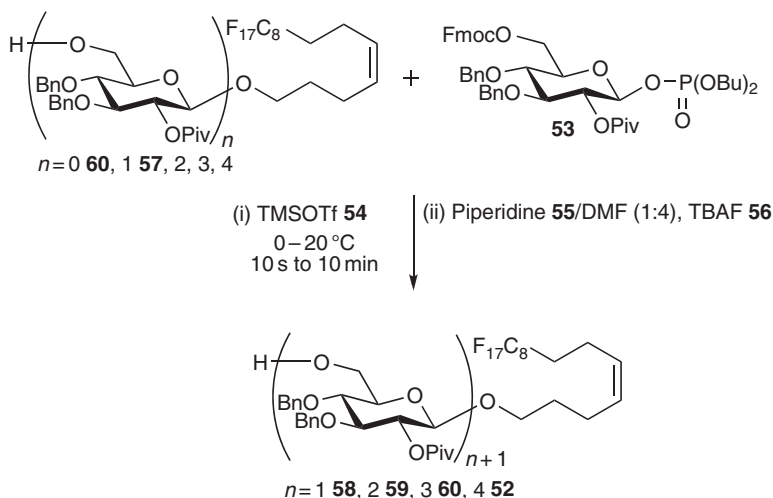

Scheme 17   General reaction scheme illustrating the iterative steps used to synthesize the β-(1 → 6)-linked ᴅ-glucopyranoside homotetramer **52**.

Using this approach, the authors identified a residence time of 30 s and a reaction temperature of 20 °C to be optimal for the synthesis of mono-glycoside **57** (99% yield), which represented an improvement on conventional reaction conditions where reaction times were of the order of 30 min and temperatures typically −78 to −40 °C. After fluorous solid-phase extraction and treatment with silica gel, the monoglycoside **57** was subsequently reacted with glycosyl phosphate **53** to afford the respective disaccharide **58**, in 97% yield, with a residence time of 20 s at 20 °C. Up to this point, the residual starting material was detected within the reaction product; consequently, the authors increased the proportion of glycosyl phosphate **53** from 2.0 to 3.0 eq. and TBAF **56** from 1.5 to 2.0 eq., which resulted in complete conversion to the trisaccharide **59** (90% yield) in conjunction with a residence time of 60 s. The final step of the reaction involved the glycosylation of the previously prepared trisaccharide **59** to afford the tetrasaccharide **52**; again a residence time of 60 s was required to afford the desired product in 95% yield. Upon scaling this process, the authors successfully attained a throughput of 11.3 mmol day^{-1} for monosaccharide **57** from fluoroalkenol **60**.

2.3 The use of toxic or hazardous reagents

In addition to reactant/intermediate instability preventing the use of certain synthetic routes on a large scale, the toxicity of reagents can also precludes the use of certain transformations on a production scale. On the grounds of safety, the use of toxic or hazardous reagents and radical-based reactions are avoided due to problems associated with reaction control. As such, to date, the industry has overcome these problems through the use of alternative reagents and reaction pathways; however, *via* novel reaction methodology these reagents and techniques can be used safely and efficiently.

With this in mind, Odedra et al. (2008) evaluated the use of tris(trimethylsilyl)silane **61** as an effective reducing agent, replacing the highly toxic reagent tin hydride, for the removal of various functional groups using a glass microreactor. Building on synthetic methodology, recently reviewed by Chatgilialoglu (2008), the researchers evaluated the use tris(trimethylsilyl)silane **61** in a glass microreactor for safe and facile radical-based reductions (Scheme 18). A typical continuous flow deoxygenation/dehalogenation involved the introduction of a premixed solution of tris(trimethylsilyl)silane **61** and azobisisobutyronitrile (AIBN) **62** (1.20 M and 10 mol%, respectively) from one inlet and a solution of the substrate (1.00 M) from a second inlet. Employing a glass microreactor whereby the outlet was coupled to a back-pressure regulator (BPR), enabled the authors to superheat the reaction solvent (toluene), thus promoting the reaction without the need to employ chlorinated or toxic
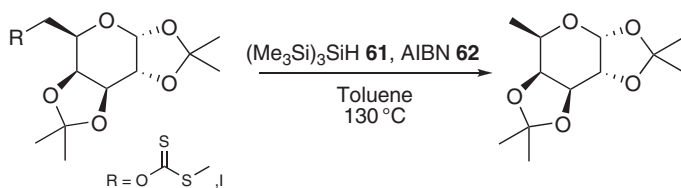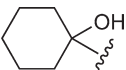
Scheme 18 Examples of the tris(trimethylsilyl)silane **61**-mediated deoxygenation and dehalogenation reactions conducted under continuous flow.

solvent systems. Using this approach the authors evaluated the generality of the flow methodology, reporting isolated yields ranging from 70 to 94% for the radical-mediated deoxygenation reactions and 67–98% for the dehalogenations.

In addition to the seven deoxygenation and dehalogenation reactions demonstrated, the authors adapted the methodology to the hydrosilylation of a series of alkynes and alkenes. To conduct such reactions, a premixed solution of the alkyne or alkene (1.00 M), tris(trimethylsilyl) silane **61** (1.2 M) and AIBN **62** (10 mol%) in toluene was passed through the heated microreactor (130 °C) at a flow rate of $200 \, \mu l \, min^{-1}$, affording a residence time of 5 min.

As Table 5 illustrates, compared to batchwise reactions the increased heat and mass transfer obtained within the microfluidic reactor afforded enhanced *cis/trans* selectivity for reactions employing alkynes and more generically a dramatic reduction in reaction time (cf. conventional batch reactions).

Table 5 Summary of the results obtained for the continuous flow hydrosilylations using tris(trimethylsilyl)silane **61**

R	Z:E Ratio[a]	Yield (%)[b]
Ph **32**	98:2 (84:16)[c]	96 (88)[c]
n-C$_6$H$_{13}$	77:23	91
	11:89	94

[a]Z:E ratio determined by ^{1}H NMR spectroscopy.
[b]Isolate yield.
[c]Literature value.

2.3.1 Fluorinations

With an increasing number of pharmaceutical agents containing fluorinated moieties, due to an observed enhancement in metabolic stability (cf. protonated analogs), the need for fluorinated precursors for use in drug discovery programs and subsequently in active pharmaceutical ingredient (API) production is ever rising. Owing to their rarity in nature, efficient synthetic protocols are required in order to access such fluorinated precursors; of the synthetic transformations available to the modern organic chemist, elemental fluorine (F_2) **63** and the nucleophilic fluorinating agent diethylaminosulfur trifluoride (DAST) **64** are the most extensively used. Unfortunately, DAST **64** is widely viewed as being too hazardous to employ on a large scale due to its tendency to detonate at temperatures in excess of 90 °C; as such, this powerful fluorinating agent currently fails to fulfill its synthetic potential.

Owing to the highly exothermic nature associated with converting a C–H bond to a C–F bond using elemental fluorine, the transformation has been long considered too dangerous to carry out on a large scale. However, the technique is of great synthetic utility, and as such a significant amount of research has been undertaken into conducting direct fluorination under continuous flow (Chambers et al., 2008).

In a thin-film nickel reactor, Chambers et al. (Chambers and Spink, 1999, 2001, 2005) demonstrated biphasic fluorination of a range of compounds, such as ethyl acetoacetate **65**. Employing 10% elemental fluorine **63** in a nitrogen carrier gas, the authors demonstrated a facile route to the selective preparation of the monofluorinated diketone, 2-fluoro-3-oxo-butyric acid ethyl ester **66**, with only small quantities of the product undergoing further fluorination to afford 2,2-difluoro-3-oxo-butyric acid ethyl ester **67** (Scheme 19). The group subsequently reported the fluorination of compounds such as nitrotoluene and ethyl-2-chloroacetoacetate, again demonstrating reaction control leading to excellent conversions and selectivities. As an extension to this, Chambers et al. recently published a manuscript detailing the successful scale-out of their reactor, whereby 30 reaction channels were operated in parallel. Using this approach, enabled the efficient heat transfer and gas/liquid mixing obtained in a single channel to be maintained and provided a safe alternative to hazardous batchwise fluorinations.
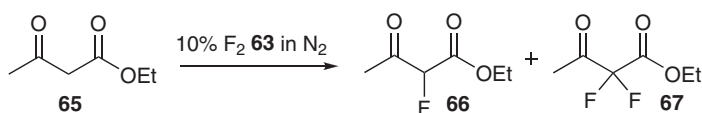
Scheme 19   Selective fluorination of a β-diketoester using elemental fluorine.

Gustafsson et al. (2008a) demonstrated a facile approach to the fluorination of a series of alcohols, carboxylic acids, aldehydes, and ketones harnessing the synthetic utility of DAST **64** in a polytetrafluoroethylene (PTFE)-based flow reactor, with an internal volume of 16.0 ml. Employing a 75 psi BPR, the authors were able to access reaction temperatures above the boiling point of the solvent under investigation. To conduct a reaction, the reactant and DAST **64** were introduced from separate inlets and mixed using a T-mixer, prior to entering the reaction channel, where a solution of sat. $NaHCO_3$ (aq.) was then introduced, after the BPR to quench the reaction mixture prior to collection of the reaction products. Upon investigating the deoxyfluorination conditions in a range of solvents, including toluene and THF, the authors rapidly identified dichloromethane (DCM) as the best solvent to use. Employing a reactor temperature of 70 °C, coupled with 1.0 eq. of DAST **64**, for the deoxyfluorination of alcohols and 2.0 eq. when using substrates containing a carbonyl moiety; the effect of reactant residence time was evaluated (8–32 min).

The authors quickly identified 16 min as being the optimum residence time and as Table 6 illustrates, under the aforementioned conditions an array of fluorinated materials were synthesized in moderate to excellent yield following an aqueous extraction and purification via column chromatography on silica gel. In addition to the array of deoxyfluorinations successfully demonstrated, the authors also evaluated the ease of performing halogen exchange, synthesizing an acyl fluoride from an acyl chloride in 80% yield.

In addition to the use of elemental fluorine **63** and DAST **64**, Miyake and Kitazume (2003) demonstrated the introduction of fluorine into a series of small organic compounds via trifluoromethylation of carbonyl compounds (Table 7), Michael addition (Scheme 20a), and Horner–Wadsworth–Emmons (Scheme 20b) reactions.
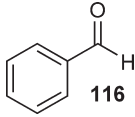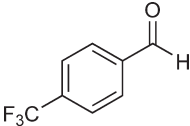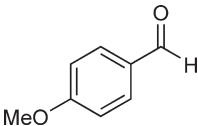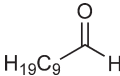
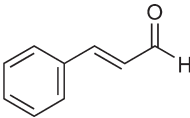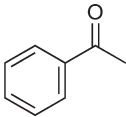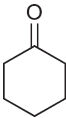Employing a glass microreactor, with channel dimensions $= 100 \, \mu m$ (wide) $\times 40 \, \mu m$ (deep) and 8.0 cm (long), the authors investigated the trifluoromethylation of an array of aldehydes and ketones (Table 7). To perform a reaction, a solution of aldehyde/ketone (1.5 M) and trifluoromethyl(trimethyl)silane **68** (2.25 M) in THF was introduced into the microreactor from one inlet and a solution of TBAF **55** in THF from a second inlet affording a total flow rate of $1.0 \, \mu l \, min^{-1}$ and reaction time of 20 s. All microreactions were conducted at room temperature and the reaction products collected off-line in aq. HCl (1.0 N) prior to extraction of the trifluoromethylated products into diethyl ether. The resulting reaction mixtures were subsequently analyzed by ^1H and ^{19}F nuclear magnetic resonance (NMR) spectroscopy in order to determine the reaction yield. Using the aforementioned protocol, the authors were able to obtain the target trifluoromethylated alcohols in excellent yields when employing aromatic and aliphatic aldehydes (63–89% yield) as precursors; however,

Table 6   A selection of the substrates fluorinated by Gustafsson et al. (2008a) using a PTFE reactor

Substrate	Product	Yield (%)[a]
		70[b]
		61[c]
	(α:β 5:4)	89
	(α:β 1:4)	100
		100
		81
		89
		100

[a]Isolated yield.
[b]5:1 mixture of diastereomers.
[c]6:1 mixture of diastereomers.

Table 7 Summary of the results obtained for the continuous flow trifluoromethylation reactions of carbonyl-containing compounds

$$R-CHO + CF_3SiMe_3\ \textbf{68} \xrightarrow[THF]{TBAF\ \textbf{55}} \xrightarrow{H^+} R-CH(OH)-CF_3$$

Substrate	Microreactor	Batch reactor
	Yield (%)[a]	Yield (%)[a]
![benzaldehyde] **116**	89	76[b]
F_3C-benzaldehyde	83	97[b]
MeO-benzaldehyde	63	–
$H_{19}C_9$-CHO	74	–
cinnamaldehyde	12	–
acetophenone	42	–
cyclohexanone	7	–

[a]Yields determined by ^{19}F NMR spectroscopy.
[b]Batch reaction (5 h).

reactions of ketones afforded poor to moderate yields (7–42% yield). The authors were also pleased to find that the microreactions afforded comparable yields to those obtained under conventional batch conditions employing reaction times of 20 s compared to 5 h (Table 7).
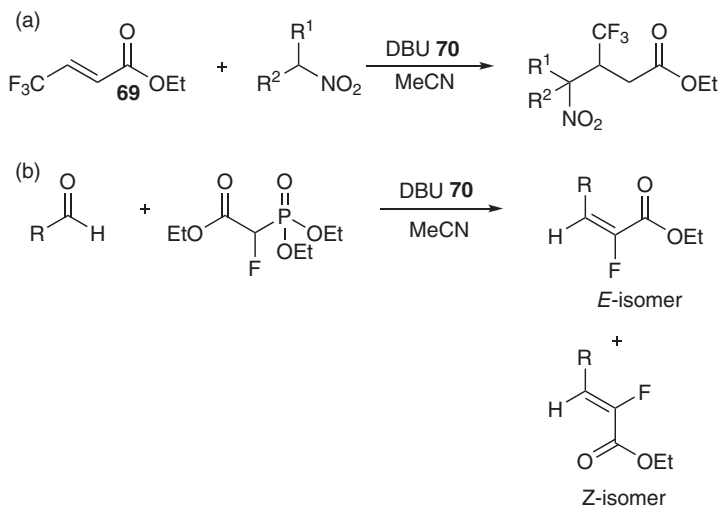
Scheme 20 A selection of the reactions investigated by Miyake and Kitazume (2003) for the incorporation of fluorine into small organic molecules (a) Michael addition and (b) Horner–Wadsworth–Emmons.

Based on previous success with the Michael addition of CF_3-containing acrylates in batch, Miyake and Kitazume (2003) and coworkers subsequently investigated the reaction under continuous flow as a means of rapidly generating a series of synthetically useful fluorinated alkanes (Scheme 20a). Again employing a reaction time of 20 s, the target compounds were obtained in isolated yields ranging from 80 to 93% which compared favorably with the results previously obtained in batch whereby yields of 90–99% were obtained with a reaction time of 30 min. In a final example, the authors reported the Horner–Wadsworth–Emmons reaction of a series of aldehydes (1.7 M) with triethyl-2-fluoro-2-phosphonoacetate **69** (2.6 M), in the presence of 1,8-dizabicycloundec-7-ene (DBU) **70**, to afford a series of α-fluoro-α,β-unsaturated esters, as illustrated in Scheme 20b. Employing dimethoxyethane (DME) as the reaction solvent and a total flow rate of 1.0 µl min^{-1}, the reaction products were collected off-line in aq. HCl (1.0 N) prior to extraction of the organics into diethyl ether. Upon removal of the solvent, the residue was analyzed by ^{19}F NMR spectroscopy and the yields determined using benzotrifluoride as an internal standard. The stereochemistry of the reaction products was confirmed by ^{1}H NMR coupling constants and the chemical shifts of the olefinic protons. Using this methodology, the authors successfully synthesized the target compounds in moderate to excellent yields; see Table 8, reporting analogous stereoselectivities to those obtained in a conventional batch reactor.

Table 8 Comparison of the stereoselectivities obtained in batch and a microreactor for the Horner–Wadsworth–Emmons reaction

R	Microreactor	Batch reactor
	Yield (%)[a]	Yield (%)[b]
C_6H_5	78	>99
	(77:23)[c]	(70:30)
4-$CF_3C_6H_4$	88	86
	(68:32)	(64:36)
4-$MeOC_6H_4$	58	>99
	(74:26)	(76:24)
n-Nonyl	81	66
	(64:36)	(64:36)

[a]Yields determined by ^{19}F NMR spectroscopy.
[b]Isolated yields, batch reaction conducted for 30 min.
[c]The number in parentheses represent the *Z:E* ratio, determined by ^{19}F NMR spectroscopy.
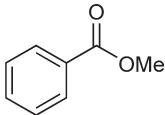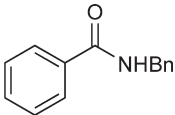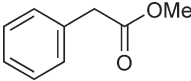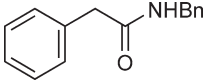
2.3.2 Trimethylaluminum
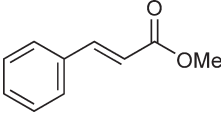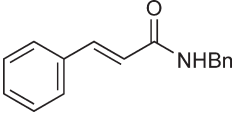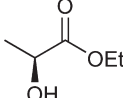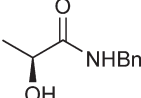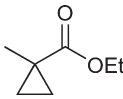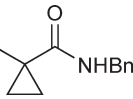
The pyrophoric nature of trimethylaluminum ($AlMe_3$) **71** and the instability associated with the aluminum–amide intermediates make $AlMe_3$ **71** difficult to handle safely at scale, as such its use is precluded for the large-scale synthesis of amides. The ease of reactant manipulation obtained through the use of microreactors, however, affords the potential to use such reagents for the continuous flow synthesis of amides, providing a practical route to their use in large-scale production. Performing reactions on an 8.0 mmol scale, later increased to 0.2 mol, Ponten et al. (2008) demonstrated the continuous flow synthesis of an array of amides, derived from a series of methyl or ether esters and benzylamine **20**; attaining excellent isolated yields as illustrated in Table 9.

In addition to the examples provided, the authors also demonstrated the use of anilines and aliphatic amines as substrates, reporting isolated yields ranging from 65 to 98% (see Section 3), whereby this methodology is demonstrated for the synthesis of the pharmaceutically important molecules rimonabant (**72**) and efaproxiral (**73**) (Schemes 65 and 66, respectively).

2.3.3 The use of butyllithium in microreactors

The reaction of organolithium compounds with carbon-based electrophiles represents one of the most useful synthetic methodologies for the formation of C–C bonds; as such, several groups have investigated these reactions in microstructured devices.

Table 9 A selection of the trimethylaluminum-mediated reactions conducted under continuous flow

Ester	Product	Yield (%)
		96
		98
		95
		70
		86

An early example of an investigation into the use of *n*-BuLi **74** under continuous flow conditions was demonstrated by Schwalbe et al. (2004) and involved the *in situ* generation of C_2F_5–Li **75** and its subsequent nucleophilic addition to benzophenone **76** as depicted in Scheme 21.
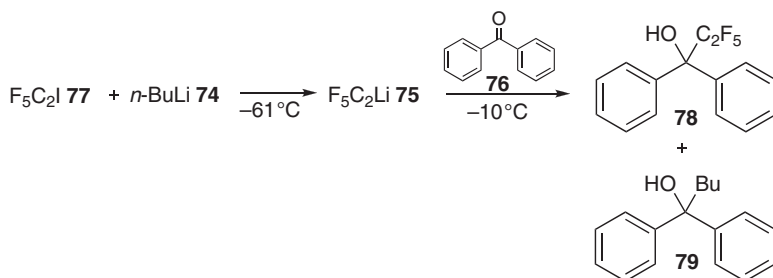
Scheme 21 Demonstration of the *in situ* generation of a short-lived organometallic species **75** and its nucleophilic addition to benzophenone **76**.

Employing a two-stage microreactor, the authors were able to conduct the first step and second steps of the reaction at different temperatures, -61 and $-10\,°C$, respectively, using two external cooling baths. To perform a reaction, solutions of *n*-BuLi **74** (0.82 M in hexane) and C_2F_5I **77** (0.75 M in DCM) were pumped into the reactor at a flow rate equivalent to a residence time of 4 min. A solution of benzophenone **76** (0.62 M) in DCM was then introduced into the second reactor and a residence time of 17 min employed. The reaction products were collected prior to performing an off-line aqueous extraction and the reaction products analyzed by GC. Employing the aforementioned reaction conditions, the authors were able to obtain the target product **78** in 51% yield, representing an increase of 37% (cf. batch reactions). The authors did however report the formation of a competing side product **79** (35%) attributed to incomplete halogen–lithium exchange in the first stage of the reaction. The reaction nonetheless illustrated the use of conventionally hazardous reagents under continuous flow, along with the feasibility of conducting serial reaction steps at different temperatures.

A recent example reported by Goto et al. (2008) exploited the high rate of halogen–lithium exchange to enable the coupling of fenchone (**80**) and 2-bromopyridine **81** in a single step, compared to the more conventional two-step procedure (Scheme 22). Using this approach, it was proposed that the rapid bromine–lithium exchange could be performed chemoselectively, in the presence of a trapping agent such as a ketone. To evaluate this hypothesis, the authors selected the alkylation of the pyridinoalcohol (fenchone) (**80**) with 2-bromopyridine **81** as a model reaction and employed a stainless-steel flow reactor, comprising of a 2 ml microreactor cell and a 15 ml residence time unit. To perform a reaction, *n*-BuLi **74** (0.5–1.0 M) in hexane was added to a solution of fenchone (**80**) (0.5–1.0 M) and 2-bromopyridine **81** (0.46 M) in anhydrous THF at a flow rate of $5\,ml\,min^{-1}$. Maintaining the reactor at $-25\,°C$, the authors evaluated the effect of reactant stoichiometry on the reaction at a fixed residence time of 3 min. The reaction mixture was collected in ice–H_2O to quench the reaction and the organic material extracted into ether prior to analysis by GC–MS and ^1H NMR spectroscopy.
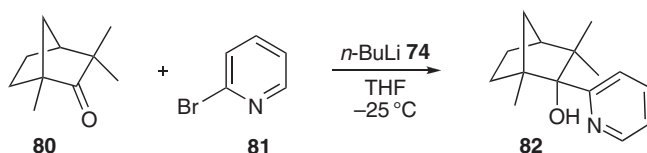
Scheme 22   Model reaction used to demonstrate the one-step coupling of fenchone (**80**) and 2-bromopyridine **81**.

Table 10 Illustration of the optimization strategy used for the one-step coupling of fenchone (**80**) and 2-bromopyridine **81** in a flow reactor

Fenchone (**80**): Halide **81**:*n*-BuLi **74**	Temperature (°C)	Yield (%)[a]
1:1:1	−25	56
2:1:1.5	−25	71
2:1:2	−25	91
2:1:1.5	0	68

[a]Isolated yield.

As Table 10 illustrates, using this approach the authors were able to rapidly optimize the reaction conditions, obtaining the target **82** in 91% yield when employing 2 eq. of fenchone (**80**) and *n*-BuLi **74**. In all cases only a single diastereomer was observed and the authors found that conducting the reaction at 0 °C resulted in a mere 3% reduction in yield. Furthermore, the reaction conditions were found to be suitable for a range of aliphatic/aromatic ketones and brominated compounds.

Nagaki et al. (2009) recently demonstrated the use of a microflow reactor for the *in situ* preparation of an oxiranyl anion derived from styrene oxide **83** and *sec*-BuLi **84**. As Table 10 illustrates, the authors evaluated the preparative synthesis of a series of substituted epoxides, by reacting 1,2-epoxyethylphenyllithium **85** with a series of electrophiles in a microflow system comprising of two T-mixers and two microtube reactors. The generation of 1,2-epoxyethylphenyllithium **85**, from styrene oxide **83** (0.10 M, 6.00 ml min^{-1}) and *sec*-BuLi **84** (0.75 M, 1.92 ml min^{-1}), was conducted in the first micromixer and was followed by trapping with MeI **86** (0.45 M, 3.84 ml min^{-1}) in the second mixer. Using this approach, the authors investigated the effect of temperature (−78 to −48 °C) and residence time (1–25 s) on the generation of intermediate **87** and subsequently the formation of 2-methyl-2-phenyloxirane.

Conducting reactions at −48 °C, the formation of oxirane occurred rapidly, indicating that the deprotonation of styrene oxide **83** is rapid; however, this was accompanied by decomposition of the oxiranyl anion **87**. Reducing the reactor temperature to −78 °C, the anion **87** was found to be stable for up to 25 s, enabling efficient reaction with a series of electrophiles to afford the respective substituted epoxide in high yield, as illustrated in Table 11.

Nagaki et al. (2008) also demonstrated the use of *sec*-BuLi **84** in a microflow system for the anionic polymerization of styrene **88**, as a means of attaining a high degree of control over the molecular weight distribution of the resulting polymer. Employing a solution of styrene **88** (2.0 M) in THF and *sec*-BuLi **84** (0.2 M) in hexane and a tubular reactor

Table 11 Summary of the reaction products generated via the deprotonation of styrene oxide **83** in a microflow reactor ($R_T = 24$ s, $-78\,^{\circ}$C)

Electrophile	Product	Yield (%)[a]	Throughput (g h^{-1})
MeI **86**		88	4.2
Me$_3$SiCl		72	5.0
Benzaldehyde **116**		84[a]	6.8
Acetophenone		70[b]	6.1
Benzophenone **76**		82	9.0

[a]Diastereomer ratio 82:18.
[b]67:33, as determined by ^{1}H NMR.

[250 μm (i.d.) $\times$ 50 cm (long)], the effect of reactor temperature (24 to $-78\,^{\circ}$C) on molecular weight (M_n) and molecular weight distribution (M_w/M_n) was initially investigated. As Table 12 illustrates, the M_n of the resulting polymer was directly linked to the reactor temperature and excellent M_w/M_n were obtained in all cases.

Table 12 Effect of molecular weight (M_n) and molecular weight distribution (M_w/M_n) when conducting anionic polymerizations under continuous flow

| Temperature (°C) | Flow Rate (ml min^{-1}) | | M_n | M_w/M_n |
	sec-BuLi **84**	Styrene **88**		
24	2.0	6.0	3400	1.10
0	2.0	6.0	3300	1.08
−28	2.0	6.0	3600	1.07
−48	2.0	6.0	3700	1.08
−78	2.0	6.0	4000	1.43

Employing a microreactor temperature of 0 °C, the authors demonstrated a linear relationship between the monomer **88** and initiator **84** ratio, enabling a specific molecular weight polymer to be prepared with ease. Based on these observations, the authors went on to evaluate the end functionalization of the polymers using a series of silanes such as chlorodimethylvinylsilane, with the investigation concluded with block copolymerization using functionalized polymers with different end groups. Using this approach, the authors were able to attain a high level of molecular weight distribution under relatively high reaction temperatures (0−24 °C), opening up the opportunity to prepare structurally well-defined polymers, copolymers, and block copolymers.

Using a stainless-steel micromixer coupled to a residence time unit, Tietze and Liu (2008) reported the development of a continuous flow process for the synthesis of an aminonaphthalene derivative, which is a precursor in the synthesis of novel anticancer agents. A key reaction in the compounds synthesis was the nucleophilic substitution reaction, illustrated in Scheme 23, to afford the phosphonosuccinate **89**; see Section 3 for details of the total synthesis achieved utilizing a series of microreaction steps. Prior to evaluating the use of *n*-BuLi **74** for the continuous flow process, the authors investigated the use of NaH **90** and organolithium bases such as lithium diisopropylamide (LDA) in batch where isolated yields of 70–91% were obtained after <24 h. The relative insolubility of the by-product NaBr precluded the use of NaH **90** in the continuous process; however, the increased solubility of LiBr meant that organo-lithium bases had potential to be employed in the system. Of the bases investigated, *n*-BuLi **74** was found to yield the most homogeneous solution and was subsequently employed in the microreactor, affording 70% yield of the phosphonosuccinate, ethyl 2-(diethoxyphosphoryl)acetate **89**, with a residence time of 24 min and a reactor temperature of 40 °C; representing a 13% increase in yield compared to analogous batch reactions conducted over 36 h.

2.3.4 Nitrations

The nitration of aromatics is often a rapid and exothermic process which frequently requires dropwise addition of the nitrating solution in order to prevent rapid evolution of heat, which can lead to undesirable
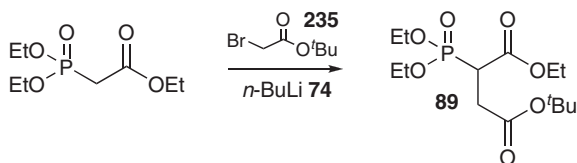

Scheme 23 Synthesis of intermediate **89** used in the preparation of gram quantities of an aminonaphthalene derivative **91**.

decomposition of the target compound and even thermal runaway. As such, the nitration of aromatics was one of the early miniaturized reactions to be reported, with Burns and Ramshaw (2002) investigating the use of a stainless-steel continuous flow reactor for the nitration of benzene **92** and toluene **93** using two-phase slugs of organic and aqueous reactants.

Ducry and Roberge (2005) subsequently reported the autocatalytic nitration of phenol **94** within a glass microreactor [$10 \times 500\,\mu m$ (wide) channels, internal volume $= 2.0$ ml] and evaluated the effect of reactant stoichiometry on the ratio of products obtained (Scheme 24). Employing a phenol **94** solution (6%) in CH_3CO_2H (6%) and water (71%) (feed 1) and a 65% HNO_3 **95** solution (feed 2), the ratio of feedstocks was varied between 3.9:1 and 2.3:1 which corresponded to 1.1–1.8 equivalents of HNO_3 **95**. Using this approach, the effect of reaction temperature was also evaluated and it was observed that at $55\,^{\circ}C$, autocatalysis started immediately, at $45\,^{\circ}C$ a 1 min delay was observed, and at lower temperatures, autocatalysis did not start. Through the use of a continuous flow process, the authors reported a reduction in the formation of polymeric side products (up to 70% in batch), an overall increase in product purity, and higher yields than were obtained within a batch reaction.

Employing a micromixer (T-mixer, $800\,\mu m$) and a stainless-steel reaction tube [$1,380\,\mu m$ (i.d.) $\times 12$ m (long)] Kulkarni et al. (2008) investigated the aromatic nitration of salicylic acid **101** under continuous flow. Using a reactant feedstock of salicylic acid **101** in acetic acid **6** (1:16) and nitric acid **95**, reactions were conducted at $20\,^{\circ}C$ and the effect of residence time evaluated. To ensure that the results obtained were indicative of the reaction occurring within the microreactor, the reaction products were collected in a vial, stored within an ice bath, and unreacted HNO_3 **95** quenched with urea and MeOH prior to analysis of the supernatant by HPLC. Using this approach, the authors were able to prevent the undesirable decarboxylation, to 2-nitrophenol **97**, observing only the formation of the monoinitrated products, 5-nitro-salicylic acid **102** (60%) and 3-nitro-salicylic acid **103** (18%) (Scheme 25). Employing increased reaction
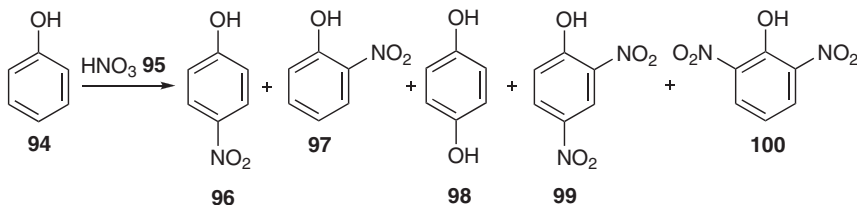
Scheme 24 Summary of the potential reaction products obtained when nitrating phenol **94**, mononitrated phenols **96** and **97**, hydroquinone **98**, and dinitrated phenols **99** and **100**.
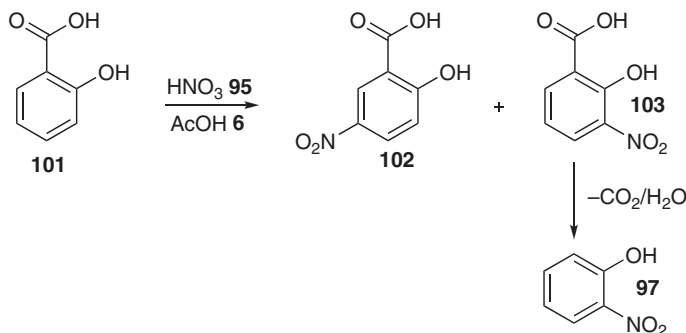
Scheme 25 Possible products obtained from the nitration of salicylic acid **101**.

temperatures the authors observed an increase in the reactions selectivity toward the synthesis of 5-nitro-salicylic acid **102**, obtaining 65% at 50 °C. The nitration of salicylic acid **101** was also the subject of a recent patent, whereby nitrations were conducted in 10–30 s, at 75 °C, within a glass microreactor (Kulkarni, 2007).

DSM recently published details of a collaboration with Corning Incorporated, which resulted in the development of a glass microreactor capable of performing a selective organic nitration, using neat HNO_3 **95**, under cGMP conditions (Scheme 26) (Braune et al., 2008). As nitration reactions are notoriously difficult to perform on a commercial scale, the main challenge was the target production volumes which were in the range of tons day^{-1}. The authors comment that although the reaction enthalpy is moderate, it is the potential exothermic decomposition of the product **104** that is problematic. Side reactions can also arise from oxidation of the starting material **105** and other components of the reaction mixture, as such careful control of the reaction conditions is required.

To perform the organic nitration, the substrate **105** and solvent were brought together in a microstructure that afforded a fine emulsion; this was followed by the addition of neat nitric acid **95** at which point the reaction started immediately. After the reaction had continued for the required time, it was stopped by the addition of water at a reduced temperature, prior to neutralization with NaOH. Neutralization was achieved in managed stages in order to control the release of heat into the reactor. Using this approach, a reactor volume of 150 ml allows the
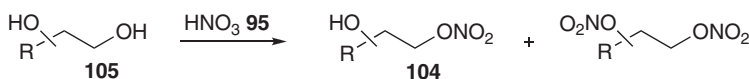
Scheme 26 Selective nitration investigated under flow by DSM using a Corning Incorporated glass reactor.

production of $13\,kg\,h^{-1}$ of **104** with intrinsically high levels of safety unattainable in conventional batch techniques. Having demonstrated the viability of the microreactor, no scale-up steps were required in order to increase the throughput to meet previously discussed targets; the authors simply employed a production unit consisting of eight microreactors (two banks of four microreactors) and the unit operated under the previous conditions. Employing such a system has enabled DSM to produce $100\,kg\,h^{-1}$ **104** providing an annual capacity of 800 tons if operated continuously. The investigation illustrated the ability to safely operate hazardous reactions, attain the desired chemical selectivity, design a predictable and reliable production unit, and prepare high-quality chemicals in a short time frame, all of which was achieved through the use of microreaction technology.

2.3.5 Exothermic reactions

Along with the challenges associated with the handling and use of large volumes of hazardous or toxic materials, the scale-up of exothermic reactions can also be problematic due to the difficulties associated with the efficient removal of heat generated. With this in mind, Schwalbe et al. (2004) evaluated the Paal–Knorr synthesis under continuous flow (Scheme 27). Due to the exothermic nature of the reaction, when adding ethanolamine **106** to acetylacetone **107** in batch, it was necessary to add the reagents over an extended period of time; consequently, even though the reaction was rapid, the dropwise addition of the reactants increased the reaction time considerably. In comparison, performing the reaction in a stainless-steel continuous flow reactor, with a residence time of 5.2 min, the authors were able to employ neat reactants to afford the target pyrrole **108** in 91% yield in a throughput of $260.0\,g\,h^{-1}$.

2.4 The incorporation of catalysts into microreactors

Having demonstrated the many practical advantages associated with the use of miniaturized continuous flow reactors for catalyst free, or homogeneous reactions, the following section focuses on the additional advantages that can be obtained through the use of heterogeneous catalysts, biocatalysts, reagents, and scavengers within such devices.
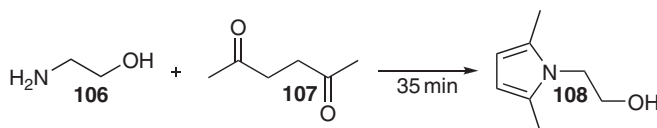

Scheme 27 Exothermic Paal–Knorr reaction conducted in a CYTOS flow reactor.

2.4.1 Base-promoted microreactions

Wiles et al. (2004a, 2007a) demonstrated the incorporation of a series of silica-supported bases into an EOF-based capillary reactor, as a means of increasing the efficiency of the Knoevenagel condensation (cf. conventional batchwise protocols). To conduct a reaction, the solid-supported base was packed into a borosilicate glass capillary [500 µm (i.d.) × 3.0 cm (long)] and held in place by two microporous silica frits. A premixed solution of the aldehyde and ethyl cyanoacetate **109**/malononitrile **110** (1.00 M in MeCN, respectively) was then mobilized through the packed bed, where the base-catalyzed condensation reaction occurred, and the reaction products collected at the reactor outlet in MeCN, prior to off-line analysis by GC–MS. Using this approach, the authors investigated the reactivity of a range of substituted aromatic aldehydes, obtaining conversions in the range of 99–100% and solid-supported catalysts **111–114** (Scheme 28). Compared to traditional stirred or shaken reactors, the use of a continuous flow system proved advantageous as it led to reduced degradation of the solid-supported catalyst, leading to enhanced reagent lifetimes and between run reproducibility.

Having demonstrated the principle using small quantities of catalytic material, typically 5 mg, the authors later demonstrated the ability to generate the aforementioned materials with a throughput ranging from 0.57 to 0.94 g h^{-1} by simply increasing the size of the packed bed employed [3,000 µm (i.d.) × 3 cm (long)].

Employing silica-supported piperazine **113** (0.10 g, 1.70 mmol N g^{-1}), the authors demonstrated the use of EOF for the semipreparative scale synthesis of a series of α,β-unsaturated compounds and as previously observed in the capillary-based reactor, the compounds were obtained in excellent isolated yield and product purity (Table 13).
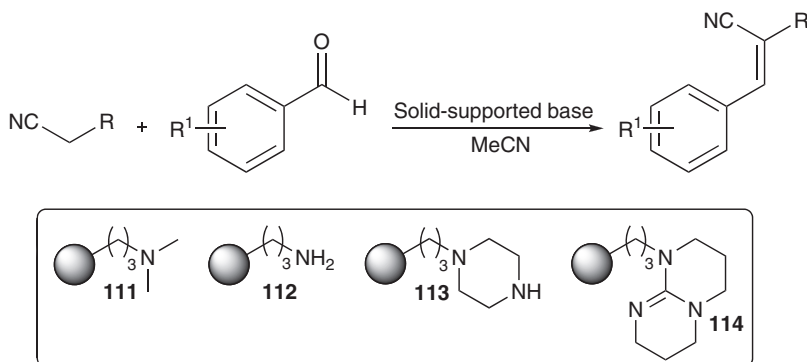
Scheme 28 General reaction scheme illustrating the Knoevenagel condensation conducted using EOF as a pumping mechanism.

Table 13 A selection of the α,β-unsaturated compounds synthesized using a silica-supported base **113** and EOF as the pumping mechanism

R^1	R^2	R^3	R^4	Flow rate ($\mu l\,min^{-1}$)	Yield (g)[a]	Yield (%)
H	H	H	$CO_2C_2H_5$	62.0	0.75	99.7
H	CO_2CH_3	H	$CO_2C_2H_5$	56.1	0.87	99.8
OCH_3	H	OCH_3	$CO_2C_2H_5$	50.1	0.78	99.9
H	OBn	H	$CO_2C_2H_5$	51.1	0.94	99.7
H	Br	H	$CO_2C_2H_5$	55.1	2.30[b]	99.4
H	H	H	CN	62.1	0.57	99.4
H	CO_2CH_3	H	CN	60.4	0.76	98.8
OCH_3	H	OCH_3	CN	55.7	0.71	99.2
H	OBn	H	CN	48.4	0.75	99.4
H	Br	H	CN	48.3	1.70[b]	99.8

[a]Unless otherwise stated, reactions were conducted for 1.0 h.
[b]Reaction conducted for 2.5 h.
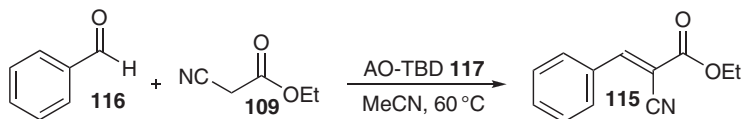
Scheme 29   Model reaction employed by McQuade et al. for the evaluation of an immobilized base **117**.

Bogdan et al. (2007) subsequently investigated the synthesis of (E)-ethyl-2-cyano-3-phenylacrylate **115** (Scheme 29) via the base-catalyzed condensation of ethyl cyanoacetate **109** and benzaldehyde **116** in a tubular reactor [1.6 mm (i.d.) × 10–60 cm (length)] packed with polymer-supported 1,5,7-triazabicyclo[4.4.0]undec-3-ene **117**. Employing a premixed solution of ethyl cyanoacetate **109** and benzaldehyde **116** (0.43 and 0.39 M, respectively), the reactor was heated to 60 °C using a HPLC column heater and the effect of residence time evaluated (25–300 s). Using the aforementioned procedure, the authors found a residence time of 300 s afforded the target compound **115** in 93% conversion and a throughput of 0.2 g h^{-1}.
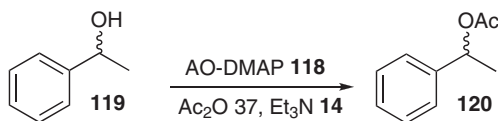
Scheme 30 Evaluation of AO-DMAP **118** as a catalyst for acylation of 2° alcohols.

Having proved the synthetic utility of their system, the authors subsequently evaluated a second supported base, 4-dimethylaminopyridine (AO-DMAP) **118**, toward the acylation of 2° alcohols (Scheme 30). Employing a premixed solution of phenyl-1-ethanol **119**, Et$_3$N **14** and acetic anhydride **37** (0.33, 0.50, and 0.50 M) in hexane, reactions were conducted at room temperature and the effect of residence time evaluated (10–50 s). Using a 60 cm packed bed, the authors were able to obtain near quantitative conversions to **120** employing residence times <20 s, with flow reactions providing superior results to those obtained in analogous batch reactions.

More recently, Costantini et al. (2009) reported a novel technique for the incorporation of an organic base, 1,5,7-triazabicyclo[4.4.0]dec-5-ene (TBD), into silicon microchannels [100 μm (wide) × 100 μm (deep) × 1.03 m (length)] which involved derivatization of a PGMA polymer brush wall coating (150 nm). To assess the catalytic properties of the derivatized polymer brushes, the authors employed the Knoevenagel condensation as a model reaction, using MeCN as the reaction solvent and a reaction temperature of 65 °C (Scheme 31). Using this approach, the authors were able to produce the target condensation product **121** with an hourly output of 7.5×10^{-5} M (using only 2.9×10^{-5} mmol of TBD **122**), with no leaching of the base observed.

Baxendale et al. (2008) reported a bifurcated approach to the synthesis of thiazoles and imidazoles by coupling a glass microreactor and a packed-bed reactor to achieve a base-mediated condensation reaction. As Scheme 32 illustrates, reactions focused on the use of ethyl isocyanoacetate **123**, as the cyanide source, with variations made via the isothiocyanate reagent, as illustrated in Table 13.

Initial investigations employed a reaction temperature of 55 °C and a flow rate of 100 μl min^{-1} with ethyl isocyanoacetate **123** (0.75 M)
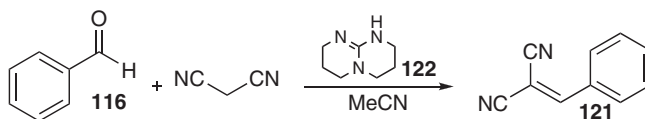
Scheme 31 Model reaction used to demonstrate the catalytic efficiency of derivatized polymer bushes.
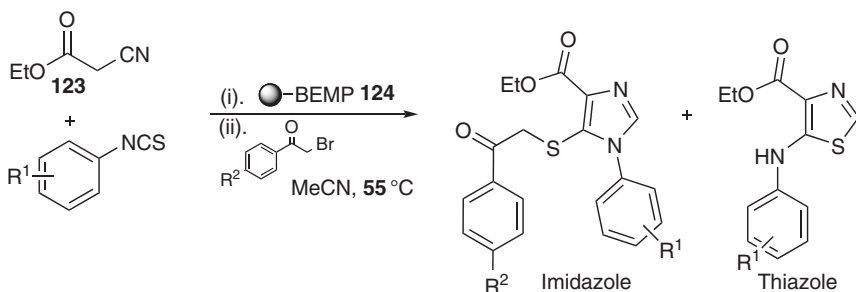
Scheme 32 Schematic illustrating the general reaction conditions employed for the continuous flow synthesis of thiazoles and imidazoles.

4-bromophenylisothiocyanate (0.75 M) reacted in the presence of 2-*tert*-butylimino-2-diethylamino-1,3-dimethylperhydro-1,3,2-diazaphosphorine on polystyrene (PS-BEMP) **124** to afford the target thiazole in excellent purity (95%) but only 58% yield. Assuming that the reminder of the thiazole was trapped on the polymer-supported base **124**, the authors passed a solution of electrophile (0.75 M) through the packed bed to afford a new product, the respective imidazole (38%). Optimal conditions were found to be 1:1 ratio of coupling reagents (0.75 M in MeCN), 1.6 eq. of PS-BEMP **124**, and a flow rate of 50 μl min^{-1} (for each reactant solution employed). Using the aforementioned conditions, the authors evaluated the effect of changing the functionality on the isothiocyanate precursor and as summarized in Table 14, an electronic effect can be seen with methoxy substituents favoring the selective formation of the thiazole.

Table 14 Summary of the results obtained for the continuous flow synthesis of thiazoles and imidazoles

R^1	R^2	Isolated yield		Combined yield (%)
		Thiazole (%)	Imidazole (%)	
4-Cl	OMe	47.5	47.5	95.1
4-Br	Br	53.0	30.0	83.0
4-OMe	H	96.0	4.0	100.0
3-F	Br	68.0	28.0	96.0
3-OMe	Br	84.0	5.0	89.0
2-OMe	H	90.0	7.0	97.0
3,5-CF$_3$	OMe	83.5	10.5	94.0
3,4-Cl	CN	53.0	26.0	79.0

2.4.2 Acid-catalyzed microreactions

Using a similar reaction setup to that reported for the Knoevenagel condensation, Wiles et al. (2005) investigated the acid-catalyzed protection of aldehydes as their respective dimethyl acetal (Scheme 33). Again, reactions were performed by pumping a premixed solution of benzaldehyde **116** and trimethylorthoformate **125** (1.0 and 2.5 M, respectively, in MeCN) through the packed-bed reactor containing Amberlyst-15 **126** $(5.0 \times 10^{-3} \, \text{g}, 4.20 \, \text{mmol} \, \text{g}^{-1})$. Off-line analysis of the reaction products by GC–MS was then used to determine the conversion of aldehyde **116** to acetal **127** and the flow rate adjusted accordingly. Using this approach, dimethoxymethyl benzene **127** was obtained in 99.8% yield (% RSD $= 0.13$, $n = 5$) and a throughput of $2.5 \times 10^{-2} \, \text{g} \, \text{h}^{-1}$. The authors subsequently investigated the synthesis of a series of dimethyl acetals (Table 15), all of which were obtained in excellent yield (>95.4%) and purity, without the need for additional off-line purification.

Using the same reactor, a premixed solution of aldehyde or ketone and dithiol (1.0 M, 1:1) in anhydrous MeCN was passed through the Amberlyst-15 **126** containing packed bed. The reaction products were again collected in MeCN and analyzed every 10 min by GC–MS. Once optimized, the reactions were conducted for 1 h, to produce the required quantity of each 1,3-dithiane or 1,3-dithiolane, the reaction products were then concentrated *in vacuo* and analyzed by ^{1}H NMR spectroscopy (Tables 16 and 17) (Wiles et al., 2007b).
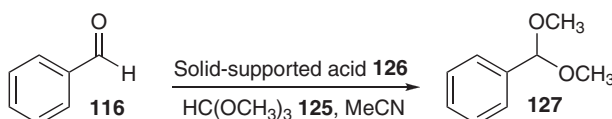
Scheme 33 An example of the protection of an aldehyde **116** as its dimethyl acetal **127** performed using a solid-supported acid catalyst under EOF-driven continuous flow.

Table 15 A selection of the results obtained for the synthesis of dimethyl acetals under continuous flow

Aldehyde	Flow rate (μl min^{-1})	Yield (%)
Benzaldehyde **116**	1.75	99.8
4-Bromobenzaldehyde **134**	1.00	99.9
4-Chlorobenzaldehyde	1.60	99.8
4-Cyanobenzaldehyde	2.00	99.6
2-Naphthaldehyde	1.40	99.8
Methyl-4-formylbenzoate	0.60	99.9
3,5-Dimethoxybenzaldehyde **268**	0.50	98.8

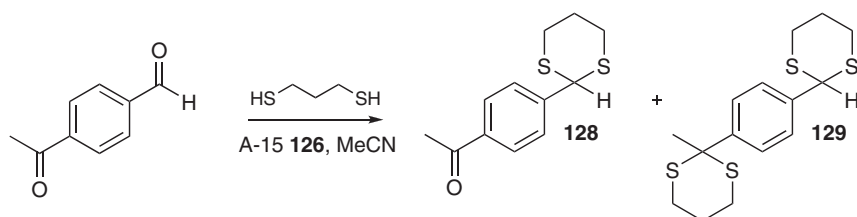**Table 16** A selection of the continuous flow thioacetalizations reported by Wiles and coworkers (2004a)

Aldehyde	n	Flow rate (μl min^{-1})	Yield (%)
Benzaldehyde 116	2	63.7	99.97
	1	63.4	99.97
4-Bromobenzaldehyde 134	2	61.4	99.92
	1	61.2	99.96
4-Chlorobenzaldehyde	2	61.7	99.91
	1	61.9	99.95
4-Cyanobenzaldehyde	2	65.4	99.94
	1	64.6	99.96
4-Benzyloxybenzaldehyde	2	61.1	99.22
	1	60.9	99.93
4-Methylbenzaldehyde	2	69.7	99.97
	1	69	99.93
4-Biphenylcarboxaldehyde	2	63	99.06
	1	63	99.97
2-Naphthaldehyde	2	60.4	99.94
	1	60.2	99.98
2-Furaldehyde	2	67.9	99.92
	1	67.5	99.97
3,5-Dimethoxybenzaldehyde 268	2	67.9	99.91
	1	67.7	99.93

In addition to developing a facile route to the synthesis of thioacetals and thioketals, optimization of the reagents residence time within the packed bed enabled the authors to demonstrate the chemoselective protection of aldehydic functionalities in the presence of ketonic moieties (Scheme 34).

Compared to batch protocols, the flow reaction afforded the target compound **128** in quantitative yield and purity, with no sign of the competing ketal **129** formation. Although the flow reactions proceeded to near quantitative conversion in all cases, should the 1,3-dithiane or 1,3-dithiolane be used in subsequent reaction steps where Pd catalysts are employed for example, it is crucial than no dithiol residues are present. With this in mind, the authors packed a plug of silica gel impregnated

Table 17   A summary of the continuous flow thioketalizations performed using EOF

Ketone	n	Flow rate ($\mu l\,min^{-1}$)	Yield (%)
Acetophenone	2	41.5	99.57
	1	41.3	99.96
Propiophenone	2	40.2	99.97
	1	40.3	99.96
Butyrophenone	2	41.6	99.9
	1	41.6	99.9
Cyclohexanone	2	42.2	99.62
	1	42.1	99.98
Benzophenone **76**	2	40.2	99.81
	1	40.1	99.91
4-Nitroacetophenone	2	40.9	99.95
	1	41	99.95
2-Methoxyacetophenone	2	40.9	99.93
	1	41.9	99.93
4-Chloroacetophenone	2	40.9	99.87
	1	40.8	99.91
4-Hydroxyacetophenone	2	42.2	99.76
	1	42.1	99.83
4-Bromoacetophenone	2	40.2	99.94
	1	40.1	99.97

Scheme 34   Potential reaction products attainable in the protection of bifunctional compounds.

with copper sulfate into the flow reactor in order to scavenge the $<2 \times 10^{-3}\%$ dithiol present in the reaction mixture. As the scavenger turned from blue to yellow upon saturation, exhaustion of the scavenger was self-indicating.
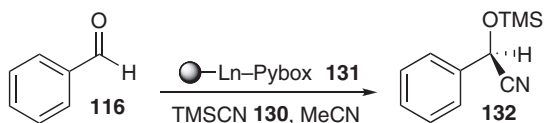
Scheme 35 An example of enantioselective synthesis performed in a packed-bed microreactor.

Another example of a Lewis acid-catalyzed reaction conducted in a miniaturized packed-bed reactor was demonstrated by Lundgren et al. (2004). As Scheme 35 illustrates, the model reaction selected involved the enantioselective addition of trimethylsilyl cyanide (TMSCN) **130** to benzaldehyde **116**. Microreactions were conducted by pumping a premixed solution of benzaldehyde **116** and TMSCN **130**, in MeCN, through a packed bed containing a polymer-supported lanthanide–pybox catalyst **131** under EOF conditions. The reaction products were diluted upon collection with MeCN and analyzed chromatographically, off-line, in order to determine both the conversion and enantioselectivity of the cyanohydrin prepared. Compared to standard batch techniques, this approach proved advantageous as it enabled the enantioselective synthesis of cyanohydrins **132**, without the need for additional extraction steps in order to recover, and potentially reuse, the catalyst from solution. In the same year, the authors also communicated the results of an investigation into the use of a series of additives, this time employing a homogeneous catalyst, for the same model reaction.

More recently Wiles and Watts (2008b, 2008c) reported the fabrication of a borosilicate glass microreactor capable of performing solution-phase syntheses, followed by heterogeneously catalyzed reaction steps and utilized this approach for the multicomponent synthesis of 51 α-aminonitriles. Initial investigations were conducted using a polymer-supported ethylenediaminetetraacetic acid ruthenium (III) chloride (PS-RuCl$_3$) **133** as the catalyst (10 mg, 0.26 mmol g^{-1}). To perform a reaction, the authors reacted a range of aromatic and aliphatic amines (0.4 M in MeCN) with 4-bromobenzaldehyde **134** (0.4 M in MeCN) in a microchannel [150 μm (wide) × 50 μm (deep) × 5.6 cm (long)], the *in situ* synthesized imine (0.2 M) was then mixed with TMSCN **130** (0.2 M in MeCN) prior to passing through the catalyst bed, where the nucleophilic cyanide addition occurred to afford the target α-aminonitrile with throughputs ranging from 17.2 and 25.4 mg h^{-1} (Table 18).

In order to increase the throughput of the system, the authors subsequently investigated the use of an alternative catalyst, polymer-supported scandium triflate (PS-Sc(OTf)$_2$) **135**. As Table 18 illustrates, compared to PS-RuCl$_3$ **133**, the PS-Sc(OTf)$_2$ **135** was found to be a more active catalyst toward the Strecker reaction and afforded the target α-aminonitriles in

Table 18   Comparison of PS-RuCl$_3$ **133** and PS-Sc(OTf)$_2$ **135** catalysts toward the Strecker reaction, conducted under continuous flow

Product	PS-Catalyst	Throughput (mg h^{-1})
	133 135	17.2 34.4
	133 135	18.1 36.1
	133 135	18.9 38.0
	133 135	19.7 39.5
	133 135	32 63.6

34.4–63.6 mg h^{-1}. Having demonstrated the ability to synthesize a series of pharmaceutically interesting α-aminonitriles under continuous flow, the authors used the methodology to prepare a library of 50 compounds, constructed from 10 substituted aldehydes and 5 amines, whereby excellent yields and purities were obtained in all cases.

2.4.3 Metal-catalyzed reactions

As a means of increasing the efficiency of a series of commonly employed C–C cross coupling reactions, including the Suzuki–Miyaura and Heck–Mizoroki, Mennecke et al. (2008) developed an oxime-based palladacycle catalyst and evaluated its coordinative immobilization within a PASSflow (polymer-assisted solution-phase synthesis under flow conditions) reactor. Employing a flow reactor comprising of (polyvinyl) pyridine-coated Raschig rings, functionalized with a palladacycle **136** $(10\,mmol\,Pd\,ring^{-1})$, the authors initially evaluated the Suzuki–Miyaura reaction, as illustrated in Table 19. The reactions were conducted by circulating a solution of aryl bromide (1.00 mmol), boronic acid (1.50 mmol), and cesium fluoride **137** (2.4 mmol) in DMF–H_2O (10:1, 5 ml), through the heated reactor (100 °C) at a flow rate of $2.5\,ml\,min^{-1}$. After a period of 24 h, the reactor was rinsed with DMF–H_2O and the washings diluted with H_2O prior to extraction with ethyl acetate. The resulting reaction products were subsequently purified by flash chromatography on silica gel to afford the target substituted biphenyl in moderate to excellent yield.

In addition to the Suzuki–Miyaura reaction, the authors also found the catalyst **136** to be active toward the arylation of olefins with aryl halides as illustrated in Table 20. Again to conduct a reaction, the authors circulated a solution containing 4-iodoacetophenone **138** (1.00 mmol), the alkene (3.00 mmol) under investigation, and tributylamine **139** (3.00 mmol) in anhydrous DMF (3 ml), through the heated reactor (120 °C) at a flow rate of $2\,ml\,min^{-1}$. After 24 h, the flow reactor was rinsed with DMF and the

Table 19 Summary of the results obtained for the continuous flow Suzuki–Miyaura reaction using an immobilized Pd (II) catalyst **136**
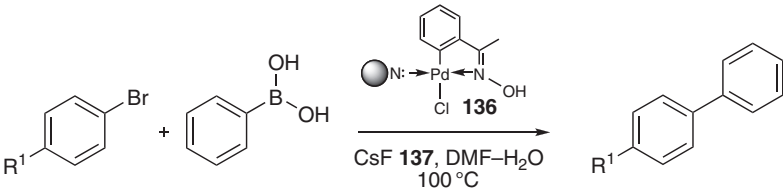

R^1	Residence time (h)	Yield (%)
H	24	89
CH_3	24	56
$COCH_3$	9	91
OCH_3	24	50

Table 20 A selection of the results obtained for the Heck-Mizoriki reaction under continuous flow

| R^1	Residence time (h)	Yield (%)^a
CO$_2$Cy	2	99
CO$_2$t-Bu	4	99
CN	4	97 (5:1)^b

^{a}Unless otherwise stated, only the *E* isomer was isolated.
^{b}The number in parentheses represents the *E/Z* ratio.

reaction products diluted with water prior to extraction into ethyl acetate, to afford the target product in excellent purity.

Using an immobilized salen complex **140**, Annis and Jacobsen (1999) investigated the hydrolytic kinetic resolution of *rac*-4-hydroxy-butene oxide **141**. By simply pumping a solution racemate **141** through a column containing the silica-supported catalyst **140**, the authors were able to generate the desired triol **142** in excellent *ee*, as summarized in Scheme 36. The approach was found to be advantageous compared to those resolutions conducted in analogous batch reactions, as the technique negates the need for laborious purifications in order to isolate the product and recover the catalyst.

In addition to employing packed beds, a small group of researchers have demonstrated the use of wall coating as a means of incorporating heterogeneous catalysts into continuous flow systems. One such example
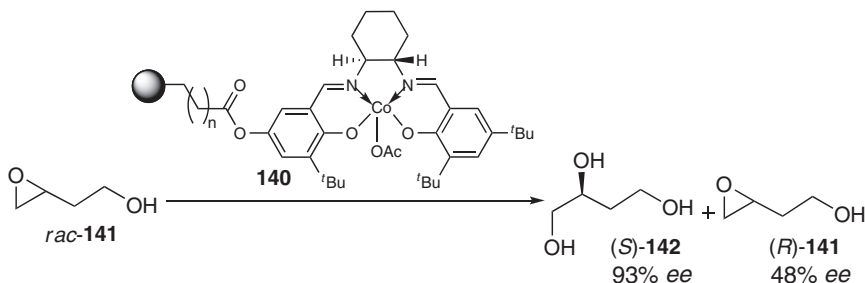
Scheme 36 Kinetic resolution of *rac*-4-hdroxy-1-butene oxide **141**.
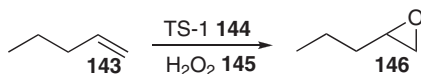
Scheme 37 The use of a wall-coated microreactor in the epoxidation of 1-pentene **143**.

was the epoxidation of 1-pentene **143**, reported by Wan et al. (2002), which was achieved using a microchannel coated with a zeolite layer **144** (Scheme 37). Coating a silicon microchannel [500 μm or 1,000 μm (wide) 250 μm (deep)] with a 3-μm-thick layer of TS-1 zeolite **144**, the oxidation of 1-pentene **143** was investigated in the presence of hydrogen peroxide **145** and afforded epoxypentane **146**. Reducing the channel width to 500 μm, the authors were able to double the conversion to **146** an observation that is attributed to an increase in the surface to volume ratio.

In addition to packed and wall-coated systems, numerous researchers have investigated the fabrication of membranes, within microchannels, in which catalytic material can be incorporated. Employing a protocol developed by Kenis et al. (1999), Uozumi et al. (2006) deposited a poly(acrylamide)-triarylphosphane palladium membrane (PA-TAP-Pd) (1.3 μm (wide), $0.37 \, mmol \, g^{-1}$ Pd) within a glass microchannel [100 μm (wide) × 40 μm (deep) × 1.4 cm (long)]. Once formed, the membrane was used to catalyze a series of Suzuki–Miyaura C–C bond-forming reactions, the results of which are summarized in Table 21.

To perform a reaction, the authors employed two reactant streams, the first contained the aryl iodide (6.3×10^{-3} M) in EtOAc/2-PrOH (1:2.5) and

Table 21 Summary of the results obtained for the Suzuki-Miyaura coupling reactions conducted using an *in situ* fabricated PA-TAP-Pd membrane

R^1	R^2	Yield (%)
H	4-MeO	99
H	3-Me	96
H	2-Me	99
3-EtCO$_2$	4-Me	99
3-Cl	4-MeO	88
4-CF$_3$	4-MeO	99

the second the aryl boronic acid $(9.4 \times 10^{-3} M)$ in aq. Na_2CO_3 $(1.8 \times 10^{-2} M)$. The reagents were infused through the heated reactor $(50\,°C)$ at a flow rate of $2.5\,\mu l\,min^{-1}$, which afforded a residence time of 4 s, and the biphasic reaction products collected prior to off-line analysis by GC and ^1H NMR spectroscopy. As Table 21 illustrates, in all cases excellent yields were obtained, ranging from 88 to 99%, demonstrating the high catalytic activity of the PA-TAP-Pd membrane. Importantly, in the absence of the membrane no coupling products were obtained.

Within the pharmaceutical industry, another important part of a reaction process is product purification and although the use of microreaction technology has provided overwhelming evidence to show that reactions are more efficient and products are synthesized in higher purity (cf. batch procedures), trace metal contamination still presents a problem. Hinchcliffe et al. (2007) recently developed a reactor capable of removing trace metal contaminants, such as Pd, Co, Cu, and Hg, from reaction mixtures under continuous flow. Using the Pd-catalyzed Suzuki reaction as a model, the authors screened a series of commercially available solid-supported scavengers, ranging from silica gel, carbon, and various QuadraPure^{TM} resins (thiourea, iminodiacetate and aminomethyl phosphonic acid) for the removal of Pd at a concentration of 60 ppm. Of the materials evaluated, QuadraPure^{TM} thiourea-derived was found to be the best scavenger, removing >99% of Pd from the reaction mixture in a single pass. Coupled with the fact that the proportion of trace metal contaminants detected within continuous flow reaction products are inherently low, due to reduced catalysts degradation, the use of a scavenger cartridge at the end of a reaction sequence presents a relatively long-term solution to this problem.

### 2.4.4 Multiple catalyst systems

Using a series of PASSflow reactors, with typical dimensions of 5 mm (i.d.) $\times$ 10 cm (long), Kirschning et al. (Kirschning and Gas 2003; Kirschning et al., 2001, 2006) demonstrated the ability to combine a series of immobilized reagents in order to perform a sequence of reaction steps. In one example, the group demonstrated an oxidation, followed by a silyl deprotection and reductive amination steps to afford a derivatized steroid 147, as illustrated in Scheme 38, in excellent yield and purity.

In 2007, Wiles et al. (2007c) demonstrated the ability to employ solid-supported catalysts in series within an EOF-based microreactor. As summarized in Scheme 39, the model reaction sequence involved combining a previously investigated acid-catalyzed deprotection with a base-catalyzed condensation reaction to enable the synthesis of α,β-unsaturated carbonyl compounds from dimethyl acetals.

The microreactor comprised of a borosilicate glass capillary [500 μm (i.d.) $\times$ 3.0 cm (long)], connected to two reservoirs, one contained the
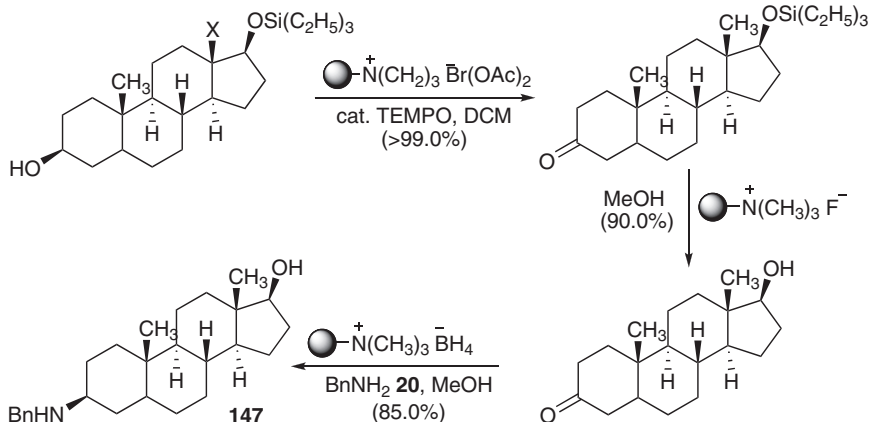
Scheme 38 Polymer-assisted derivatization of a steroid under continuous flow conditions.
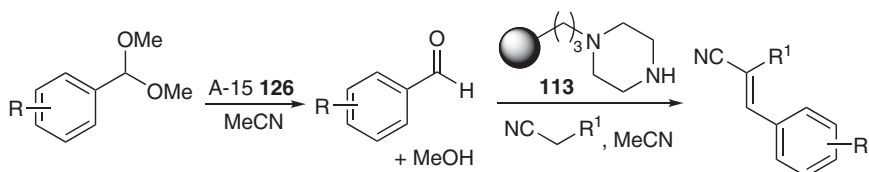
Scheme 39 General reaction scheme illustrating the multistep synthesis of an α,β-unsaturated compound.

reactant solution and the other served to collect the reaction products. To retain the solid-supported catalysts, a microporous silica (MPS) frit was placed at one end of the capillary and Amberlyst-15 **126** (2.5 mg) dry packed against it, a second frit followed and the solid-supported base **113** (2.5 mg) was packed into the reactor and held in place by a third MPS frit; this way the catalysts remained spatially resolved.

A typical procedure for the microreactions involved passing a solution of dimethyl acetal and activated methylene (1.0 M, respectively) in MeCN, through the solid-supported acid, where deprotection to afford the aldehyde occurred, followed by the supported base, where the *in situ* generated aldehyde condensed with the activated methylene to afford the desired α,β-unsaturated compound. Using EOF as the pumping technique, the reaction products were collected in MeCN, analyzed off-line by GC–MS and the conversion of starting materials to product quantified. Should any starting materials remain, the flow rate was reduced, by reducing the applied field, and the reaction repeated until optimized. Once successfully optimized,

the reactions were operated continuously for 2.5 h, the reaction solvent was then removed *in vacuo* and the "crude" product analyzed by ^{1}H NMR spectroscopy. Where compounds had not previously been reported within the literature, elemental analysis was performed using the product generated under flow conditions. Using this approach, the authors synthesized 20 α,β-unsaturated compounds in isolated yields of 99.1–99.9%, >99.9% purity utilizing residence times in the range of 0.6–1.25 min, depending on the reactants employed. To illustrate the efficiency of employing a series of solid-supported catalysts in a microreactor, the authors performed an analogous batch reaction and found that a reaction time of 24 h was required in order to obtain comparable conversions (cf. ~1 min residence times within the microreactor).

Having demonstrated the ability to incorporate multiple heterogeneous catalysts into an EOF-based flow reactor, the authors evaluated an increase in packed-bed size as a means of increasing the throughput of the flow reactor from mg h^{-1} to g h^{-1}. As the diffusion distance between the reactant solution and the solid-supported catalysts remains the same, the reaction efficiency attained in the capillary reactor was maintained and the increased flow rate employed afforded a higher throughput. In practice, this was achieved by increasing the reaction channel to 3 mm (i.d.), packing with A-15 **126** (36 mg) and silica-supported piperazine **113** (50 mg) and employing a flow rate of 54.9 μl min^{-1} afforded a throughput of 0.93 g h^{-1} in analytical purity (Wiles et al., 2007d).

In another example employing multiple supported catalysts and reagents, Smith et al. (2007a) presented a modular flow reactor in which 14 1,4-disubstituted-1,2,3-triazoles were synthesized. Coupling an immobilized copper(I) iodide species **148** with two scavenger modules (immobilized thiourea **149** and phosphane resin **150**), the authors reported the [3 + 2] cycloaddition of an array of azides and terminal acetylene (30 μl min^{-1}) to afford the desired 1,4-disubstituted 1,2,3-triazoles (Scheme 40) in moderate to excellent yield (70–93%).

In analytical mode, the reactor was optimized to afford between 20 and 200 mg of product; however in the case of propargylic alcohol
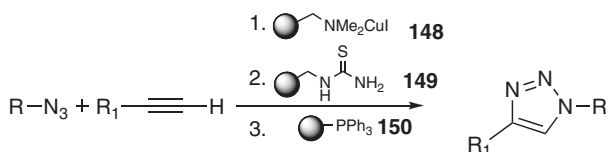
Scheme 40 Schematic illustrating the principle associated with the use of multiple solid-supported reagents in a single pressure-driven flow reactor.

($R^1 = CH_2OH$) and benzyl azide ($R = CH_2PH$), the reactor was operated continuously for 3 h to afford 1.50 g of the desired product in 85% yield and 95% purity. Additional examples reported by the group included amides and guanidines whereby purification was facilitated by the use of tagged phosphane reagents (Smith et al., 2007b).

Wiles and Watts (2007b) developed a microreactor to enable the parallel screening of catalysts and supported reagents, using the synthesis of tetrahydropyranyl ethers as a model reaction (Table 22). Employing a borosilicate glass microreactor containing four identical reaction channels [280 µm (wide) × 90 µm (deep) × 2.0 cm (long)], the authors evaluated a series of polymer-and silica-supported Lewis acid catalysts for their efficiency toward the protection of benzyl alcohol 35 as 2-(benzyloxy) tetrahydropyran 151. In each case, 1 mg of catalyst was employed and as Table 22 illustrates, excellent conversions were obtained for all catalysts; however, the higher loading of the silica-supported sulfonic acid

Table 22 Summary of the results obtained for the synthesis of 2-(benzyloxy)tetrahydropyran **151**, employing an array of solid-supported catalysts

| Channel no.	Supported Lewis acid	Loading (mmol g^{-1})	Flow rate (µl min^{-1})	Conversion (%)
1		3.50	1.10	100.0 (0.0)[a]
2	135	0.60	1.60	99.9 (3.5 × 10^{-4})[a]
3	152	4.20	1.80	100.0 (0.0)[a]
4	(SO$_3$)$_3$ Yb	2.00	1.50	99.9 (2.6 × 10^{-4})[a]

[a]The numbers in parentheses represent the % RSD, where $n = 15$.

derivative **152** enabled the reactions to be performed at a high throughput. Having identified the most active catalyst, the reactor was subsequently used to protect a further 14 alcohols whereby isolated yields $\geq$ 99.4% were obtained; in addition, employing MeOH as the reaction solvent enabled facile deprotection of the THP ethers. Using this approach, catalytic turnover numbers in excess of 2,760 were obtained with the catalyst showing no sign of degradation.

2.4.5 Biocatalysis

In addition to the wide range of chemically catalyzed reactions conducted in microreactors, the past 2 years has seen a large amount of interest in the use of biocatalysts within such systems (Honda et al., 2006). Of these, one of the most noteworthy examples is the fused silica microreactor reported by Belder et al. (2006), who fabricated an integrated system capable of synthesis, separation and detection. Using the enantioselective synthesis of 3-phenoxypropane-1,2-diol **153** as a model reaction, the authors evaluated the hydrolysis of 2-phenoxymethyloxirane **154** using an epoxide hydrolase enzyme (Scheme 41). The next step of the process involved the electrophoretic separation of the resulting reaction mixture, which was achieved in 90 s, followed by fluorescence detection of the two enantiomers using a deep-UV laser (Nd:YAG, 266 nm). Using this technique enabled three mutants of the epoxide hydrolase *Aspergillus niger* affording conversions in the range of 22–43% and *ee* values of 49–95%.

In 2006, Wang et al. (2006) reported the fabrication and evaluation of a polydimethylsiloxane (PDMS) microreactor capable of performing 32 enzyme-catalyzed click reactions in parallel (Table 22). The reactor consisted of several components including a nanoliter rotary mixer, a chaotic mixer, and a microfluidic multiplexer, which enabled discrete aliquots of reactants (57 s reactant^{-1}) to be introduced into the reaction channel and allowed multiple reactions to be performed in parallel. Using this approach, the authors performed 10 *in situ* click reactions between acetylene **155** and 10 different azides in the presence of (1) bovine carbonic anhydrase II (bCAII) **156**, (2) bCAII **156** and an inhibitor, (3) in the absence of bCAII **156**, and (4) two blank solutions containing only bCAII **156** and PBS solution. Using this approach, the reactions were performed in two batches and employing DMSO/EtOH (1:4) as the reaction solvent, the
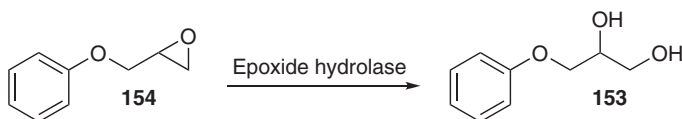
Scheme 41 Model reaction used to demonstrate the biocatalytic hydrolysis of 2-phenoxymethyloxirane **154**.

reaction mixtures were subsequently heated at 37 °C for 40 h prior to analysis by LC–MS. In addition to the speed of processing, the microreactor also enabled the quantities of reactants to be reduced with a typical reaction consuming 4 μl of reaction mixture (19 μg bCAII **156**, 2.4 nmol acetylene **155**, 3.6 nmol azide) [cf. 100 μl (94 μg bCAII **156**, 6.0 nmol acetylene **155**, 40.0 nmol azide) in a batch protocol]; a 2–12-fold reduction depending on the reactant. The authors were also pleased to confirm that the same results were obtained in the microreactor as within a 96-well plate (batch reaction), reporting the same nine compounds as hits out of 20 click compounds; a selection of which are illustrated in Table 23.
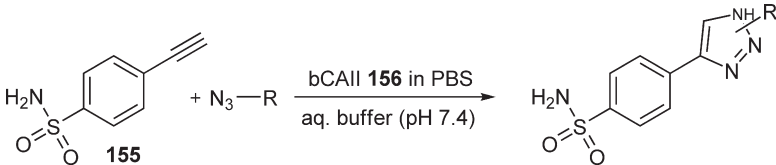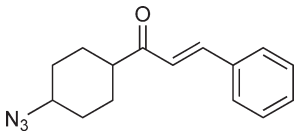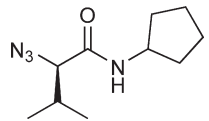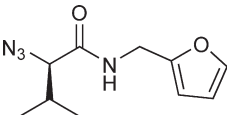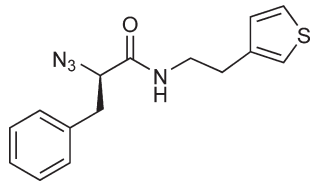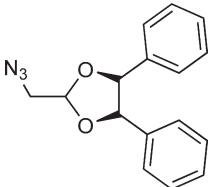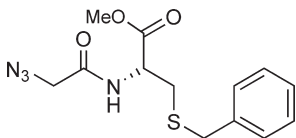
In order to increase the efficiency of biocatalytic transformations conducted under continuous flow conditions, Honda et al. (2006, 2007) reported an integrated microfluidic system, consisting of an immobilized enzymatic microreactor and an in-line liquid–liquid extraction device, capable of achieving the optical resolution of racemic amino acids under continuous flow whilst enabling efficient recycle of the enzyme. As Scheme 42 illustrates, the first step of the optical resolution was an enzyme-catalyzed enantioselective hydrolysis of a racemic mixture of acetyl-D,L-phenylalanine to afford L-phenylalanine **157** (99.2–99.9% *ee*) and unreacted acetyl-D-phenylalanine **158**. Acidification of the reaction products, prior to the addition of EtOAc, enabled efficient continuous extraction of L-phenylalanine **157** into the aqueous stream, whilst acetyl-D-phenylalanine **158** remained in the organic fraction (84–92% efficiency). Employing the optimal reaction conditions of 0.5 μl min^{-1} for the enzymatic reaction and 2.0 μl min^{-1} for the liquid–liquid extraction, the authors were able to resolve 240 nmol h^{-1} of the racemate.
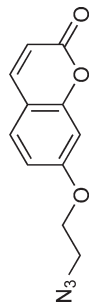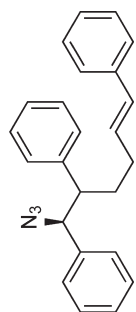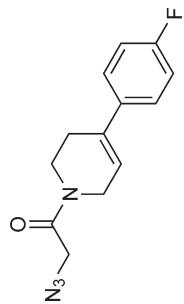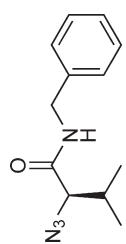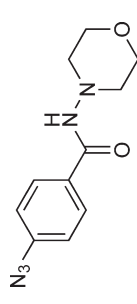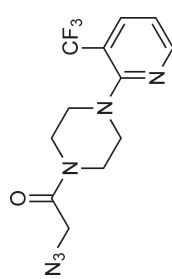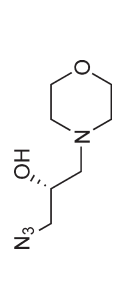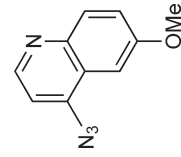
Employing a multichannel PDMS microreactor [350 μm (wide) × 250 μm (deep) × 6.4 mm (long)], in which the thermophilic enzyme β-glycosidase was immobilized, Thomsen et al. (2007) evaluated the hydrolysis of 2-nitrophenyl-β-D-galactopyranoside. Heating the reactor to 80 °C, the authors were able to continuously hydrolyze 2-nitrophenyl-β-D-galactopyranoside and monitored the reaction efficiency via generation of 2-nitrophenol **97**.

Again using the principle of PASSflow, Drager et al. (2007) recently reported the development of a polymeric matrix that was capable of performing automatic purification and immobilization of His$_6$-tagged proteins, followed by their use as highly active biocatalysts. Using the polymeric support illustrated in Figure 1, the authors conducted the immobilization of two enzymes, benzaldehyde lyase (BAL) and *Bacillus subtilis* (BsubpNBE), and evaluated the resulting biocatalysts toward the benzoin reaction (Scheme 43) and the regioselective hydrolysis of esters.

Initial investigations into the efficacy of the immobilization strategy were conducted using the benzoin reaction whereby employing benzaldehyde **116** (5.5×10^{-2} M) in phosphate buffer (pH 7, containing 10%

Table 23 Summary of the 20 click reactions conducted within a PDMS microreactor, highlighting those which were identified to be a hit

Azide	Result	Azide	Result
	Hit		Hit
	Hit		Hit
	No hit		No hit

No hit

Hit

No hit

No hit

Hit

Hit

No hit

No hit

Scheme 42 Continuous flow optical resolution of acetyl-D,L-phenylalanine using an immobilized aminoacylase enzyme.
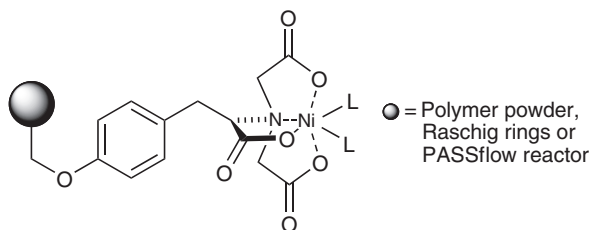
Figure 1 Illustration of the tyrosine-based matrix used for the immobilization of His$_6$-tagged proteins.
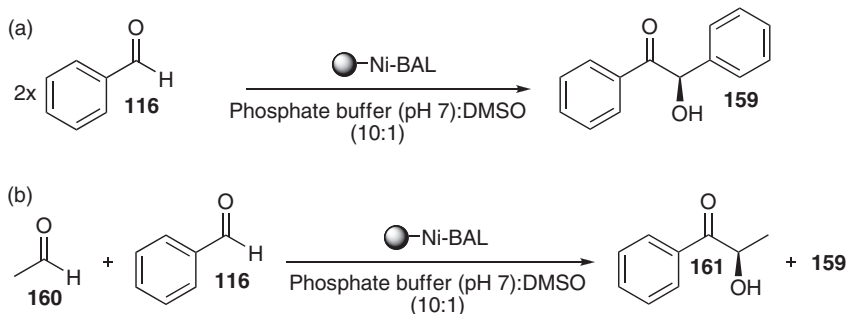
Scheme 43 An example of the (a) benzoin reaction and (b) cross-benzoin reaction conducted using immobilized His$_6$-tag BAL.

DMSO), a reaction temperature of 37 °C, and a residence time of 90 min, achieved by recirculating the reaction mixture through the PASSflow reactor at a flow rate of 1.0 ml min^{-1}, the authors were able to attain 99.5% conversion of **116** to (R)-benzoin **159**, determined by off-line GC analysis. Increasing the reactant concentration from 5.5×10^{-2} to 0.2 M, resulted in a reduction in benzoin **159** production of 5.9%, with longer reaction times required to attain high conversions with further increases in reactant concentration (typically 9 h for 1.0 M **116**). The authors subsequently demonstrated the cross-benzoin reaction between acetaldehyde

160 (2.3×10^{-1} M) and benzaldehyde **116** (4.6×10^{-2} M) whereby the target compound (R)-2-hydroxy-1-phenylpropan-1-one **161** was obtained in 92% isolated yield; (R)-benzoin **159** was obtained as a minor by-product in 8% yield.

Having confirmed that the immobilization strategy was robust enough to be used in conjunction with a continuous flow reactor, the authors evaluated the immobilization of a second His$_6$-tag enzyme, BsubpNBE, and employed the synthesis of 6-O-acetyl-D-glucal **162** (Scheme 44) as a model reaction.

In comparison to the previous example, the ester hydrolysis was significantly slower requiring a reaction time of 60 h to consume tri-O-acetyl-D-glucal **163** and afford the target compound **161** in 80% yield, with D-glycal **164** as a minor by-product (12.0%).

Along with problems associated with enzyme recovery and reuse, difficulties associated with the efficient recycle of cofactors have also contributed to the limited industrial uptake of biocatalysis. With this in mind, Yoon et al. (2005) reported a PDMS microfluidic system [channel dimensions = 250 μm (wide) × 3 cm (long)] capable of electrochemically regenerating nicotinamide cofactors and thus reducing the costs associated with the use of enzymes that require the presence of a cofactor. The authors found that by employing multistream laminar flow, comprising of a buffer stream and a reagent stream, regeneration of the cofactor could be achieved at the surface of a gold electrode. Using the conversion of achiral pyruvate **165** to L-lactate **166** in the presence of an enzyme (Scheme 45), the authors were able to demonstrate efficient enzyme/cofactor regeneration, equivalent to a turnover number of 75.6 h^{-1}.
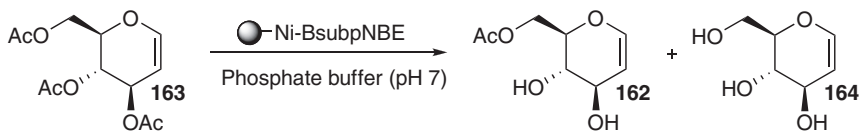
Scheme 44   The continuous flow ester hydrolysis achieved using a flow reactor containing immobilized His$_6$-tag BsubpNBE.
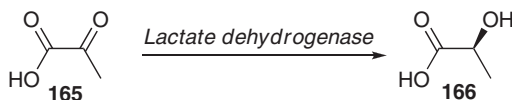
Scheme 45   Enzymatic synthesis of L-lactate **166**, employing electrochemical cofactor regeneration.

Csajagi et al. (2008) recently demonstrated the enantioselective acyla-
tion of racemic alcohols in a continuous flow bioreactor, using *Candida
antarctica* lipase B (CaLB) **167**. Employing a packed-bed reactor, containing
0.40 g of enzyme **167**, and pumping a solution of *rac*-phenyl-1-ethanol **119**
(10 mg ml^{-1}) in hexane:THF:vinyl acetate **168** (2:1:1) at a flow rate of
100 µl min^{-1} (at 25 °C), the authors found the reactor reached steady
state after 30 min of operation. Under the aforementioned conditions, the
(*R*)-acetate **169** was obtained in 50% conversion and 99.2% *ee* and residual
(*S*)-alcohol **170** in 98.9% *ee* with a residence time of 8.2 min; analogous
results were obtained in batch, however, required 24 h to afford 50%
conversion of **119**–**169**. Having devised a rapid technique for the evalua-
tion of immobilized biocatalysts, the authors compared a series of lipase
enzymes for the model reaction illustrated in Scheme 46, whereby CaLB
167, lipase *Pseudomonas cepacia* IM, and Amano lipase AK were found to
afford the highest throughputs of 10.2, 10.2, and 10.6 µmol min^{-1} g^{-1},
respectively.

To demonstrate the synthetic application of this methodology, the
authors subsequently demonstrated its use for the preparative kinetic
resolutions of a series of 2° alcohols, Table 24, whereby 20 ml solutions
of each racemic alcohol were passed through the bioreactor (3.3 h) and
found to afford analogous results to those obtained during the initial
optimization experiments. The authors successfully demonstrated the
use of immobilized and lyophilized enzymes within a continuous flow
reactor, presenting a synthetically viable approach to the kinetic resolution
of racemic alcohols.

Due to their cost, instability and limited longevity, enzymes are not
widely employed in production scale syntheses; however, through their
incorporation into flow reactors, biocatalysts can be readily employed in
the synthesis of high value products.

2.5 The use of solid-supported reagents in noncatalytic flow processes

From the examples above it can be seen that the incorporation of
solid-supported catalysts into flow reactors can afford extremely efficient
processes; however, recently numerous authors have reported the use of
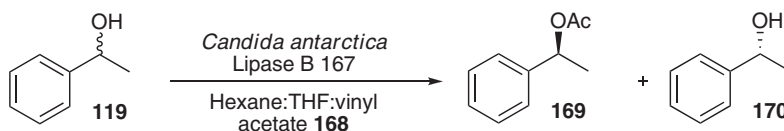
Scheme 46 Schematic illustrating the biochemical acylation of *rac*-phenyl-1-ethanol **119**.

Table 24 Examples of the preparative-scale kinetic resolutions conducted under flow

Compound	Yield (%)[a]	ee[b]	$[\alpha]_D^{25}$[c]	E[d]
OAc (R)-**169**	40	98.5	−62.8	
OH (S)-**170**	48	99.1	+125.3	>>>200
OAc (R)⁻	26	77.4	+2.0	
OH (S)⁻	41	99.0	+7.1	>200
OAc (R)⁻	34	56.4	+4.9	
OH (S)⁻	41	85.1	−23.3	22

[a]Products isolated from the reactor output stream.
[b]Determined by enantioselective GC.
[c]Specific rotations (∼1.0, CHCl₃).
[d]Due to sensitivity to experimental errors, enantiomer selectivity values calculated in the range 25–500 are
 reported as >200 and those above 500 as >>>200.

solid-supported reagents and scavengers, which have a finite lifetime in
the absence of regeneration techniques, under flow conditions and illu-
strated a series of novel techniques that are useful to the modern day
synthetic chemist.

Over the past decade, numerous authors have reported the continuous
flow synthesis of peptides via serial deprotection and coupling steps
(Flogel et al., 2006; Watts et al., 2002), to date, there have been no reports
of continuous flow protections, followed by reaction of an unprotected
moiety and selective deprotection. Owing to the complex nature of pro-
tecting group chemistry, it was the aim of a recent study, conducted by
Wild et al. (2009), to develop a noncovalent protecting group strategy
which would enable the facile N-protection of bifunctional compounds

and subsequent reaction of the unprotected functionality to afford the target molecule in excellent yield and selectivity. With this aim in mind, the authors investigated the use of crown ethers as noncovalent protecting groups as they have been shown to efficiently sequester ammonium ions, forming a stable adduct via hydrogen bonding. Using this principle, several authors have reported the use of crown ethers as N-protecting groups in solution; however, widespread application of the methodology has been precluded by problems associated with product isolation and reuse of the crown ether. To address this, Wild et al. (2009) prepared a solid-supported 18-crown-6 ether derivative and subsequently demonstrated its use as a novel N-protecting group within a packed-bed flow reactor. To illustrate the selectivity of the technique, the O-acetylation of tyramine **171** was conducted using acetyl chloride **19**, in the absence of a protecting group, which resulted in a complex mixture consisting of the desired tyramine acetate **172** (23%), tyramine *N*-acetate **173** (12%), tyramine diacetate **174** (20%), and residual starting material (45%) (Scheme 47), when conducted in a batch reaction.

In comparison, employing the reaction strategy depicted in Scheme 48 whereby the trifluoroacetic acid (TFA) salt of tyramine **175** was N-protected by the immobilized crown ether [step (a)], O-acetylated with acetic anhydride **37** in the presence of an organic base **14** [step (c)], and then simultaneously deprotected and the crown ether regenerated
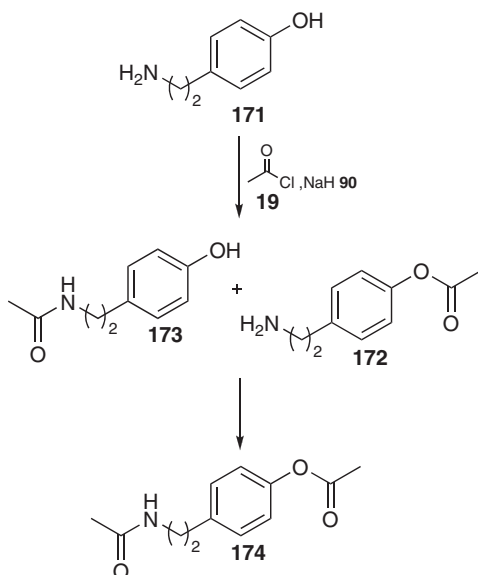
Scheme 47 Schematic illustrating the reaction products obtained when conducting the acetylation of tyramine **171** in the absence of a protecting group.
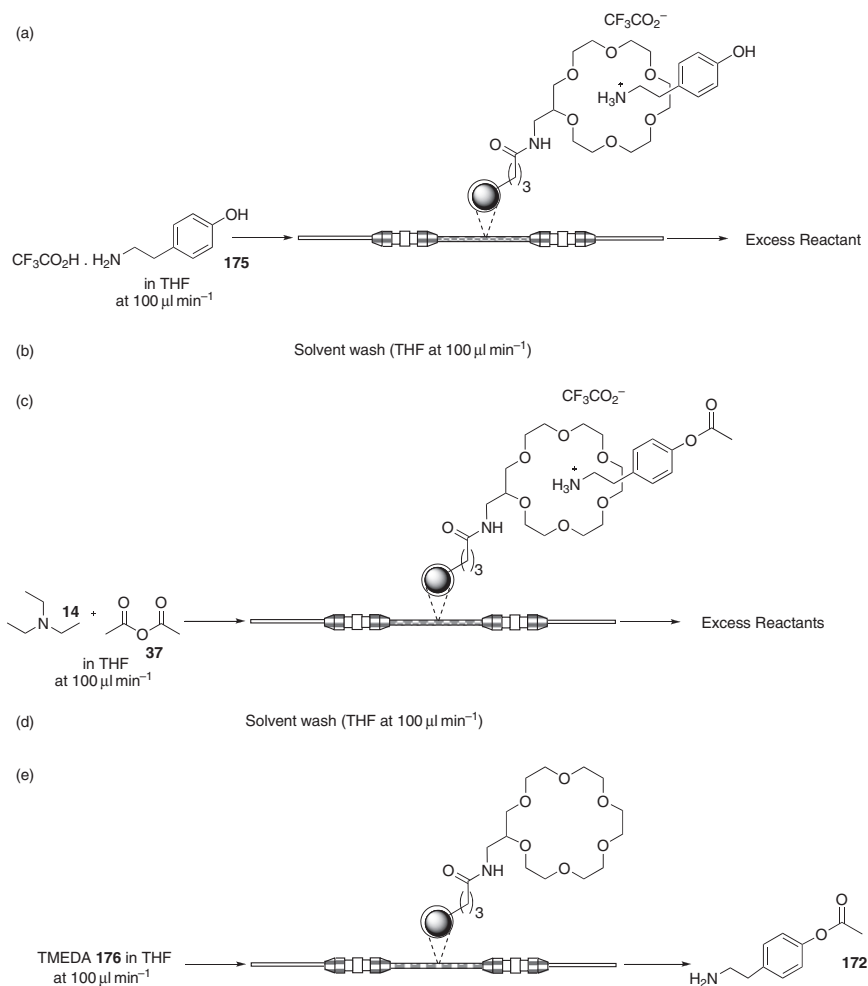
Scheme 48   Reaction protocol employed for the continuous flow acetylation of tyramine, using an immobilized 18-crown-6 ether derivative (0.15 g, 0.16 mmol g^{-1}).

using a solution of $N,N,N'N'$-tetramethylethylenediamine **176** [step (e)], the target compound tyramine acetate **172** was obtained in quantitative yield (2.4×10^{-2} mmol reaction^{-1}) and selectivity. The authors also investigated the generality of the protecting group strategy finding that HCl, TFA, and p-TSA salts could be complexed readily and several bifunctional compounds were also reacted to afford the O-product in all cases. It is acknowledged that automation of the methodology would increase the efficiency of the process, making it a practical alternative to conventional solution-phase protection/deprotection chemistry.
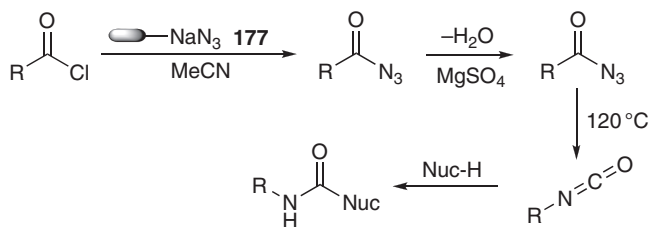
Scheme 49 Generalization of the polymer-assisted Curtius rearrangement conducted under continuous flow.

One of the more recent solid-supported reagents utilized by Ley and co-workers is an azide monolith, used to synthesize a series of azides from their respective acyl halide, as illustrated in Scheme 49 (Baumann et al., 2008a). The authors report the fabrication of the azide monolith **177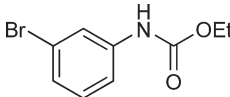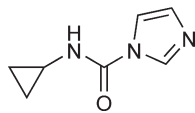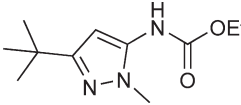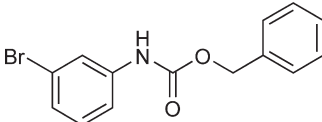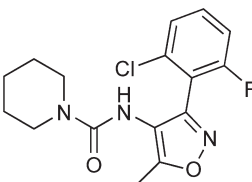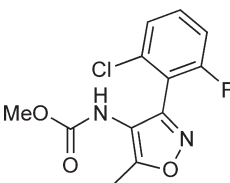** ($2.00 \, mmol \, g^{-1}$) in a glass Omnifit reactor [15 mm (i.d.) × 10 cm (long)] via thermal polymerization and quantified the columns total void volume (6.4 ml) using mercury intrusion analysis.

To synthesize a series of organic azides, the authors pumped a solution of the acyl chloride (1.0 M in MeCN) through the azide monolith **177**, at room temperature ($0.5 \, ml \, min^{-1}$), to afford a residence time of 13 min. In the case of the substrate 3-bromobenzoyl chloride, removal of the reaction solvent *in vacuo* afforded the respective azide, 3-bromobenzoyl azide, in quantitative yield and excellent purity. Having demonstrated the successful conversion of acyl chlorides to acyl halides, the next step of the investigation was to decompose the acyl azide under flow, *in situ*, to afford the respective isocyanate.

As Scheme 49 illustrates, this was achieved by firstly passing the acyl azide solution through a drying agent to remove any residual moisture and then superheating the reaction mixture in a convection flow coil to 120 °C. The isocyanate was then collected in a sealed vial, containing a nucleophile (1.0–4.0 eq.), and the reaction mixture heated to 100 °C, for 10 min, in a microwave to afford the reaction products summarized in Table 25. In both cases, the azide monolith **177** was used as a stoichiometric reagent and as such required regeneration after 1–10 mmol of organic azide had been prepared. Monolith regeneration proved facile and was achieved by simply pumping a solution of sodium azide through the depleted column to afford the original loading. The authors also reported the Curtius rearrangement starting from carboxylic acids and demonstrated the simultaneous trapping of the isocyanate intermediate with an array of nucleophiles to afford the target compounds in 75–95% yield and >90% purity (Baumann et al., 2008b).

Table 25 Summary of the products generated using azide monoliths (2.0 mmol g^{-1}) under continuous flow

Product	Yield (%)
	84
	73
	90
	64
	76
	78

The selective oxidation of primary alcohols is notoriously difficult to achieve selectively as further oxidation of the product to the respective carboxylic acid occurs rapidly, as depicted in Scheme 50. Wiles et al. (2006) therefore proposed that it should be possible to isolate either the aldehyde or the carboxylic acid, depending on the reaction times employed. To demonstrate this, the authors constructed a packed-bed reactor [3 mm (i.d.) × 5.0 cm (long)] containing silica-supported Jones' reagent (0.15 g, 0.15 mmol), a Cr(VI)-based oxidant, and by exploiting the high surface to volume ratio obtained within continuous flow reactors, the
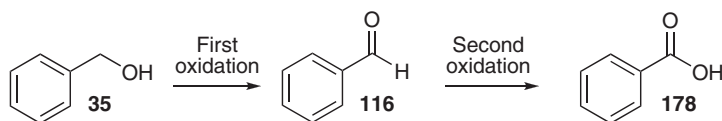
Scheme 50   Illustration of the overoxidation of benzyl alcohol **35** to benzoic acid **178**, observed in a stirred batch reactor.

authors were able to selectively oxidize an array of aromatic primary alcohols to either the aldehyde or carboxylic acid, depending on the reactant residence time within the packed bed.

Under pressure-driven flow, a reactant stream of the aromatic alcohol under investigation $(1.0 \times 10^{-2}\,M)$ in DCM was pumped through the packed bed and the effect of residence time evaluated by varying the flow rate; reaction products were analyzed by GC–MS and the conversion to the aldehyde and carboxylic acid was quantified. Conducting the first reactions at a flow rate of $300\,\mu l\,min^{-1}$ (21 s) afforded consumption of the alcohol **35** to afford a mixture of the aldehyde **116** and carboxylic acid **178**, reducing the flow rate to $50\,\mu l\,min^{-1}$ (126 s) converted all available aldehyde **116** to benzoic acid **178**. Consequently, in order to selectively synthesize benzaldehyde **116**, the flow rate was increased to $650\,\mu l\,min^{-1}$, affording a reaction time of 9.7 s, and the aldehyde **116** isolated in quantitative yield. Having successfully identified a means of the chemoselective oxidation of primary alcohols, a series of substituted alcohols were investigated, demonstrating no substrate dependency with respect to aromatic alcohols (Table 26). In addition to affording a chemoselective technique, the use of a solid-supported oxidant was advantageous as no metal contaminated waste streams were generated, as is the case with homogeneous Cr(VI)-based oxidants.

Unfortunately, the technique was not suitable for the oxidation of aliphatic aldehydes as the increase in polarity of the reaction stream (cf. aromatic alcohols) led to leaching of the Jones' reagent from the solid support. The methodology did however enable the facile oxidation of secondary alcohols to their respective ketone, as no competing overoxidation products could be formed, the reactions were conducted at a flow rate of $650\,\mu l\,min^{-1}$ (residence time $= 9.7$ s) to again afford the respective ketones in excellent yield (99.0–100.0%) and quantitative purity. Although the oxidant employed was not catalytic, the solid-supported reagent was self-indicating and turned from orange to green upon exhaustion.

2.6 Photochemical reactions

Along with improving those synthetic transformations that are routinely employed in the development and identification of lead compounds, there are many interesting synthetic procedures that are investigated within

Table 26 Summary of the results obtained for the chemoselective oxidation of primary alcohols

Alcohol	Flow rate ($\mu l\,min^{-1}$)	Product distribution (%)	
		Aldehyde	Carboxylic acid
Benzyl alcohol **35**	650	100 (99.1)[a]	0
	50	0	100 (99.6)
3,5-Dimethoxybenzyl alcohol	650	100 (99.5)	0
	50	0	100 (99.3)
4-Bromobenzyl alcohol	650	100 (99.0)	0
	50	0	100 (98.3)
4-Chlorobenzyl alcohol	650	100 (99.3)	0
	50	0	100 (99.4)
4-Cyanobenzyl alcohol	650	100 (98.5)	0
	50	0	100 (99.0)
Methyl-4-formylbenzyl alcohol	650	100 (99.2)	0
	50	0	100 (99.6)
4-Methylbenzyl alcohol	650	100 (99.2)	0
	50	0	100 (95.6)
4-Benzyloxybenzyl alcohol	650	100 (99.5)	0
	50	0	100 (99.8)
4-Aminobenzyl alcohol	650	100 (100)	0
	50	0	100 (99.8)
4-Dimethylaminobenzyl alcohol	650	100 (99.3)	0
	50	0	100 (99.6)
Biphen-4-yl methanol	650	100 (99.7)	0
	50	0	100 (99.5)
(5-Nitrothiophen-2-yl)-methanol	650	100 (99.8)	0
	50	0	100 (99.7)
2-Benzyloxybenzyl alcohol	650	100 (99.7)	0
	50	0	100 (99.8)
2-Naphthalen-2-yl methanol	650	100 (99.9)	0
	50	0	100 (99.9)
4-Acetylbenzylalcohol	650	100 (99.8)	0
	50	0	100 (99.8)

[a]The number in parentheses represents the isolated yield (%).

research laboratories which fail to be adopted when it comes to target manufacture. One such technique is photochemistry, which despite its ability to efficiently generate reactive intermediates many contributing factors have precluded the use of photochemistry on a large scale, such as difficulties associated with scaling light sources. As such,

photochemical syntheses represent one of the most interesting applications of this emerging technology as MRT has the potential to enable the many synthetically useful photochemical transformations reported by academic researchers to be used for the industrial-scale synthesis of fine chemicals and pharmaceutical agents. The following discussion therefore highlights the current problems associated with photochemistry, and subsequently describes how the microreaction technology has the potential to resolve the most fundamental of these issues.
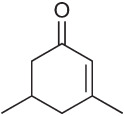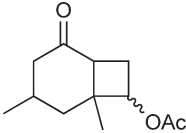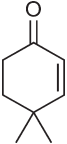
2.6.1 Homogeneous photochemistry
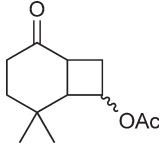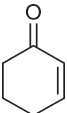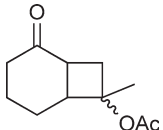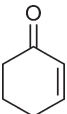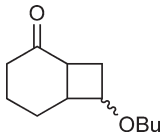
Utilizing a commercially available microreactor, fabricated from FOR-TURAN® glass, Fukuyama et al. (2004) evaluated a series of [2 + 2] cycloadditions as a means of reducing the reaction times conventionally associated with the synthetic transformation (Table 27). Using a high-pressure mercury lamp (300 W), the reaction of cyclohex-2-enone **179** with vinyl acetate **168** (Scheme 51), to afford the cycloadduct **180**, was used to compare photochemical efficiency within the microreactor [1,000 μm (wide) × 500 μm (deep)] and a conventional batch reactor (10 ml).

In line with the literature, irradiating the batch reactor for 2 h afforded only yielded 8% **180**; however, employing a residence time of 2 h within the microreactor, achieved by pumping the reaction mixture through the microchannel at a flow rate of 8.3 μl min^{-1}, the authors obtained adduct **180** in 88% yield. The enhanced irradiation efficiency obtained within the flow reactor therefore enabled a dramatic increase in reaction yield, coupled with a reduction in the overall reaction time required. With this in mind, the authors investigated the generality of the technique and as Table 26 illustrates, moderate to good yields were obtained for a range of substituted cyclohex-2-enones and vinylic compounds.

Another example of this was reported by Hook et al. (2005), whereby a series of photocycloadditions were performed using a standard, water-cooled immersion well, wrapped in fluorinated ethylene propylene (FEP) tubing (channel dimensions = 700 μm). In the first instance, the authors demonstrated the synthesis of 6-butyl-3-azabicyclo[3.2.0]hept-6-ene-2,4-dione **181** (Scheme 52a), which was achieved by pumping a solution of maleimide **182** (0.10 M) and 1-hexyne **183** (0.15 M), in MeCN, through the reactor at 2.0 ml min^{-1}; affording the target compound **181** in 95% yield with a throughput of 2.1 g h^{-1}. Additional photochemical transformations performed by the group included the synthesis of 7,8-dimethyl-1,2,3,9a-tetrahydropyrrolo[1,2-*a*]azepine-6,9-dione **184** (Scheme 52b) which was obtained in 80.0% yield at an impressive throughput of 7.4 g h^{-1}.

Mukae et al. (2007) also compared a Pyrex batch reaction vessel (8 mm) with several Pyrex microreactors [channel dimensions = 100 μm (wide) × 40 μm (deep) 1.20 cm (long)] for the photocycloaddition of

Table 27 Photochemical [2 + 2] cycloaddition conducted in a FORTURAN® glass microreactor

Substituted cyclohex-2-enone	Vinylic substrate	Cycloadduct	Irradiation time (h)	Yield (%)
	168		2	70
	168		3.2	62
179			3.2	64
179			3.2	67
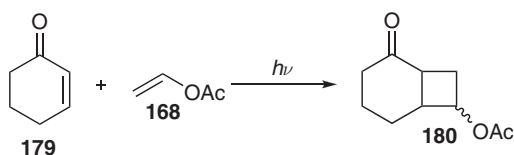
Scheme 51 Photochemical [2 + 2] cycloaddition of cyclohex-2-eneone **179** with vinyl acetate **168**.

2-(2-alkenyloxymethyl)-naphthalene-1-carbonitriles **186**, as depicted in Scheme 53. Using a xenon lamp (500 W) as the light source, the effect of alkene substitution, solvent, residence time, and microchannel dimensions on the cycloaddition was evaluated.

Under standard batch conditions, the target products were obtained in 74% yield with an irradiation time of 3 h, compared with analogous yields in the microreactor with an irradiation time of only 1 min. In addition to
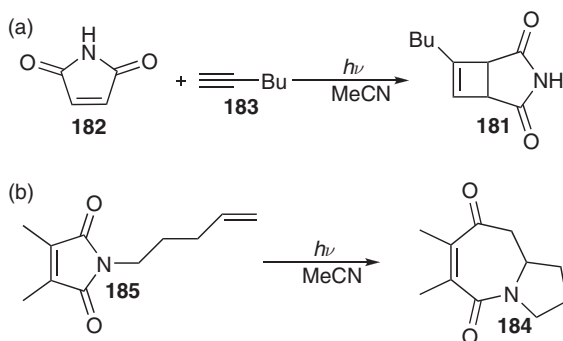
Scheme 52 (a) [2 + 2] Photocycloaddition of maleimide **182** and 1-hexyne **183** to afford **181** and (b) intramolecular [5 + 2] photocycloaddition of 3,4-dimethyl-1-pent-4-enylpyrrole-2,5-dione **185**.
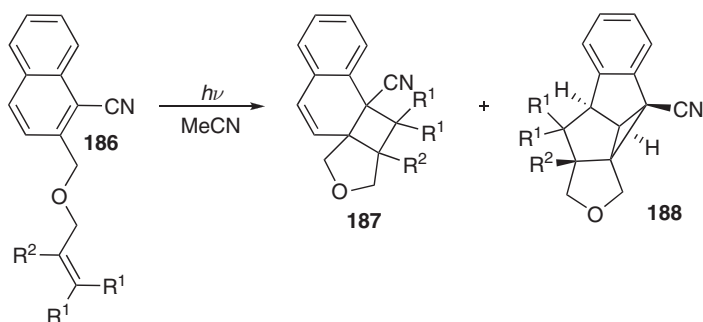
Scheme 53 Photochemical synthesis of a series of 2-(2-alkenyloxymethyl)-naphthalene-1-carbonitriles.

the obvious increase in photon efficiency obtained, the authors also noted an increase in reaction regioselectivity when conducting the reaction under flow conditions an observation which is attributed to the ability to remove the initial products **187** from the reactor prior to the second reaction, an undesirable photocycloreversion, which affords products of the type **188**. In addition, the authors also demonstrated the ability to boost the throughput of the reactor by simply increasing the width of the reaction channel (100–2,500 μm) whilst maintaining the original channel depth, illustrating the ease with which such reactions can be scaled. Using this approach a 25-fold increase in reactor throughput was obtained, with no observable decrease in reaction selectivity.

With numerous researchers investigating the advantages associated with thermally or biocatalytically controlled asymmetric syntheses, some of which have been performed in continuous flow reactors, few have considered the prospects of photochemical asymmetric synthesis, an idea
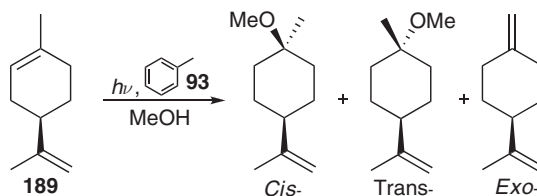
Scheme 54 Asymmetric addition of MeOH to (R)-(+)-(Z)-limonene (**189**) performed in a quartz microreactor.

recently communicated by Sakeda et al. (2007). Using the asymmetric photochemical addition of methanol to (R)-(+)-(Z)-limonene (**189**) as a model reaction (Scheme 54), the authors compared three quartz micro-reactors, with a standard laboratory cell as a means of highlighting the synthetic potential of this approach.

Employing a low-pressure Hg lamp ($\lambda = 254$ nm) the authors evaluated the effect of channel geometry on photon efficiency and diastereomeric excess (*de*) (see Table 28) by pumping a methanolic solution of (R)-(+)-(Z)-limonene (**189**) (25 mM) and toluene **93** (10 mM) through the various quartz reactors. Initial investigations were conducted using a microreactor with channel dimensions of 500 μm (wide) × 300 μm (deep) and focused on determining the effect of irradiation time on the conversion of (R)-(+)-(Z)-limonene (**189**). Using this approach, a linear relationship between irradiation time and conversion was observed; however, the authors did observe a decrease in *de* with prolonged exposure times. Based on this observation, a series of microchannel geometries were subsequently evaluated and it was found that shallow channels, typically <40 μm, afforded increased photon efficiency; which is attributed to illumination homogeneity. Furthermore, a slight increase in *de* was observed in all flow experiments when compared to the batch cell, a feature that was explained by the suppression of side reactions within the continuous flow reactors.

Table 28 Summary of the results obtained for the asymmetric addition of MeOH to (R)-(+)-(Z)-limonene (**189**) in batch and a microreactor with an irradiation time of 36 s

| Reactor	Dimensions	Photon efficiency	*de* (%)
Batch	100 μm × 3 mm	0.06	28.7
Micro	500 μm × 300 μm	0.11	30.6
Micro	400 μm × 40 μm	0.27	29.4
Micro	200 μm × 20 μm	0.29	30.0

2.6.2 Heterogeneous photochemistry

The homogeneous photochemical reactions described thus far serve to illustrate the effectiveness achieved as a result of combining photochemistry and microreactors; however, organic photochemistry is not limited to homogeneous reactions, with many synthetically useful transformations conducted using catalytic processes. Miniaturized catalytic photochemistry initially focusing on the photodegradation of substrates (Gorges et al., 2004; Li et al., 2003); however, more recently researchers have reported the use of such systems for a series of common organic reactions including reductions, alkylations, and cyclizations, a selection of which are discussed below.

An early example of a photochemical cyclization was reported by Takei et al. (2005) who demonstrated the synthesis of L-pipecolinic acid **190** from an aqueous solution of L-lysine **191**, as illustrated in Scheme 55. To achieve this photocatalytic transformation, the authors fabricated a Pyrex microreactor in which the channel cover plate was coated with a 300 nm layer of TiO_2 anatase (100 nm particles), prior to thermal bonding, to afford a titania-coated microreactor (TCM); the titania film was subsequently loaded with platinum (0.2 wt%), by photodeposition, to enable the TCM to be used for redox-combined photosynthesis. To conduct the reaction, the authors pumped a solution of L-lysine (**191**) (2.0 mM) through the reactor using a syringe pump and irradiated the TiO_2 film through a photomask using a high-pressure mercury lamp ($110 \, mW \, cm^{-1}$). The resulting reaction mixture was subsequently collected and analyzed off-line by chiral HPLC in order to determine the proportion of L-lysine (**191**) converted to D- and L-pipecolinic acid **190**/**192**.

Employing a flow rate of $1 \, \mu l \, min^{-1}$ and a residence time of 0.86 min, the authors obtained 87% conversion of L-lysine (**191**), exhibiting 22% selectivity for pipecolinic acid and 14% yield of L-pipecolinic acid **190**. To demonstrate the TCM's efficiency, the authors also performed the reaction in batch employing 2 wt% Pt-loaded TiO_2 particles, which afforded the same surface to volume ratio of catalyst as calculated to be within the TCM, whereby a reaction time of 60 min afforded analogous results. The authors concluded that the increased reaction efficiency observed within the TCM was attributed to the efficient irradiation of the reaction mixture; however, for a true comparison they noted that measurement of the quantum yield of each system would be required.
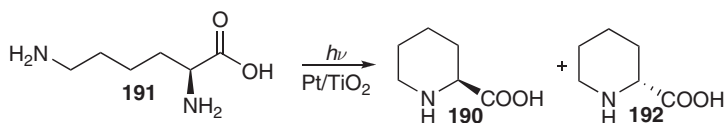
Scheme 55   Photocatalytic synthesis of L-pipecolinic acid **190** and D-pipecolinic acid **192**.
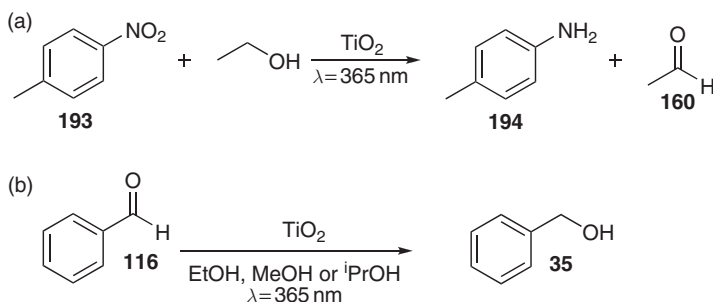
Scheme 56 Illustration of the photocatalytic reductions conducted by Matsushita et al. (2006) in a quartz microreactor.

In an analogous manner, Matsushita et al. (2006) investigated the use of a quartz microreactor [channel dimensions $= 500 \, \mu m$ (wide) $\times 100 \, \mu m$ (deep) $\times 0.40 \, cm$ (long)], in which the bottom and sides of the microchannel were coated with TiO_2 (anatase), for the photocatalytic reduction of 4-nitrotoluene **193** (Scheme 56a) and benzaldehyde **116** (Scheme 56b) using a UV-LED ($\lambda = 365 \, nm$). As the photoreduction of an analyte requires a corresponding oxidation step to occur, a series of alcohols were evaluated as potential reaction solvents.

In theory, alcohols with low pK_a's afford a greater proportion of protons and alkoxy radicals, it was therefore proposed that MeOH would be an ideal solvent for this transformation; however, due to the kinetic instability of the methoxy radical the authors found the reductions to be more successful when conducted in EtOH. In addition, it was found that saturating the reactant stream with nitrogen, thus excluding dissolved oxygen, promoted the reaction as the electrons in the conduction band of the excited TiO_2 layer were not captured by oxygen. With this knowledge in hand, the authors evaluated the efficiency of the TiO_2-coated quartz reactor toward the reduction of 4-nitrotoluene **193** to afford 4-aminotoluene **194** and acetaldehyde **160**, as a function of reactant residence time within the microreactor. Employing 4-nitrotoluene **193** in N_2-saturated EtOH ($1.0 \times 10^{-4} \, M$), in the absence of light, 0% conversion to 4-aminotoluene **194** was observed, this was subsequently increased to 8.3% with an irradiation time of 10 s and finally to 45.7% **194** when a residence time of 60 s was employed. Having demonstrated the ability to perform photocatalytic reduction of a nitro group to an amine, the authors investigated the reduction of benzaldehyde **116** (Scheme 56b). As the nitro group is more readily reduced than an aldehydic functionality, it came as no surprise to the authors that only 10.7% conversion to benzyl alcohol **35** was observed when employing an irradiation time of 60 s. Consequently, further studies are currently underway by the group in order to optimize the excitation wavelength and
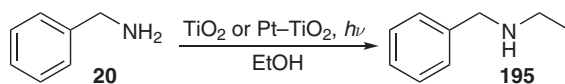
Scheme 57 The model reaction used to demonstrate the photochemical N-alkylation conducted in a quartz microreactor.

microreactor design for the reduction of multifunctional compounds (Matsushita et al., 2008).

Matsushita et al. (2007) subsequently demonstrated the ability to N-alkylate amines (Scheme 57) under continuous flow, again employing a quartz microreaction channel coated with a TiO_2 or Pt-loaded TiO_2 layer. As Table 28 illustrates, the illuminated specific surface area per unit of liquid attained within a microchannel is large even without taking into account the surface roughness of the catalyst; however, it can be seen that a shallow reaction channel provides optimal photon efficiency.

Having observed no photochemical alkylation in batch when employing TiO_2 particles and 84% N-alkylation (with 2.4% dialkylation after 5 h and 74.1% after 10 h) using the Pt–TiO_2 catalyst (5 h), initial flow reactions were conducted using a microreactor coated with Pt–TiO_2. Employing a series of UV-LEDs ($\lambda = 365$ nm, 2.2 m W cm^{-2}) as the light source, the authors pumped a solution of benzylamine **20** (1 mM) in EtOH through the Pt–TiO_2-coated microchannel and evaluated the effect of flow rate (2–40 μl min^{-1}) and conversion to N-ethylbenzylamine **195**. Using a residence time of 2.5 min, the authors were pleased to observe 85% yield of N-ethylbenzylamine **195** with no sign of the dialkylated by-product. Having successfully performed a photochemical N-alkylation using the batch evaluated catalyst, the authors investigated the use of a Pt-free TiO_2-coated microchannel and were surprised to find that with an irradiation time of 90 s, 98% **195** was obtained. As Table 29 illustrates, increasing the surface to volume ratio by reducing the channel depth affords a more efficient reaction system and compared to batch where 0% **195** was obtained using TiO_2, excellent yields of N-ethylbenzylamine **195** can be

Table 29 Illustration of the effect of channel depth on the illuminated specific surface areas per unit of liquid in a microreactor (constant channel width of 500 μm) and the yield of N-ethylbenzylamine **195** obtained using a TiO_2 wall coating

| Channel depth (μm)	Illuminated surface area (m^2 m^{-3})	Yield (%)
300	7.3×10^3	98
500	6.0×10^3	94
1,000	4.0×10^3	70

obtained with irradiation times as low as 1.5 min. It was also encouraging to see that the use of different solvent systems also enabled the authors to access *N*-methyl and *N*-propyl derivatives, providing a facile route to *N*-alkyl amines.

Wootton et al. (2002) investigated the use of a microreactor for the continuous photochemical generation of singlet oxygen and subsequently demonstrated the principle for the synthesis of ascaridole **196** (Scheme 58). To perform the reaction, a methanolic solution of α-terpinene **197** and Rose bengal (**198**) (photosensitizer) was introduced into the reactor at a flow rate of $1 \mu l \min^{-1}$, where it was mixed with a constant stream of oxygen ($15 \mu l \min^{-1}$), prior to irradiation with a 20 W tungsten lamp. As a safety precaution, the reaction products were degassed with nitrogen in order to prevent the accumulation of oxygenated solvents. Using the aforementioned protocol, the authors report 85% conversion of α-terpinene **197** to ascaridole **196**, demonstrating efficient photon transfer using a commercially available light source.

Another interesting photochemical transformation conducted in a microfabricated reactor, was the photochemical chlorination of toluene-2,4-diisocyanate reported by Ehrich et al. (2002). Employing a falling film microreactor [channel dimensions $= 600 \mu m$ (wide) $\times 300 \mu m$ (deep) $\times 6.6$ cm (long)], consisting of 32 parallel microchannels, the authors investigated the photochemical generation of chlorine radicals from gaseous chlorine using tetrachloroethane as the reaction solvent. By varying the flow rate of chlorine (14–56 ml $\min^{-1}$) and toluene-2,4-diisocyanate (0.1–0.6 ml $\min^{-1}$) feeds and the reactor temperature, the authors were able to optimize the production of benzyl chloride-2,4-diisocyanate. Employing a residence time of just 9 s and a reactor temperature of 130 °C, afforded benzyl chloride-2,4-diisocyanate in 81% yield with a space time yield of 401 mol h^{-1}, which far exceeds the throughput of 1.3 mol h^{-1} attained in a conventional reactor.

See Section 3 for a discussion of the photochemical synthesis of an endothelin receptor antagonist **199** using the Barton reaction and the synthesis of a precursor to (–)-rose oxide **200** which is of industrial interest to fragrance manufacturers.
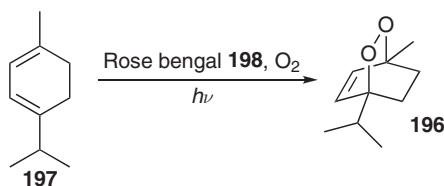
Scheme 58   An early example of the photochemical generation of singlet oxygen within a glass microreactor.

3. COMPOUNDS OF INTEREST AND INDUSTRIAL APPLICATIONS OF MICROREACTION TECHNOLOGY

Having discussed some of the advantages associated with the use of microreaction technology as a tool to conduct high-throughput organic synthesis, the final section of this chapter focuses on some of the compounds generated under continuous flow that are of synthetic and/or industrial interest.

Along with the halogen–lithium exchange reactions detailed in Section 2.3.3, numerous hydrogen–lithium exchange reactions have been reported to benefit from being conducted under continuous flow conditions. Such reactions are typically performed at low temperatures, that is, −78 °C, owing to the exothermic nature of the transformation and to prevent decomposition of unstable intermediates. The use of cryogenic reaction temperatures is however disadvantageous when considering employing reactions on a production scale. With this in mind, examples have featured within the literature that demonstrates the ability to increase reaction temperature, by conducting the reactions within miniaturized, continuous flow reactors. One such example of this is the synthesis of a sprio lactone **201** which is a fragment of neuropeptide Y, a receptor antagonist for the treatment of obesity (Takasuga et al., 2006).

As Scheme 59 illustrates, the reaction involves the hydrogen–lithium exchange of phenyl isonicotinamide **202**, in the presence of *n*-BuLi **74**/LiBr **203**, followed by a reaction with ethyl-4-oxocyclohexanecarboxylate **204** to afford the target spiro lactone **201** as a mixture of *cis*/*trans* isomers. In the presence of any residual dilithiated intermediate **205**, the spiro lactone **201** can undergo a second reaction to afford the by-product **206**. Conducting the reaction in a microflow reactor, comprising of static mixers and
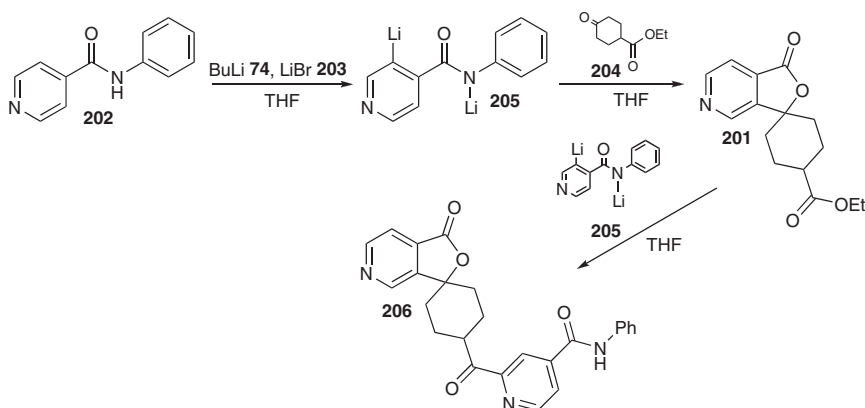
Scheme 59 Selective synthesis of a spiro lactone derivative **201** achieved using continuous flow methodology.

Table 30 Summary of the results obtained for the continuous flow synthesis of a spiro lactone **201**

Reactor temperature (°C)	Flow rate (ml min^{-1})	Yield **201** (%)	Cis/ trans	Yield **206** (%)	Residual **202** (%)
−80	3.3	92.5	1.10	0.5	5.5
−80	3.3	93.3	1.12	0.8	6.9
−80	3.8	92.4	1.12	0.8	6.5
−10	5.3	51.8	1.75	32.5	10.1
−40	5.3	67.8	1.39	15.1	7.9
−80	7.2	90.9	1.18	1.9	8.1

stainless-steel tube reactors [0.25–2 mm (i.d.) × 0.01–20 m (length)], Takasuga et al. (2006) obtained yields in excess of 90% **201**; employing a reaction temperature of −80 °C and a reaction time estimated to be 20 s. The authors also noted that the yield decreased with increasing temperature and observed a change in selectivity upon varying the reactor temperature. In comparison, when increasing from an 800 tank to a 2,000 l tank (jacket temperature −90 °C, reaction mixture = −66 °C), the investigators observed a reduction in yield from 82.9 to 77.3% and an increase in the addition time from 15 to 36 min. The increased yield in the flow reactor can be attributed to the efficient removal of heat from the reaction mixture, preventing undesirable decomposition products obtained at increased temperatures, as illustrated in Table 30.

Compared with the above examples, whereby an array of pharmaceutically important molecules have been synthesized under pressure-driven flow, Garcia-Egido et al. (2002) reported the synthesis of fanetizole (**207**), an active compound for the treatment of rheumatoid arthritis, utilizing EOF. Employing a borosilicate glass microreactor fabricated at The University of Hull, the authors demonstrated the first example of a heated EOF-controlled reaction. As Scheme 60 illustrates, using
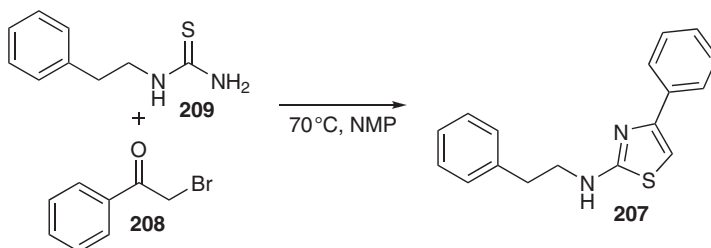
Scheme 60 Synthesis of fanetozole (**207**) under continuous flow.

*N*-methylpyrrolidone (NMP) as the reaction solvent, 2-bromoacetophenone **208** (1.4×10^{-2} M) and phenylethylthiourea **209** (2.1×10^{-2} M) were reacted to afford the target molecule **207** in quantitative conversion with respect to 2-bromoacetophenone **208**.

Employing a stainless-steel continuous flow reactor, Zhang et al. (2004) described the synthesis of gram to kilogram quantities of material for use in early clinical studies. One reaction reported by the authors was the exothermic synthesis of *N*-methoxycarbonyl-L-*tert*-leucine **210**, as illustrated in Scheme 61. By continuously adding a solution of methyl chloroformate **211** to L-*tert*-leucine **212**, in the presence of aq. NaOH **26**, at a reactor temperature of $-40\,°C$ afforded the target compound **210** in 91% yield with a throughput of $83.0\,g\,h^{-1}$.

Using a stainless-steel microreactor, Ushiogi et al. (2007) reported a microflow system capable of synthesizing unsymmetrical diarylethenes, a process that is notoriously difficult to achieve in conventional batch systems. As Scheme 62 illustrates, diarylethenes are of synthetic interest due to their ability to change color via a reversible switching between two distinct isomers, which occurs as a result of light absorption.

With conventional protocols requiring low reaction temperatures, typically $-78\,°C$, to prevent side reactions from occurring, scaling the reaction for industrial production of such compounds has proved difficult. As such, the authors evaluated the process under continuous flow, proposing that the effective temperature control and accurate residence times attainable within miniaturized flow reactors would enable the synthesis of diarylethenes at temperatures above $-78\,°C$ and thus facilitate the large-scale synthesis of such compounds.
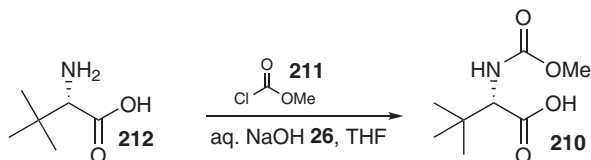
Scheme 61 An example of the reaction protocol employed for the exothermic synthesis of carbamates.
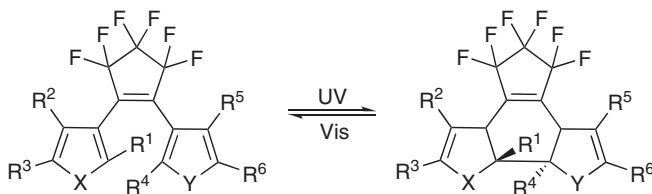
Scheme 62 Illustration of the photochromism exhibited by diarylethenes.
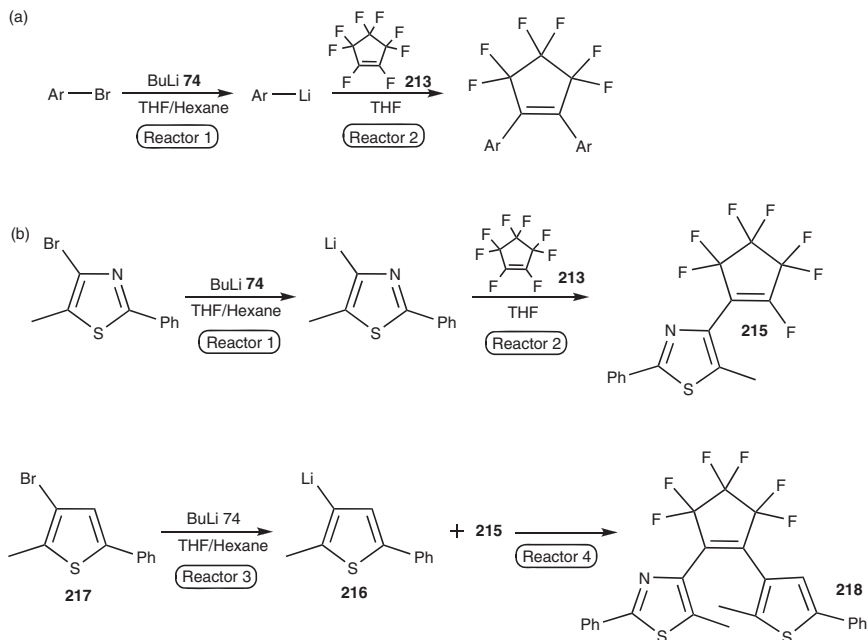
Scheme 63 Schematic detailing the general protocol employed for the continuous flow synthesis of (a) symmetrical and (b) unsymmetrical diarylethenes.

Initial investigations centered on the synthesis of symmetrical diarylethenes and focused on identifying the effect of reactor temperature on the reaction yield. The first step of the reaction was a halogen–lithium exchange between an aryl bromide (0.3 M, 7.5 ml min^{-1}) and n-butyllithium **74** (1.5 M, 1.5 ml min^{-1}), traditionally performed at low reaction temperatures to avoid decomposition of the aryllithium intermediate (Scheme 63a). The second step involved the reaction of two equivalents of the aryllithium compound with octafluorocyclopentene **213** (0.75 M, 1.5 ml min^{-1}) to afford the target diarylethene **214**. Utilizing a stainless-steel microreactor consisting of two T-micromixers and two residence time units, the aforementioned reaction was conducted at a range of reaction temperatures (−45 to 15 °C) achieved by immersing the microreactor in a cooling bath, whereby 0 °C provided an optimum reaction temperature. Employing a residence time of 3.4 s in the first reactor and 2.9 s in the second, the authors isolated a range of diarylethenes in yields ranging from 47 to 87% depending on the aryl bromide used. In comparison to batch reactions conducted at −78 °C, this represented a dramatic increase in yield, with the monoarylated dominating in batch. The authors noted however that employing only 1 eq. of BuLi **74** within the flow reactor afforded the monoaryl derivative as the major product (Table 31). As such, it was

Table 31 Comparison of the product distribution obtained in batch and microflow systems for the arylation of octafluorocyclopentene **213**


| | | Isolated yield (%) | |
		Diarylethene	Monoarylethene
Reactor	Reaction temperature (°C)		
Batch	−78 (3 h)[a]	10	52
Micro	0 (9 s)[a]	51	11

[a]The numbers in parentheses represent the reaction times employed.

proposed that by employing two different aryl halides, unsymmetrical diarylethenes could be obtained in high yield.

Using a convergent synthetic approach, the authors were able to adapt their flow process to enable the synthesis of unsymmetrical diarylethenes in good isolated yield. As depicted in Scheme 63b, the methodology involved preparing one monoarylated product **215** (reactors 1 and 2), as previously discussed, and the aryllithium intermediate **216** of a second aryl bromide **217** in parallel (reactor 3). The reactant streams were then converged in reactor 4, to afford the target unsymmetrical diarylethene **218** in an isolated yield of 53%. Owing to the different photochromic properties of such compounds, the synthetic methodology presented affords a facile route to the fine tuning of the compounds physical properties, whilst providing a method capable of producing any successful materials on a large scale.

Panke et al. (2003) also demonstrated enhanced reaction control, with respect to the temperature-sensitive synthesis of 2-methyl-4-nitro-5-propyl-2H-pyrazole-3-carboxylic acid **219**, a key intermediate in the synthesis of the lifestyle drug Sildenafil® (**220**) (Scheme 64). When performing the nitration of 2-methyl-5-propyl-2H-pyrazole-3-carboxylic acid **219** under adiabatic conditions, with a dilution of $6.01 \, kg^{-1}$), Dale et al. (2000) observed a temperature rise of 42 °C (from 50 to 92 °C) upon addition of the nitrating solution. As Scheme 63 illustrates, this proved problematic as at 100 °C decomposition of the product **219** was observed and in order to reduce thermal decomposition of pyrazole **219**, and increase process safety, the authors investigated addition of the nitrating solution in three aliquots, which resulted in a reduced reaction temperature of 71 °C and an increase in chemoselectivity; unfortunately, the reaction time was increased from 8 to 10 h.
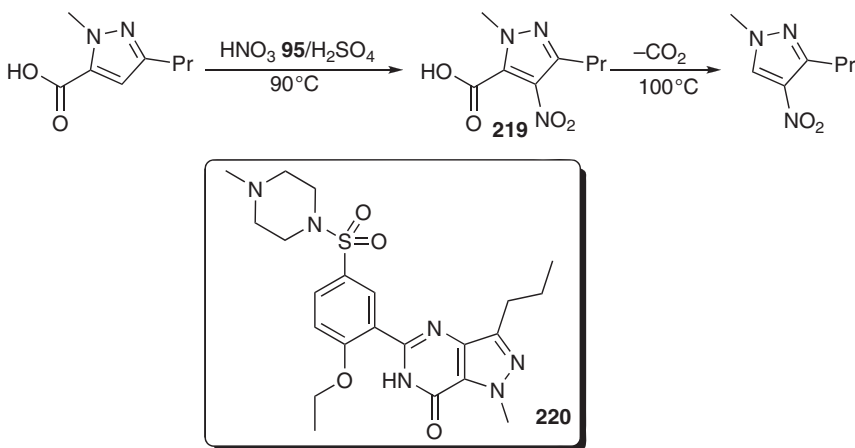
Scheme 64   An illustration of the temperature-sensitive synthesis of 2-methyl-4-nitro-5-propyl-2H-pyrazole-3-carboxylic acid **219**, a key intermediate of Sildenafil® (**220**).

By conducting the reaction in a flow reactor, where the heat of reaction can be rapidly dissipated, the authors were able to maintain a reaction temperature of 90 °C as a result of adding the nitrating mixture continuously. Coupled with a residence time of 35 min, the authors were able to attain a throughput of 5.5 g h^{-1} with an overall yield of 73% **219**. In addition to the dramatic reduction in residence time (10 h–35 min) and the increased process safety, the continuous flow methodology afforded a facile route to the chemoselective synthesis of 2-methyl-4-nitro-5-propyl-2H-pyrazole-3-carboxylic acid **219**.

Having earlier demonstrated the use of AlMe$_3$ **71** for the efficient synthesis of amides from a series of simple methyl and ethyl esters, Gustafsson et al. (2008b) extended their investigation to include the synthesis of two pharmaceutically relevant compounds, rimonabant (**72**) (SR141716) (Scheme 65) and efaproxiral (RSR13) (**73**) (Scheme 66). In both cases, the established synthetic protocols involved the formation of an amide bond, in the first instance from and acid chloride and 1-aminopiperidine **221** and secondly from the reaction of the ester or carboxylic acid and a substituted aniline precursor. Based on their previous success employing AlMe$_3$ **71** in a PTFE tubing (1 mm i.d.)-based continuous flow reactor, the authors investigated the synthesis of rimonabant (**72**) and efaproxiral (**73**) under continuous flow conditions.

As Scheme 65 illustrates, the first step of the rimonabant (**72**) flow synthesis involved the treatment of 4-chloropropiophenone **222** with LiHMDS **223** for 1 min prior to the addition of ethyl oxalate **224** at 50 °C where it reacted for 5 min; after work up and purification, the resulting β-ketoester **225** was isolated in 70% yield. Treatment of **225** with the HCl
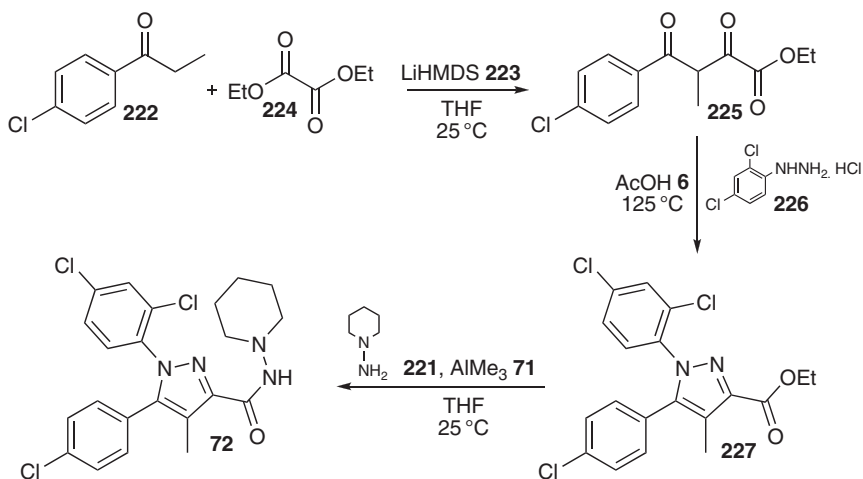
Scheme 65 Synthetic route employed for the continuous flow synthesis of rimonabant (**72**).
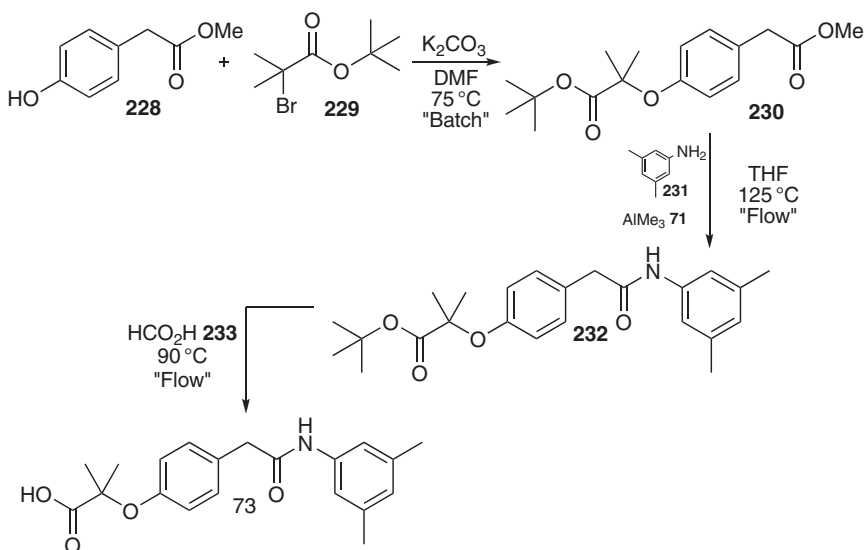
Scheme 66 Combination of batch and flow methodology for the synthesis of the pharmaceutical agent, efaproxiral (**73**).

salt of 4-chlorophenylhydrazine **226**, in acetic acid **6**, at 125 °C afforded pyrazole **227** in 80% yield with a residence time of 16 min. The final step of the synthesis involved the formation of an amide bond which was achieved via the treatment of pyrazole **227** with AlMe₃ **71** and

1-aminopiperidine **221** in THF at 125 °C for 2 min. Using this approach, the authors reported the isolation of the antiobesity drug rimonabant (**72**) in an overall yield of 49%, demonstrating the ability to continuously synthesize drug molecules on the gram scale.

In synthesis of their second drug target, Seeberger et al. combined batch and flow regimes as a means of obtaining efaproxiral (**73**), a pharmaceutical agent used for the enhancement of radiation therapy. This mode of operation was selected as the authors acknowledged potential problems associated with the heterogeneous nature of the inorganic base/ organic solvent mixture that was required to alkylate the phenol derivative **228** (Scheme 66). In batch, the authors alkylated phenol **228** with the *tert*-butyl ester of 2-bromo-2-methyl-propionic acid **229** to afford the methyl ester **230** in 75% yield. The second step of the reaction involved an aluminum-mediated amide bond formation between the ester **230** and 3,5-dimethylaniline **231** which was conducted under continuous flow, using a residence time of 2 min, affording the amide **232** in 77% yield and quantitative selectivity toward the methyl ester. The final step involved hydrolysis of the *tert*-butyl ester, which was achieved under flow using formic acid **233** at 90 °C, affording efaproxiral (**73**) in 89 % yield. Using this combination of batch and flow reactions, the authors were able to synthesize the target compound **73** at 24 mmol h^{-1}.

In a recent example of industrial interest, Tietze and Liu (2008) reported the development of a continuous flow process for the synthesis of an aminonaphthalene derivative **91** on a kilogram scale, for use as a starting material toward the preparation of novel anticancer agents such as the duocarmycin prodrug **234** (Scheme 67). Initial investigations focused on modifying the existing batch procedure and utilizing numerous single microreaction steps in series, thus enabling comparison of the developed flow protocol with existing synthetic methodology.

As Scheme 68 illustrates, the first step of the reaction was the synthesis of the *tert*-butyl ester **235** from bromoacetyl bromide **236**. Owing to the
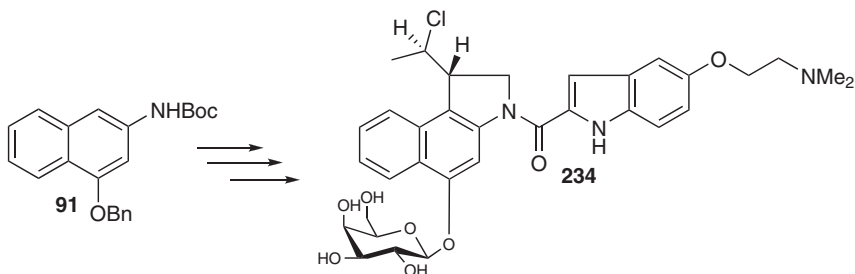
Scheme 67   Schematic illustrating compound **91** as a building block in the synthesis of the prodrug **234**.
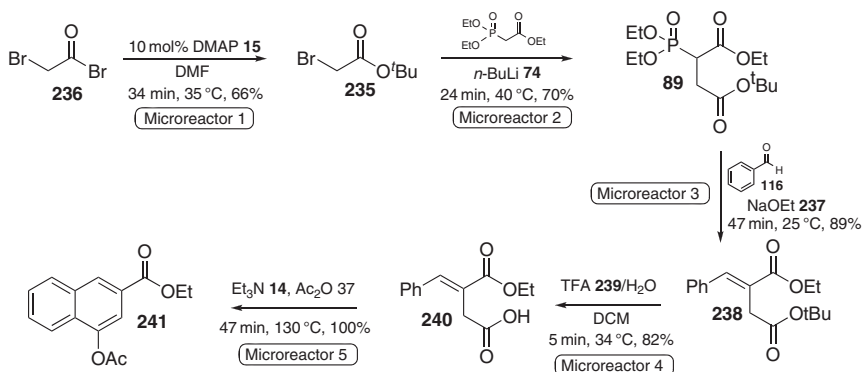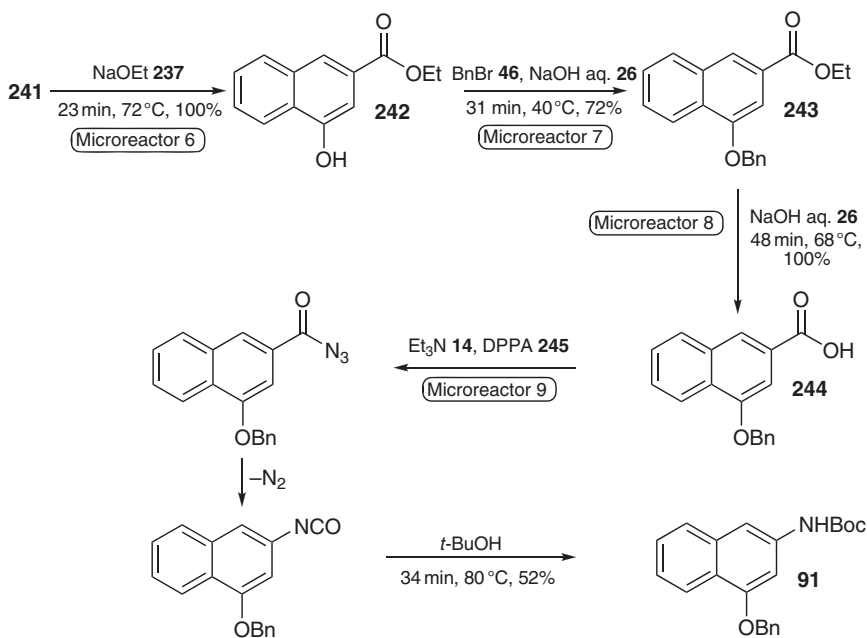
Scheme 68 Schematic illustrating the first five microreactions used in the synthesis of **91**.

precipitation of an ammonium salt, solvents such as diethyl ether and THF were unsuitable for use within the flow reactor; a short solvent study was therefore conducted and DMF identified as the ideal solvent. Employing 10% DMAP **15** in DMF, a reaction temperature of 35 °C and a residence time of 34 min, the authors were able to isolate the target *tert*-butyl ester **235** in 66% yield. The *tert*-butyl ester **235** was subsequently used in the synthesis of the phosphonosuccinate **89**; details discussed previously and can be found summarized in Scheme 23.

In a third microreactor, the anion of 4-*tert*-butyl 1-ethyl-2-(diethoxyphosphoryl)succinate was prepared *in situ* using sodium ethoxide **237** (in EtOH) and the Wittig–Horner olefination with benzaldehyde **116** performed using a residence time of 47 min to afford (E)-*tert*-butyl-1-ethyl-2-benzylidenesuccinate **238** in excellent selectivity (89% yield). In a fourth reactor, the acid-catalyzed (TFA **239**) *tert*-butyl ester deprotection was achieved using a residence time of 5 min at 34 °C and employing DCM as the reaction solvent to afford (E)-3-(ethoxycarbonyl)-4-phenylbut-3-enoic acid **246** in 82% yield. The deprotection was subsequently followed by a Friedel–Crafts acylation, using triethylamine **14** and acetic anhydride **37**, to afford 4-acetoxy-naphthalene-2-carboxylic acid ethyl ester **241** in quantitative yield when conducted at 130 °C (residence time = 47 min).

In the first step illustrated in Scheme 69, the carboxylic acid ethyl ester **241** undergoes quantitative solvolysis, using NaOEt **237** (30 mol%), the resulting naphthol derivative **242** was subsequently protected as its benzyl ether **244** using aq. NaOH **26** and benzyl bromide **46** to afford ethyl-4-(benzyloxy)-2-naphthoate **243** in 72% yield. Quantitative hydrolysis of the ethyl ester **243** followed, using aq. NaOH **26** at 68 °C for 48 min. The carboxylic acid **244** was used directly with the Shioiri–Yamada reagent

Scheme 69 Schematic illustrating the final four microreactions used to obtain the target (4-benzyloxynaphthalen-2-yl)-carbamic acid *tert*-butyl ester **91**.

DPPA **245** in the presence of *tert*-butanol to afford the target product **91** via a Curtius rearrangement (52% yield).

The authors were pleased to report that in most cases, similar or better results were obtained when comparing the reaction steps performed under continuous flow and batch, the continuous flow approach, how-ever, had the advantages of providing increased safety and faster reac-tions, with an empirical accelerating factor of $F = 3$–10 reported.

In an analogous manner, LaPorte et al. (2008) employed three conse-cutive reactions in the development of a continuous protocol for the synthesis of 6-hydroxybuspirone **246** (Scheme 70). The authors rationa-lized the need for a continuous process as the oxidation times required at a pilot plant stage would be of the order of 16–24 h as the process was mass transfer limited and the need to cool the reaction mixture to −70 °C would be an issue for concern. To simplify studies, the authors employed a solution of the preformed enolate **247** (prepared at −70 °C using NaHMDS **44**, 3 ml min^{-1}) as the reactant feedstock for one inlet of the microreactor and oxygen (0.3 l min^{-1}) as the second feed. The microreactor was cooled to −10 °C using a recirculating coolant and afforded 65–70% conversion to **246** with a residence time of 2–3 min. To increase the yield of the target
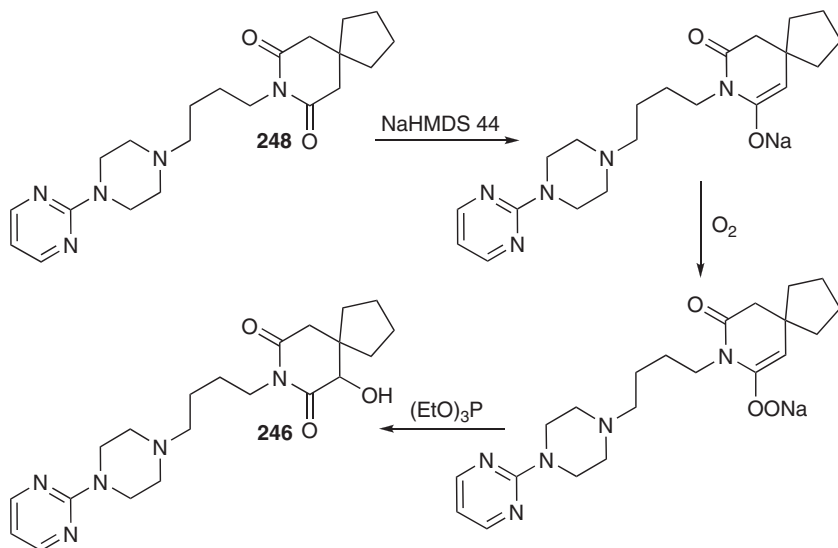
Scheme 70 Synthesis of 6-hydroxybuspirone **246** via the hydroxylation of the azapirone psychotropic agent buspirone (**248**).

product further, the authors subsequently employed a second microreactor where the reaction products from the initial reactor were reacted with a second stream of oxygen. Using this approach, the yield was increased to 85–92% with a processing time of 5–6 min with a daily production volume of 300 g day^{-1}. Based on the encouraging results obtained, the process was subsequently scaled to enable the production of 6-hydroxybuspirone **246** from buspirone (**248**) on a multi-kilo scale and incorporated in-line FTIR monitoring.

In an extension to their earlier examples of β-hydroxyketone dehydration (Scheme 7), Tanaka et al. (2007) evaluated the continuous flow synthesis of an immunoactivating natural product, pristane (2,6,10,14-tetramethylpentadecane) (**249**). Due to limited commercial availability of pristane (**249**), the authors investigated the compounds preparation in a microreactor as a means of obtaining a method suitable for production of pristane (**249**) to meet demand, which is currently ~5 kg week^{-1}. The first step of the reaction involved treating farnesol (**250**) with MnO_2 to afford the respective aldehyde, which subsequently underwent a reaction with isobutyl magnesium chloride to afford an allylic alcohol **251**. The alcohol **251** (1.0 M in THF) was subsequently dehydrated within a micromixer (Comet X-01) using p-TsOH·H_2O **12** in THF/toluene (0.2–1.0 M), at total flow rate of 600 µl min^{-1} and a reaction temperature of 90 °C, followed by catalytic hydrogenation. Under the aforementioned reaction conditions, the authors obtained the target compound **249** in 80% yield from farnesol
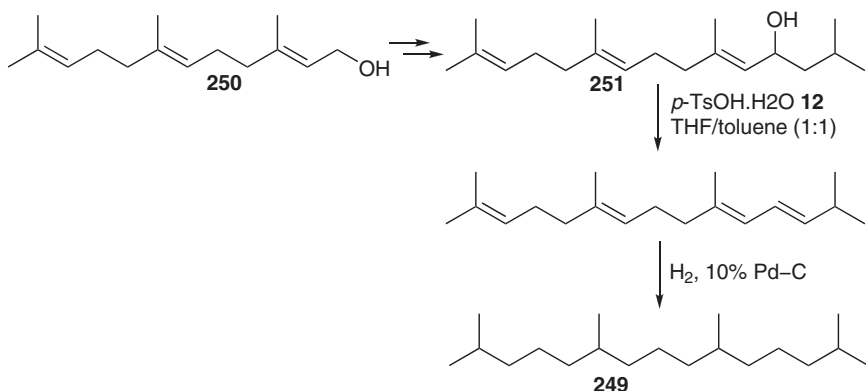
Scheme 71 Synthetic strategy employed for the continuous flow synthesis of the immunoactivating natural product, pristane (**249**).

(**250**) (Scheme 71). Compared to batch techniques, this synthetic route proved advantageous as only a simple purification was required in order to isolate the product **249** unlike the multiple distillations traditionally employed.

Cheng-Lee et al. (2005) demonstrated the multistep synthesis of a radiolabeled imaging probe in a PDMS microreactor, consisting of a complex array of reaction channels, with typical dimensions of $200 \, \mu m$ (wide) $45 \, \mu m$ (deep). Employing a sequence of five steps, comprising of (1) [^{18}F] fluoride concentration ($500 \, \mu Ci$), (2) solvent exchange from H_2O to MeCN, (3) [^{18}F]fluoride substitution of the D-mannose triflate **252** (324 ng), to afford the labeled probe **253** ($100 \, °C$ for 30 s and $120 \, °C$ for 50 s), (4) solvent exchange from MeCN to H_2O, and finally, (5) acid hydrolysis of **254** at $60 \, °C$, the authors demonstrated the synthesis of 2-[^{18}F]-FDG **254** (Scheme 72).

Using this approach, 2-[^{18}F]-FDG **254** was obtained in 38% radiochemical yield, with a purity of 97.6% (determined by radio TLC). Miniaturization of the process enabled the reaction sequence to be performed in
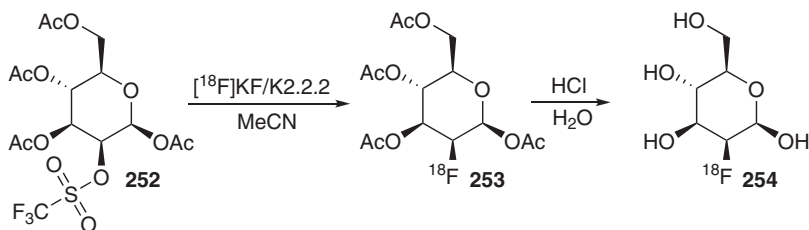
Scheme 72 Synthesis of the radiolabel 2-[^{18}F]-fluorodeoxyglucose (2-[^{18}F]-FDG) **254**.

14 min, compared to 50 min for the current automated protocol. Most importantly, however, the authors found the process to be reproducible between runs and reactors. Future work is therefore concerned with increasing the reaction chamber in order to increase the quantities of material synthesized for use in human PET imaging (10 mCi patient^{-1}).

Building on the bifurcated pathway, developed to enable the selective synthesis of thiazoles or imidazoles (Scheme 73), Baxendale et al. (2005) subsequently demonstrated the synthesis of a HIV-1 RTI analog **255** using the same reaction methodology.

As Scheme 73 illustrates to attain the target compound **255**, the authors reacted 4-bromophenyl isothiocyanate **256** with ethyl isocyanoacetate **257** in the presence of PS-BEMP **124** to afford the thiazole **258** in 58% yield and introduction of α-bromoamide **259** through the PS-BEMP **124** cartridge subsequently afforded the target compound **255** in 30% yield.

In 2005, Baxendale et al. reported the first enantioselective synthesis of 2-aryl-2,3-dihydro-3-benzofurancarboxamide neolignan (grossamide) **260** conducted under continuous flow conditions. As illustrated in Scheme 73, the first step of the reaction involved the synthesis of amide **261** *via* the coupling of ferulic acid **262** and tyramine **171**, in the presence of PS-HOBt **263**. Monitoring reaction progress by LC–MS, the authors were able to optimize this step to afford the amide **261** in 90% conversion; however, prior to performing the second reaction step it was imperative to remove any residual tyramine **171**. As Scheme 74 illustrates, this was achieved by
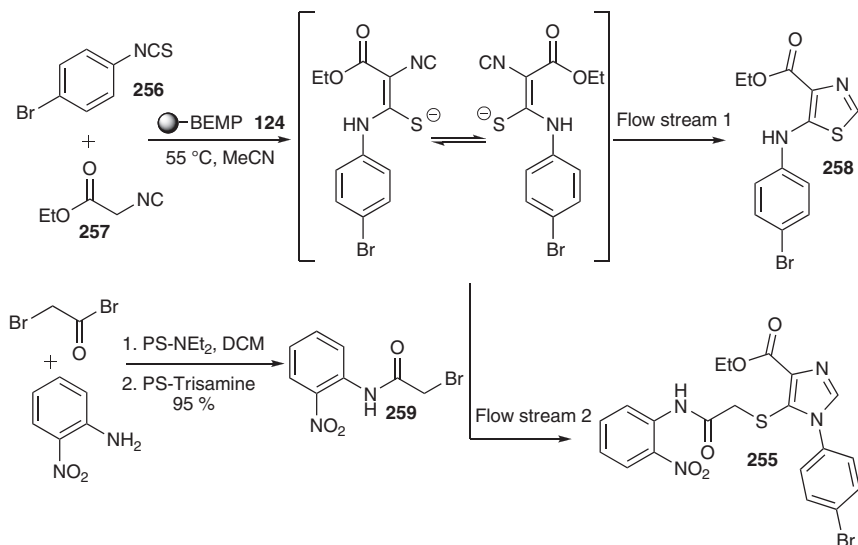
Scheme 73   The continuous flow synthesis of a HIV-1 RTI analog **255** from α-bromoamide **259**.
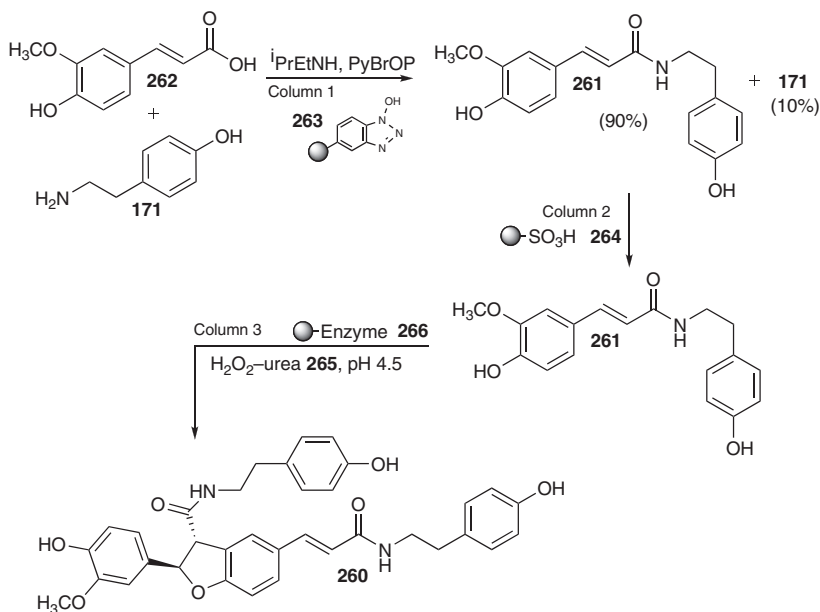
Scheme 74 Continuous flow protocol employed for the synthesis of the natural product grossamide (**260**) using a series of solid-supported reagents, catalysts and scavengers.

passing the reaction mixture through a second column containing PS-SO$_3$H **264** to afford the target intermediate **261** in excellent purity. A premixed solution of the amide **261** and H$_2$O$_2$–urea complex **265**, in aqueous buffer, was subsequently pumped through a third column, containing silica-supported peroxidase **266**, to afford grossamide (**260**) in excellent yield and purity.

Employing a series of packed columns, containing immobilized reagents, catalysts, and scavengers, in conjunction with a glass microreactor and a flow hydrogenation system, Baxendale et al. (2006) reported the flow-assisted synthesis of the alkaloid natural product ($\pm$)-oxomaritidine (**266**). As depicted in Scheme 75, the initial steps of azide **267** and aldehyde **268** synthesis were performed simultaneously in separate reaction columns and at the point of convergence, in the presence of a polymer-supported phosphine **269** at 55 °C, afforded the aza-Wittig intermediate **270**. This was followed by reduction of the imine **270**, utilizing a commercially available flow hydrogenator containing 10% Pd/C, to afford the 2° amine **271** in THF. As subsequent reaction steps required a change of reaction solvent, from THF to DCM, the amine **271** was collected on-line and solvent removal achieved using a Vapourtec V-10 solvent evaporator, the amine **271** was then redissolved in DCM, a process that took less than
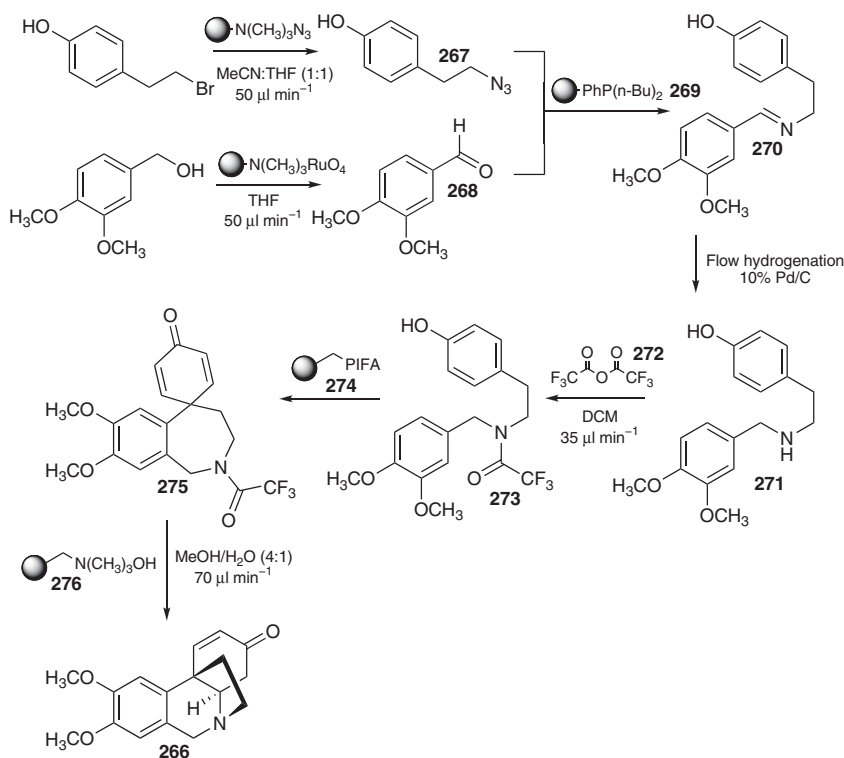
Scheme 75 Illustration of the reaction steps employed in the flow-assisted synthesis of (±)-oxomaritidine (**266**).

10 min. In the latter half of the reaction sequence, the 2° amine **271** was trifluoroacetylated (5 eq. of TFAA **272** 80 °C) within a glass microreactor to afford amide **273**, which subsequently underwent oxidative phenolic coupling, in the presence of polymer-supported (ditrifluoroacetoxyiodo)benzene **274**, to afford a seven-membered tricyclic derivative **275**. The resulting product stream was finally passed through a column reactor, containing a polymer-supported base **276**, which promoted cleavage of the amide bond followed by spontaneous 1,4-conjugate addition to generate the target compound (±)-oxomaritidine (**266**).

Employing a stainless-steel microreactor, Sugimoto et al. (2006, 2008) demonstrated the Barton reaction (nitrite photolysis) of a steroidal substrate **277** to afford **199**, a key intermediate in the synthesis of an endothelin receptor antagonist. Initial investigations employed a conventional 300 W high-pressure mercury lamp and a stainless-steel microreactor with a single serpentine reaction channel [1,000 μm (wide) × 107 μm (deep) 2.2 m (long)]. To perform a continuous Barton photolysis, a gap of 7.5 cm

was maintained between the light source and the stainless-steel micro-reactor, an acetone solution containing the nitrite **277** (9 mM) and pyridine (0.2 eq.) was then pumped through the stainless-steel reactor at a flow rate of $33\,\mu l\,min^{-1}$, and the reaction products analyzed off-line by HPLC to determine the conversion of nitrite **277** to oxime **199**.

Using a quartz cover plate, the authors observed the production of a complex reaction mixture due to the low wavelength of the mercury light source. In comparison, using a Pyrex cover plate afforded the rearranged product **199** in moderate yield (21%), whereas employing a soda-lime glass cover plate increased the yield to 59% **199**. The authors found that if the light source was positioned closer to the reactor that is 5.0 cm, the yield of **199** decreased (33%), an observation that was attributed to thermal degradation of the oxime **199** occurring as a result of the light source heating the reactor (>50 °C) (Scheme 76).

As the short wavelength light (<365 nm) emitted from the mercury lamp was not thought to be advantageous for this particular reaction, the authors replaced the light source with a 15 W black light ($\lambda_{max} = 352$ nm) as a means of avoiding the undesirable heating of the microreactor. Due to the reduced heating of the light source, the black light was able to be positioned 3.0 cm from the reactor (cf. 7.5 cm for the mercury lamp). As Table 32 illustrates, a Pyrex cover plate afforded the highest yield of oxime **199** (21%) with a marked reduction in energy consumption (cf. to the mercury lamp) and the authors found that by increasing the reactant
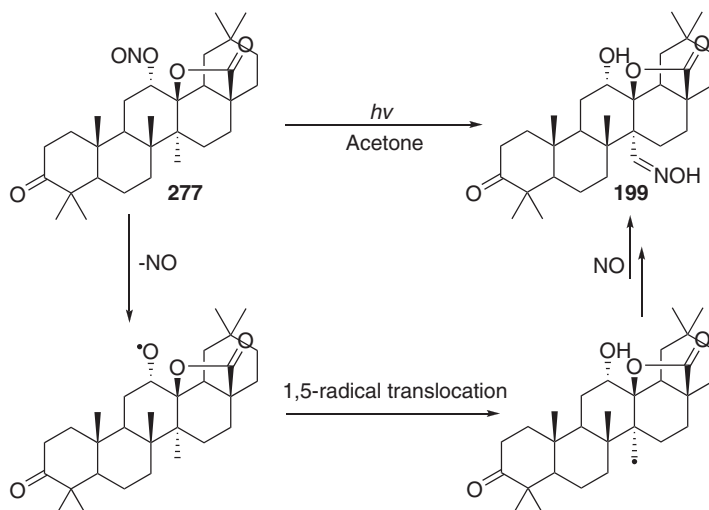
Scheme 76 Barton nitrite photolysis of a steroidal compound **277** to afford an oxime **199**.

Table 32   Summary of the results obtained during the Barton photolysis of **277**

Light source	Cover plate material	Residence time (min)	Yield (%)	Yield (W h^{-1})
300 W Hg lamp	Pyrex	6	21	0.7
300 W Hg lamp	Soda lime	6	56	1.9
15 W black light	Soda lime	6	15	10.3
15 W black light	Pyrex	6	29	19.3
15 W black light	Pyrex	12	71	23.7

residence time from 6 to 12 min, the target oxime **199** could be obtained in 71% yield; as determined by HPLC analysis.

In order to produce oxime **199** in greater quantities, the authors subsequently evaluated the use of DMF as the reaction solvent due to the increased solubility of the nitrite precursor **277** (36 mM). In conjunction with two serially connected microreactors, each containing 16 microchannels [1,000 μm (wide) × 500 μm (deep) × 1.0 m (length)] and eight black lights, the photochemical synthesis was performed continuously for 20 h at a flow rate of 250 μl min^{-1} (residence time = 32 min). After an off-line aqueous extraction and silica gel column, 3.1 g of the oxime **199** was obtained equating to an isolated yield of 60% and successfully demonstrating the ability to use photochemical synthesis for the scalable preparation of pharmaceutically relevant compounds.

A more recent example of the *in situ* photochemical generation of singlet oxygen was reported by Meyer et al. (2007) who demonstrated the synthesis of hydroperoxide **278**, a precursor to (–)-rose oxide (**200**) which is used as a fragrance in the perfume industry (Scheme 77). To demonstrate the synthetic utility of the continuous flow methodology, batch reactions were performed alongside the microreactions, using a modified Schlenk reactor (40 ml). The microreactor employed was fabricated from Borofloat® glass, possessed a total internal volume of 270 μl, and was illuminated using a diode array consisting of 4 × 10 diodes (λ 468 nm). To evaluate the microreactor, a solution of (–)-β-citronellol (**279**) (0.1 M) and Ru(^{t}bpy)$_3$Cl$_2$ **280** (1 × 10^{-3} M) in EtOH was firstly purged with compressed air for 20 min (0.4 l h^{-1}), using a peristaltic pump, the reaction mixture was subsequently cycled through the reactor over the course of the investigation, with samples analyzed off-line periodically by HPLC. In comparison to the batch reactor where only 7.5 ml of the reactor volume was illuminated (15.2 cm^2), in the microreactor all 270 μl of the reaction mixture was irradiated (6.9 cm^2) which afforded increased photonic efficiency leading to enhanced space time yields of 0.9 mmol l^{-1} min^{-1} (cf. 0.1 mmol l^{-1} min^{-1}) obtained in the batch cell.
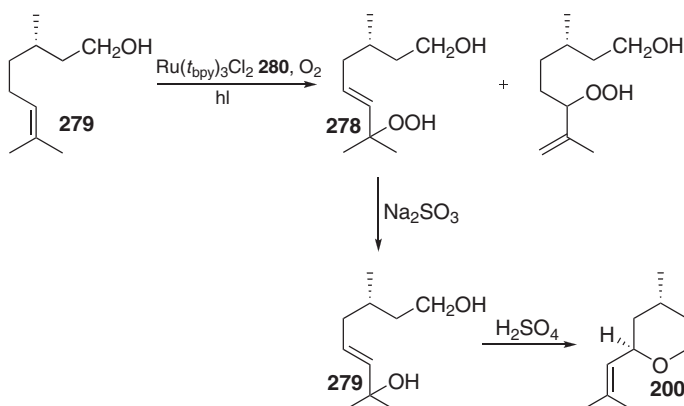
Scheme 77 Photooxygenation of (–)-β-citronellol (**279**) conducted in a glass microreactor and the subsequent use of hydroperoxide **278** in the synthesis of (–)-rose oxide (**200**).

4. CONCLUSIONS

As can be seen from the variety of reactions discussed herein, microreaction technology enables the rapid screening of both reactants and reaction conditions, thus affording a facile route to the generation of compound libraries. In addition to the time savings harnessed, the use of MRT has the potential to reduce the costs associated with high-throughput chemistry as it enables a vast array of information to be generated from reduced quantities of substrates and catalysts when compared with conventional techniques. Added to this the advantage that the reaction conditions identified can subsequently be transferred from the research laboratory to pilot-scale production and beyond, it is clear to see why the field of microreactor research has grown rapidly over the past decade.

REFERENCES

Acke, D. R., and Stevens, C. *Green Chem.* **9**, 386–390 (2007).

Acke, D. R., Stevens, C. V., and Roman, B. I. *Org. Proc. Res. Dev.* **12**, 921–928 (2008).

Annis, D. A., and Jacobsen, E. N. *J. Am. Chem. Soc.* **121**, 4147–4154 (1999).

Baumann, M., Baxendale, I. R., Ley, S. V., Nikbin, N., and Smith, C. D. *Org. Biomol. Chem.* **6**, 1587–1593 (2008).

Baumann, M., Baxendale, I. R., Ley, S. V., Nikbin, N., Smith, C. D., and Tierney, J. P. *Org. Bio. Mol. Chem.* **6**, 1577–1586 (2008b).

Baxendale, I. R., Deeley, J., Griffiths-Jones, C. M., Ley, S. V., Saaby, S., and Tranmer, G. K. *Chem. Commun.* 2566–2568 (2006).

Baxendale, I. R., Griffiths-Jones, C. M., Ley, S. V., and Tranmer, G. K. *Synlett* **3**, 427–430 (2005).

Baxendale, I. R., Ley, S. V., Smith, C. D., Tamborini, L., and Voica, A. *J. Combin. Chem.* **10**(6), 851–857 (2008).

Belder, D., Ludwig, M., Wang, L., and Reetz, M. T. *Angew. Chem. Int. Ed.* **45**, 2463–2466 (2006).

Benali, O., Deal, M., Farrant, E., Tapolczay, D., and Wheeler, R. *Org. Proc. Res. Dev.* **12**, 1007–1011 (2008).

Bogdan, A. R., Mason, B. P., Sylvester, K. T., and McQuade, D. T. *Angew. Chem. Int. Ed.* **46**, 1698–1701 (2007).

Braune, S., Pochlauer, P., Reintjens, R., Steinhofer, S., Winter, M., Lobet, O., Guidat, R., Woehl, P., and Guermeur, C. *Chem. Today* **26**, 1–4 (2008).

Burns, J. R., and Ramshaw, C. *Chem. Eng. Commun.* **189**, 1611–1628 (2002).

Carrel, F. R., Geyer, K., Codee, J. D.C., and Seeberger, P. H. *Org. Lett.* **9**(12), 2285–2288 (2007).

Chambers, R. D., Fox, M. A., Holling, D., Nakano, T., Okazoe, T., and Sandford, G. *Lab Chip* **5**, 191–198 (2005).

Chambers, R. D., Holling, D., Spink, R. C.H., and Sandford, G. *Lab Chip* **1**, 132–137 (2001).

Chambers, R. D., Sandford, G., Trmcic, J., and Okazoe, T. *Org. Proc. Res. Dev.* **12**(2), 339–344 (2008).

Chambers, R. D., and Spink, R. C.H. *Chem. Commun.* 883–884 (1999).

Chatgilialoglu, C. *Chem. Eur. J.* **14**, 2310–2320 (2008).

Cheng-Lee, C., Sui, G. D., Elizarov, A., Shu, C. Y.J., Shin, Y. S., Dooley, A. N., Huang, J., Daridon, A., Wyatt, P., Stout, D., Kolb, H. C., Witte, O. N., Satyamurthy, N., Heath, J. R., Phelps, M. E., Quake, S. R., and Tseng, H. R. *Science* **310**, 1793–1796 (2005).

Comer, E., and Organ, M. G. *Chem. Eur. J.* **44**, 7223–7227 (2005a).

Comer, E., and Organ, M. G. *J. Am. Chem. Soc.* **127**, 8160–8167 (2005b).

Costantini, F., Bula, W. P., Salvio, R., Huskens, J., Gardeniers, H. J.G.E., Reinhoudt, D. N., and Verboom, W. *J. Am. Chem. Soc.* **131**, 1650–1651 (2009).

Csajagi, C., Szatzker, G., Toke, R. R., Urge, L., Davas, F., and Poppe, L. *Tetrahedron: Asymmetry* **19**, 237–246 (2008).

Dale, J. D., Dunn, P. J., Golightly, C., Hughes, M. L., Levett, P. C., Pearce, A. K., Searle, P. M., and Ward, G. *Org. Proc. Res. Dev.* **4**, 17–22 (2000).

Drager, G., Kiss, C., Kunz, Y., and Kirschning, A. *Org. Biomol. Chem.* **5**, 3659–3664 (2007).

Ducry, L., and Roberge, D. M. *Angew. Chem. Int. Ed.* **44**, 7972–7975 (2005).

Ehrich, H., Linke, D., Morgenschweis, K., Baerns, M., and Jahnisch, K. *Chimia* **56**, 647–653 (2002).

Fernandez-Suarez, M., Wong, S. Y.F., and Warrington, B. H. *Lab Chip* **2**, 170–174 (2002).

Flogel, O., Codee, J. D.C., Seebach, D., and Seeberger, P. H. *Angew. Chem.* **45**, 7000–7003 (2006).

Fukuyama, T., Hino, Y., Kamata, N., and Ryu, I. *Chem. Lett.* **34**, 66–67 (2004).

Garcia-Egido, E., Wong, S. Y.F., and Warrington, B. H. *Lab Chip* **2**, 31–33 (2002).

Geyer, K., and Seeberger, P. H. *Helv. Chim. Acta.* **90**, 395–403 (2007).

Glasnov, T. N., and Kappe, C. O. *Macromol. Rapid Commun.* **28**, 395–410 (2007).

Gorges, R., Meyer, S., and Kreisel, G. *J. Photochem., Photobiol. A: Chem.* **167**, 95–99 (2004).

Goto, S., Velder, J., El Sheikh, S., Sakamoto, Y., Mitani, M., Elmas, S., Adler, A., Becker, A., Neudorfl, J.-M., Lex, J., and Schmalz, H.-G. *Synletters* **9**, 1361–1365 (2008).

Gustafsson, T., Gilmor, R., and Seeberger, P. H. *Chem. Commun.* 3022–3024 (2008a).

Gustafsson, T., Ponten, F., and Seeberger, P. H. *Chem. Commun.* 1100–1102 (2008b).

Hessel, V., Hofmann, C., Lob, P., Lohndorf, J., Lowe, H., and Ziogas, A. *Org. Proc. Res. Dev.* **9**, 479–489 (2005).

Hinchcliffe, A., Hughes, C., Pears, D. A., and Pitts, M. R. *Org. Proc. Res. Dev.* **11**, 477–481 (2007).

Honda, T., Miyazaki, M., Nakamura, H., and Maeda, H. *Adv. Synth. Catal.* **348**, 2163–2171 (2006).

Honda, T., Miyazaki, M., Yamaguchi, Y., Nakamura, H., and Maeda, H. *Lab Chip* **7**, 366–372 (2007).

Hook, B. D.A., Dohle, W., Hirst, P. R., Pickworth, M., Berry, M. B., Booker-Milburn, K. I. *J. Org. Chem.* **70**, 7558–7564 (2005).

Hooper, J., and Watts, P. *J. Labelled Comp. Radiopharm.* **50**, 189–196 (2007).

Kawanami, H., Matsushima, K., Sato, M., and Ikushima, Y. *Angew. Chem. Int. Ed.* **46**, 5129–5132 (2007).

Kenis, P. J.A., Ismagilov, R. F., and Whitesides, G. M. *Science* **285**, 83–85 (1999).

Kikutani, Y., Horiuchi, T., Uchiyama, K., Hisamoto, J., Tokeshi, M., and Kitamori, T. *Lab Chip* **2**, 188–192 (2002a).

Kikutani, Y., Hibara, A., Uchiyama, K., Hisamoto, J., Tokeshi, M., and Kitamori, T. *Lab Chip* **2**, 193–196 (2002b).

Kirschning, A., Altwicker, C., Drager, G., Harders, J., Hoffmann, N., Hoffmann, U., Schonfeld, H., Solodenko, W., and Kunz, U. *Angew. Chem. Int. Ed.* **40**, 3995–3998 (2001).

Kirschning, A., and Gas, J. *Chem. Eur. J.* **9**, 5708–5723 (2003).

Kirschning, A., Solodenko, W., and Mennecke, K. *Chem. Eur. J.* **12**, 5972–5990 (2006).

Kulkarni, A. A. *World Patent*, WO2007087816A1 (2007).

Kulkarni, A. A., Nivangune, N. T., Kalyani, V. S., Joshi, R. A., and Joshi, R. R. *Org. Proc. Res. Dev.* **12**, 995–1000 (2008).

LaPorte, T. L., Hamedi, M., DePue, J. S., Shen, L., Watson, D., and Hsieh, D. *Org. Proc. Res. Dev.* **12**, 956–966 (2008).

Li, X., Wang, H., Inoue, K., Uehara, M., Nakamura, H., Miyazaki, M., Abe, E., and Maeda, H. *Chem. Commun.* 964–965 (2003).

Lundgren, S., Russom, A., Jonsson, C., Stemme, G., Haswell, S. J., Anderson, H., and Moberg, C. "*8th International Conference on Miniaturised Systems for Chemistry and Life Sciences*", p. 878 (2004).

Mason, B. P., Price, K. E., Steinbacher, J. L., Bogdan, A. R., and McQuade, D. T. *Chem. Rev.* **107**(6), 2300–2318 (2007).

Matsuoka, S., Hibara, A., Ueno, M., and Kitamori, T. *Lab Chip* **6**, 1236–1238 (2006).

Matsushita, Y., Kumada, S., Wakabayashi, K., Sakeda, K., and Ichimura, T. *Chem. Lett.* **35**, 410–411 (2006).

Matsushita, Y., Ohba, N., Kumada, S., Sakeda, K., Suzuki, T., and Ichimura, T. *Chem. Eng. J.* **135S**, S303–S308 (2008).

Matsushita, Y., Ohba, N., Kumada, S., Suzuki, T., and Ichimura, T. *Catal. Commun.* **8**, 2194–2197 (2007).

Mennecke, K., and Kirschning, A. *Synthesis* **20**, 3267–3272 (2008).

Meyer, S., Tietze, D., Rau, S., Schafer, B., and Kreisel, G. *J. Photochem. Photobiol. A: Chem.* **187**, 248–253 (2007).

Miyake, N., and Kitazume, T. *J. Fluorine Chem.* **2003**, 243–246 (2003).

Mukae, H., Maeda, H., Nashihara, S., and Mizuno, K. *Bull. Chem. Soc. Jpn.* **80**, 1157–1161 (2007).

Nagaki, A., Takizawa, E., and Yoshida, J. *J. Am. Chem. Soc.* **131**(5), 1654–1655 (2009).

Nagaki, A., Tomida, Y., and Yoshida, J. *Macromolecules* **41**, 6322–6330 (2008).

Odedra, A., Geyer, K., Gustafsson, T., Gilmour, R., and Seeberger, P. H. *Chem. Commun.* 3025–3027 (2008).

Panke, Schwalbe, T., Stirner, W., Taghavi-Moghadam, S., and Wille, G. *Synthesis* 2827–2830 (2003).

Ponten, F., Gustafsson, T., and Seeberger, P. H. *Chem. Commun.* 1100–1102 (2008).

Ratner, D. M., Murphy, E. R., Jhunjhunwala, M. D., Snyder, A., Jensen, K. F., and Seeberger, P. H. *Chem. Commun.* **5**, 578–580 (2005).

Sakeda, K., Wakabayashi, K., Matsushita, Y., Ichimura, T., Suzuki, T., Wada, T., and Inoue, Y. *J. Photochem. Photobiol. A: Chem.* **192**, 66–171 (2007).

Sato, M., Matsushima, K., Kawanami, H., and Ikuhsima, Y. *Angew. Chem. Int. Ed.* **46**, 6284–6288 (2007).

Schwalbe, T., Autze, V., Hohmann, M., and Stirner, W. *Org. Proc. Res. Dev.* **8**, 440–454 (2004).

Schwalbe, T., Autze, V., and Wille, G. *Chimia* **56**, 636–646 (2002).

Smith, C. D., Baxendale, I. R., Lanners, S., Hayward, J. J., Smith, S. C., and Ley, S. V. *Org. Biomol. Chem.* **5**, 1559–1561 (2007a).

Smith, C. D., Baxendale, I. R., Tranmer, G. K., Baumann, M., Smith, S. C., Lewthwaite, R. A., and Ley, S. V. *Org. Biomol. Chem.* **5**, 1562–1568 (2007b).

Sugimoto, A., Fukuyama, T., Sumino, Y., Takagi, M., and Ryu, I. *Tetrahedron* **65**, 1593–1598 (2008).

Sugimoto, A., Sumino, Y., Takagi, M., Fukuyama, T., and Ryu, I. *Tetrahedron Lett.* **47**, 6197–6200 (2006).

Takasuga, M., Yabuki, Y., and Kato, Y. *J. Chem. Eng. Jpn.* **39**, 772–776 (2006).

Takei, G., Kitamori, T., and Kim, H. B. *Catal. Commun.* **6**, 357–360 (2005).

Tanaka, K., Motomatsu, S., Koyama, K., Tanaka, S., and Fukase, K. *Org. Lett.* **9**, 299–302 (2007).

Thomsen, M. S., Polt, P., and Nidetzky, B. *Chem. Commun.* 2527–2529 (2007).

Tietze, L. F., and Liu, D. *Arkivoc* **viii**, 193–210 (2008).

Uozumi, Y., Yamada, Y. M.A., Beppu, T., Fukuyama, N., Ueno, M., and Kitamori, T. *J. Am. Chem. Soc.* **128**, 15994–15995 (2006).

Ushiogi, Y., Hase, T., Iinuma, Y., Takata, A., and Yoshida, J. *Chem. Commun.* 2947–2949 (2007).

van Meene, E., Moonen, K., Acke, D., and Stevens, C. V. *Arkivoc* **i**, 31–45 (2006).

Wan, Y. S.S., Chau, J. L.H., Gavrilidis, A., and Yeung, K. L. *Chem. Commun.* 878–879 (2002).

Wang, J., Sui, G., Mocharla, V. P., Lin, R. J., Phelps, M. E., Kolb, H. C., and Tseng, H. R. *Angew. Chem. Int. Ed.* **45**, 5276–5281 (2006).

Watts, P., Wiles, C., Haswell, S. J., and Pombo-Villar, E. *Tetrahedron* **58**, 5427–5439 (2002).

Wild, G. P., Wiles, C., Watts, P., and Haswell, S. J. *Tetrahedron* **65**, 1618–1629 (2009).

Wiles, C., and Watts, P. *Chem. Commun.* 443–467 (2007a).

Wiles, C., and Watts, P. *Chem. Commun.* 4928–4930 (2007b).

Wiles, C., and Watts, P. *Eur. J. Org. Chem.* 1655–1671 (2008a).

Wiles, C., and Watts, P. *Org. Proc. Res. Dev.* **12**, 1001–1006 (2008b).

Wiles, C., and Watts, P. *Eur. J. Org. Chem.* 5597–5613 (2008c).

Wiles, C., Watts, P., and Haswell, S. J. *Tetrahedron* **60**, 8421–8427 (2004a).

Wiles, C., Watts, P., Haswell, S. J., and Pombo-Villar, E. *Org. Proc. Res. Dev.* **8**, 28–32 (2004b).

Wiles, C., Watts, P., Haswell, S. J., and Pombo-Villar, E. *Lab Chip* **4**, 171–173 (2004c).

Wiles, C., Watts, P., and Haswell, S. J. *Tetrahedron* **61**, 5209–5217 (2005).

Wiles, C., Watts, P., and Haswell, S. J. *Tetrahedron Lett.* **47**, 5261–5264 (2006).

Wiles, C., Watts, P., and Haswell, S. J. *Chem. Commun.* 966–968 (2007a).

Wiles, C., Watts, P., and Haswell, S. J. *Tetrahedron Lett.* **48**, 7362–7365 (2007b).

Wiles, C., Watts, P., and Haswell, S. J. *Lab Chip* **7**, 322–330 (2007c).

Wiles, C., Watts, P., and Haswell, S. J. *Chem. Commun.* 966–968 (2007d).

Wiles, C., Watts, P., Haswell, S. J., and Pombo-Villar, E. *Tetrahedron* **59**, 2886–2887 (2003).

Wootton, R. C.R., Fortt, R., and de Mello, A. J. *Org. Proc. Res. Dev.* **6**, 187–189 (2002).

Yoon, S. K., Choban, E. R., Kane, C., Tzedakis, T., Kenis, P. J.A. *J. Am. Chem. Soc.* **127**, 10466–10467 (2005).

Yoshida, J. "Flash Chemistry: Fast Organic Synthesis in Microsystems". Wiley, London (2008).

Zhang, X., Stefanick, S., and Villani, F. J. *Org. Proc. Res. Dev.* **8**, 455–460 (2004).